COATS, Richard Lee, 1936-
NEUTRON KINETICS OF A REFLECTED BURST REACTOR.

The University of Oklahoma, Ph.D., 1966
Physics, nuclear

THE UNIVERSITY OF OKLAHOMA

GRADUATE COLLEGE

NEUTRON KINETICS OF A REFLECTED BURST REACTOR

A DISSERTATION

SUBMITTED TO THE GRADUATE FACULTY

in partial fulfillment of the requirements for the

degree of

DOCTOR OF PHILOSOPHY

BY

RICHARD L.EE COATS

Norman, Oklahoma

1966

NEUTRON KINETICS OF A REFLECTED BURST REACTOR

APPROVED BY

Albert E. Miller

Jon A. Reuscher

M. L. McGuire

Robert M. St. John

Edwin H. Klehr

DISSERTATION COMMITTEE

ACKNOWLEDGMENT

To adequately express my gratitude to the many individuals from whom assistance and encouragement have been obtained in the preparation of this dissertation, would require an additional volume. In particular, appreciation is extended to A. E. Wilson, J. A. Reusher and R. L. Long for the advice and encouragement during this work.

Special thanks are extended to Paul O'Brien who revealed the problem and provided encouragement throughout the study.

Special appreciation is also extended to J. C. Connant, John Snyder and Don Cox for their "extra" effort which made possible the completion of the experimental work.

Assistance with the many drawings and graphs was provided by Kathy Summers whose help I appreciate. Thanks are given also to June Christy and Christine Edmunds for their typing assistance.

Appreciation is also extended to the A. E. C. Special Fellowship in Nuclear Science and Engineering administered through the Oak Ridge Institute of Nuclear Studies and to the Associated Rocky Mountain Universities fellowship program for providing financial assistance throughout my graduate studies.

Most sincere thanks are due to my wife and children for their patience, understanding and encouragement throughout the graduate program.

TABLE OF CONTENTS

LIST OF TABLES

LIST OF ILLUSTRATIONS

NEUTRON KINETICS OF A REFLECTED BURST REACTOR

CHAPTER I

INTRODUCTION

In recent years there has been a greater interest in fast burst fuel assemblies for the investigation of the effect of nuclear radiation upon matter. In answer to these needs there are now several fast burst reactor facilities in operation [3, 14, 15, 17, 29] and much work is being done in the design of fuel assemblies which will meet the demands of the experimenters for larger radiation dose and dose rates.

A fast reactor can be described simply as an assembly of fissionable material supported by structural materials which offer little moderation of the neutrons produced in fission. A fast burst reactor is such an assembly which by some means is made highly supercritical in a short time allowing a pulse in neutron level to occur.

The general procedure by which a neutron pulse is produced is to make the assembly super prompt critical. This means that the geometrical and material conditions are such that the system is capable of producing more neutrons than are lost even if the neutrons which are generated by the decay of certain fission products are considered lost. In this condition the neutron level in such a system can increase with a period on the order of 10 microseconds. A description of the time dependent characteristics of a typical neutron pulse is given in Appendix A.

In general the kinetic behavior of such a system can be characterized by certain inherent properties such as (1). the average number of neutrons produced per neutron lost, (2). the mean lifetime of a neutron in the assembly, (3). the fraction of the fissions which produce fission fragments that ultimately give rise to more neutrons through decay, and (4). the decay constants associated with these fission fragments.

However, external components can also affect the behavior of the fuel assembly. External reflectors have long been known to affect the pulse characteristics of fast burst fuel assemblies. A distinct difference in the characteristics of outdoor (free-field) and indoor operation of both Godiva I [1] and Godiva II [2] was observed. This difference was attributed to the return of wall reflected neutrons to the fuel assembly during indoor operation.

When materials are placed near the fuel assembly, the effect becomes even more pronounced. During operation of the White Sands Missile Range Fast Burst Reactor and of the Sandia Burst Reactor (SPR), which are basically Godiva type reactors, it has been noted that the presence of experimental equipment near the reactors greatly alters the burst characteristics. [3] The alteration manifests itself as a change in the initial period, the peak fission rate, the burst width, and the total yield from that expected based on the amount of reactivity initially inserted into the system. The disturbance appeared as though there has been a change in the basic reactor kinetic parameters. This apparent change in the kinetic parameters arises because the kinetic equations applicable to a bare assembly are used to describe the behavior of a reflected system.

The equations which are commonly used to describe the behavior of a small fast assembly are:

$$\frac{dn(t)}{dt} = \frac{k(t)\,(1 - \gamma\beta) - 1}{\ell}\, n(t) + \sum_i \gamma_i \lambda_i C_i(t) + S(t)\,\gamma_S$$

$$\frac{dC_i(t)}{dt} = \frac{\beta_i k(t)}{\ell} n(t) - \lambda_i C_i(t)$$

where

$n(t)$ = neutron density at time t,

$C_i(t)$ = density of the i^{th} delayed neutron group precursor at time t,

$S(t)$ = rate at which source neutrons are added to the core,

$k(t)$ = neutron multiplication factor for system at time t,

ℓ = prompt neutron lifetime for system,

β_i = i^{th} group fraction of total neutrons from fission,

β = $\sum_i \beta_i$

γ_i = effectiveness of i^{th} delayed neutron group in producing fission,

λ_i = decay constant of i^{th} delayed neutron group,

γ = average delayed neutron effectiveness in producing fission

γ_S = source neutron effectiveness in causing fission.

These equations are known as the single energy, space independent kinetic equations.

The derivation of these equations can be found in many places in the literature [4, 5, 7]. A general solution is given in reference [12]. These equations prove adequate for an unreflected fast burst reactor which in general is a small fuel assembly. The space effects of such a core are small and are further minimized by the relatively long mean free path of the neutrons at "fast" energies. The neutron distribution in energy is quite peaked in the high energy range and hence the single energy restriction on the equations is satisfied for a fast system.

With the presence of a reflector near the reactor, however, these equations can hardly be expected to be adequate since the reflected neutrons are not taken into account. The direct application of these equations to a reflected assembly would lead to apparent discrepancies in parameters measured by different techniques. One such apparent discrepancy is the so-called "Dollar Paradox" discussed later.

The safe operation of a fast burst reactor facility depends on the knowledge of how a given experimental arrangement will effect the burst characteristics of the fuel assembly. The ability to produce the desired dose and dose rate requested by an experimenter is also a required feature of a burst facility. With an accurate mathematical description of the entire system, prediction of the amount of reactivity required for a given burst is possible and safer operation is insured.

In the fast burst reactor design, certain limitations on the total yield which can be produced in a rigid fuel assembly have been recognized. One of the basic problems facing designers is the thermal shock wave produced in the system. This shock wave is related to the initial period and to the yield of the system. If the pulse could be shaped properly, a lesser shock effect for a given burst yield might be realized. Since reflecting surfaces exhibit a broadening effect on the pulse shape, reflectors could be used to "shape" the pulse and thereby reduce the shock effect.

As fast burst reactors become a more common tool in radiation effects studies, the need for a model which adequately expresses the reflected neutron contributions becomes greater. This model should retain as many features of the theory for the bare assembly as possible in order to conveniently extrapolate the description of a bare assembly to the reflected conditions. A cumbersome unfamiliar model would prove a hindrance to the operating personnel when making reactivity adjustments for an experiment.

The purpose of this paper is to present a model which adequately describes the neutron behavior of a reflected system and to present experimental results which substantiate the validity of this model.

CHAPTER II

REVIEW OF PREVIOUS WORK

Work describing space dependent kinetics is prevalent in the literature [46, 47, 48, 49, 50]. In most cases, however, the work is directed toward space time solutions for large homogeneous systems. Very little theoretical work has been directed toward the space dependence of small burst reactors. The reason for this is simply that the space independent kinetic equations have usually been adequate. Recent observations have, however, raised doubts as to validity of the space independent description in the case where materials in addition to the fuel are involved.

C. S. Brunson [19], in surveying various fast reactor assemblies, noticed a discrepancy between the value of a "dollar" arrived at by different means. This is the so-called "Dollar Paradox". Brunson suggests that the anomaly could be the result of

(1). a previously unknown delayed neutron group of U^{238}

(2). neutrons returning from a reflector

(3). photoneutrons in steel or other structural materials

(4). some (n, delayed n') reaction

T. F. Wimett, et al, [2], in describing the characteristic of Godiva II, was forced to postulate "pseudo-delayed groups of neutrons" to account for an effect which was attributed to room reflected neutrons. In order to extrapolate "outdoor" measured data to the "indoor" situation, two additional delayed neutron groups were postulated with decay constants and relative abundances which provided a good fit to the "indoor" data. The inhour relation was used in determining these values. After including these extra "delayed" neutron groups in the normal space independent, single energy kinetic equations, most room return effects observed were adequately reproduced. The time constants which resulted in a fit to the data were 3.5×10^{-3} seconds for one group and 5×10^{-5} seconds for the other. The second group should influence the inhour relation only for very short reactor periods. Neither group should have a significant effect for reactor periods greater than 10 seconds.

Experimental Work

John T. Mihalczo [42, 51] has done considerable work in the study of the prompt neutron lifetime in various single region enriched systems. This work also includes a study of the effect on prompt neutron lifetime when the fuel assembly consisted of two separate parts separated by a fixed distance [41]. As the separation distance was increased, the measured prompt neutron lifetime increased. This result indicates that the transit time of high energy neutrons across this gap is a significant contribution to the lifetime of the neutrons.

In a recent study, as yet unpublished, Mihalczo investigated the effect on lifetime of steel reflectors located on the ends of cylindrical critical assemblies. Again it was found that the prompt neutron lifetime increased. In all of Mihalczo's prompt neutron lifetime work, the Rossi alpha technique [45] was used. Whether or not the results can be carried over to burst conditions remains a question.

R. A. Karam of ANL used Rossi alpha techniques to study the prompt neutron lifetime parameters in the ZPR-IX, a reflected system [25]. Karam used Cohn's one energy group reflected kinetics model in an attempt to correlate the data. A one exponential fit was found unsatisfactory, which implies that the reflector adds a separate component with a decay constant different from that of the fuel. This suggests that the lifetime of the system is a weighted combination of reflector and fuel neutron lifetimes.

The only systematic experimental investigation of the effect of a reflecting surface on the kinetic behavior of a burst reactor was undertaken by Robert L. Long [3,32]. Long's work consisted of investigating the burst characteristics of the White Sands Missile Range FBR when the system was reflected by various materials. A wide variation in virtually all of the burst characteristics was noted. This change was due to an increase in the mean lifetime of the neutrons in the system. The prompt neutron decay constant was measured for each reflector system and, when used with Wimett's prompt kinetics model [15], gave satisfactory agreement between measured and calculated response of the reactor. Long used several moderating and non-moderating reflectors with the most radical changes in parameters such as prompt neutron lifetime occurring when moderating materials were used. The prompt neutron decay constant was lowered considerably when moderating reflectors were used, implying a large increase in the neutron lifetime.

The FBR and the SPR-I are both cylindrical in shape and have a cadmium shroud to pervent the return of thermal neutrons to the fuel assembly. Although the fuel of the FBR is enriched uranium with 10 weight percent molybdenum while enriched uranium metal is the fuel of the SPR-I, one can expect the same general behavior. Insight then can be gained as to the order of magnitude expected of the reflector time constants for the SPR-I assembly. Long's work serves as a basis for both the theoretical and experimental aspects of this paper and is referred to numerous times.

The time constants arising in Long's work could arise either as slowing down times in the reflector or as transit times for neutrons traveling from core to reflector and back. An experimental investigation of these time constants as a function of separation distance and thickness of the reflector would lead to isolation of the individual constants. This is the approach that is used in the present investigation. A reflector material has been chosen and systematically investigated for various geometrical configurations.

Theoretical Papers

The kinetic representation of a small unreflected burst reactor is quite simple. T. P. Wimett and John Orndoff [15] have presented what is now the common mathematical model to describe burst behavior. Their model is based on the assumptions that the space independent, single energy kinetics equations are valid and that the delayed neutron contribution can be ignored during the initial part of the burst. The validity and usefullness of the model has been demonstrated many times. However, in the presence of a reflector which can lend time constants to the system on the same order of magnitude as the reactor period, the validity of the model in this case becomes questionable.

The theoretical papers concerning space time dependence are quite numerous in the literature [46, 47, 48, 49, 50]. In most cases, however, the work is directed toward space time solutions which do not lend themselves readily to determination of the parameters of interest in this paper since the majority are concerned with a description of large thermal reactors. Very little theoretical work has been directed toward the space dependence of small burst reactors. The representation of a small assembly such as a Godiva type reactor is more straightforward than that for large thermal reactors. The reasons that little work has been directed toward the small system are that the model of Wimett has been adequate in most cases, and that the concern for the reflector induced perturbations has only recently manifested itself.

In a work primarily directed toward interpretation of the changes one might expect when the simple space independent model is replaced by a more sophisticated one, C. E. Cohn suggested a simple one energy group two region model. The regions were adjacent and each was assumed to have a characteristic prompt neutron lifetime. In Cohn's formulation, each region was to be described by a space independent kinetics model with source terms accounting for neutrons coming from the other region. For the fuel region, this is equivalent to treating the reflected neutrons as an additional delayed neutron group. Some of the more subtle space time effects have been ignored. The assumption of a two point kinetics model should, however, be well suited to the description of a burst reactor in the vicinity of a reflector. The description of a reflected burst reactor in terms of one energy group would not be realistic, especially in the case of a moderating reflector.

Calculation of the parameters in a small burst system could be handled by any one of numerous calculational techniques. The Carlson Sn method [57] has become a common tool for the description of a Godiva type reactor. To calculate various parameters in the system, one usually uses perturbation theory which is described quite well by Gordon E. Hansen and Clifford Maier [52]. To describe the behavior of a fast-thermal coupled system, however, too many energy groups would be necessary to describe the resulting neutron energy spectrum in the detail necessary. Hansen has indicated that an approach of this type would be unsatisfactory for the problem of this paper [39].

The Monte Carlo calculation techniques are well suited to calculation of neutron parameters. John T. Mihalczo and D. C. Irving [20] discuss the application of 05R general purpose Monte Carlo neutron transport code [43]. This IBM 7090 code requires 58 minutes to run 20,000 neutron histories for a Godiva I type geometry. This method is too time consuming to use for calculation of such quantities as the leakage neutron spectrum.

V. Benzi, et al, [44] have just recently published a Monte Carlo approach which considerably reduces computer time. This time savings arises from replacing the continuum of physical processes with a discrete set of possibilities. The ability of the code to describe spectrums in detail is, however, quite limited in its present form.

Related Topics

Of interest in this study is the mean lifetime of neutrons in a finite moderating geometry. To perform a detailed analysis of the effect of reflected neutrons on the burst characteristics of a reactor, knowledge of the energy spectrum of the reflector leakage neutrons and the mean time constant associated with reflected neutrons of a given energy is required. Pulse neutron experiments [53, 56] provide some insight as to the order of magnitudes of these time constants but fall far short of providing quantitative answers which can be used in the study of reflector effects. Most pulsed neutron work concerns the mean lifetime of neutrons in an infinite system. However, the primary concern of this paper is the lifetime of source energy neutrons to the cadmium cutoff energy in a very small system.

CHAPTER III

THEORETICAL DEVELOPMENT OF A SMALL REFLECTED REACTOR KINETICS MODEL

A model which may be used to describe the behavior of a reflected fast burst reactor is developed based on the following assumptions.

1. The single energy, point reactor kinetic equations are applicable to the unreflected core.
2. These equations can be extended to the case of a reflected reactor by the addition of a time dependent source term $\gamma_r R$ which represents the addition to the core of the reflected neutrons and their effectiveness in causing fission.

The validity of the first assumption has been substantiated many times for small fast reactors with no appreciable return of leakage neutrons to the core from a reflector.

The second assumption eliminates the cumbersome two-region multi-energy neutron transport equations which must otherwise be employed. Furthermore, this assumption permits one to describe the problem in terms of parameters which can be measured and which are familiar to workers in the field of reactor kinetics.

Consider the point reactor kinetic equations applicable to a sourceless, unreflected fuel assembly.

$$\frac{dn}{dt} = \frac{k(1 - \gamma\beta) - 1}{\ell} n + \sum_i \gamma_i \lambda_i C_i \tag{1}$$

$$\frac{dC_i}{dt} = \frac{\beta_i k}{\ell} n - \lambda_i C_i. \tag{2}$$

By assumption 2 the extension of these equations to the reflected core results in the following form for equation (1). The development is given in Appendix B.

$$\frac{dn}{dt} = \frac{k(1 - \gamma^* \beta^*) - 1}{\ell} n + \sum_i \gamma_i \lambda_i C_i + \gamma_r R \tag{3}$$

where γ_r = effectiveness of reflected neutrons in causing fission,

R = rate at which reflected neutrons are added to the core,

$$\gamma^* \beta^* = \sum_{i=1} \beta_i \gamma_i + \gamma_r \beta_r .$$

In order to describe the time dependent behavior of the term R, it is necessary to consider the time history of the reflected neutrons. The reflected neutrons originate as a result of fission within the fuel assembly with an average energy of 2 Mev. After undergoing, on the average, several collisions, the neutron may escape from the fuel assembly with a degraded energy. The mean lifetime of the neutron within the core is designated as ℓ and there are several ways in which one could represent this quantity. In view of the method of calculation which is described later, the following representation is employed.

$$\ell = \frac{\int_E \int_{\vec{\Omega}} \int_{\vec{r}} \ell(\vec{r}, \vec{\Omega}, E) \, S(\vec{r}, \vec{\Omega}, E) \, d\vec{r} \, d\vec{\Omega} \, dE}{\int_E \int_{\vec{\Omega}} \int_{\vec{r}} S(\vec{r}, \vec{\Omega}, E) \, d\vec{r} \, d\vec{\Omega} \, dE} \tag{4}$$

where

$\ell(\vec{r}, \vec{\Omega}, E)$ = the average lifetime of a fission neutron which appears with coordinates in $d\vec{r}$, $d\vec{\Omega}$, dE about $\vec{r}$, $\vec{\Omega}$, and E.

$s(\vec{r}, \vec{\Omega}, E)$ = the number of fission neutrons which appear with coordinates in $d\vec{r}$, $d\vec{\Omega}$, dE about $\vec{r}$, $\vec{\Omega}$, and E per volume, per unit solid angle per unit energy.

If the source function is assumed to be a separable function of $\vec{r}$, $\vec{\Omega}$, and E, $S(\vec{r}, \vec{\Omega}, E)$ can then be represented as follows:

$$S(\vec{r}, \vec{\Omega}, E) = S_{\vec{r}}(r)\, S_{\vec{\Omega}}(\vec{\Omega})\, S_E(E) \tag{5}$$

where

$S_{\vec{r}}(\vec{r})$ = the number of fission neutrons appearing in dr about $\vec{r}$ per unit volume which is simply the spatial fission distribution;

$S_{\vec{\Omega}}(\vec{\Omega})$ = the number of fission neutrons appearing in $d\vec{\Omega}$ about $\vec{\Omega}$ per unit solid angle. This is the angular distribution of the fission neutrons which for all practical cases is isotropic;

$S_E(E)$ = the number of fission neutrons appearing in dE about E per unit energy. Thus $S_E(E)$ is the fission energy spectrum.

Upon escape from the fuel the neutron must traverse the distance between the fuel assembly and is dependent upon the energy, location and direction of travel of the neutron upon escape from the fuel assembly. The mean value for τ_2 is given by:

$$\tau_2 = \frac{\int_E \int_{\vec{\Omega}} \int_{r_s} \bar{\tau}_2(\vec{r}, \vec{\Omega}, E)\, L(\vec{r}, \vec{\Omega}, E)\, P_{cr}(r, \vec{\Omega})\, dr_s\, d\vec{\Omega}\, dE}{\int_E \int_{\vec{\Omega}} \int_{r_s} L(\vec{r}, \vec{\Omega}, E)\, P_{cr}(\vec{r}, \vec{\Omega})\, dr_s\, d\vec{\Omega}\, dE} \qquad (6)$$

where

$\tau_2(\vec{r},\vec{\Omega}, E)$ = the time required for a neutron in $d\vec{r}$, $d\vec{\Omega}$, dE about $\vec{r}$, $\vec{\Omega}$, and E to travel from the fuel assembly to the reflector.

$L(\vec{r},\vec{\Omega}, E)$ = the number of leakage neutrons in $d\vec{r}$, $d\vec{\Omega}$, dE about $\vec{r}$, $\vec{\Omega}$, and E per unit surface area per unit solid angle per unit energy.

$P_{cr}(\vec{r},\vec{\Omega})$ = the probability that a neutron escaping from the fuel with coordinates $(\vec{r},\vec{\Omega})$ will arrive at the reflector.

dr_s = a unit of fuel surface located at $\vec{r}$.

$\int_{r_s}$ - integration over the surface of the fuel.

Since the leakage neutron spectrum from a fast burst fuel assembly is highly peaked in the Mev region, τ_2 is expected to be quite small compared to the other time constants which will be encountered. For this reason it is not necessary to investigate τ_2 and it is assumed that there is no spectral shift from the core to the reflector.

After reaching the reflector the neutrons may undergo scattering processes with the reflector nuclei and be further degraded in energy. The neutrons which avoid capture in the reflector ultimately escape with some energy E'. The mean time spent in the reflector by such neutrons is $\tau_3(E')$ which is dependent on the slowing down properties, the absorption and scattering cross sections and the geometrical configuration of the reflector. The technique which is used to calculate $\tau_3(E')$ requires the following representation.

$$\tau_3(E') = \frac{\int_E \int_{\vec{\Omega}} \int_{\vec{r}_r} \tau_3(\vec{r}, \vec{\Omega}, E, E') \, I(\vec{r}, \vec{\Omega}, E) \, dr_r \, d\vec{\Omega} \, dE}{\int_E \int_{\vec{\Omega}} \int_{\vec{r}_r} I(\vec{r}, \vec{\Omega}, E) \, dr_r \, d\vec{\Omega} \, dE} \tag{7}$$

where

$\tau_3(\vec{r}, \vec{\Omega}, E, E')$ = the mean residence time in the reflector of neutrons which enter the reflector with coordinates in dr_r, $d\vec{\Omega}$, dE about $\vec{r}$, $\vec{\Omega}$, E.

$I(\vec{r}, \vec{\Omega}, E)$ = the number of neutrons entering the reflector with coordinates in dr_r, $d\vec{\Omega}$, dE about $\vec{r}$, $\vec{\Omega}$, and E per unit surface area per unit solid angle per unit energy.

dr_r = a unit of reflector surface area located at $\vec{r}$.

$\int_{r_r}$ — integration over the surface of the reflector.

The neutron, if reflected in the direction of the fuel assembly, then traverses the distance between the fuel assembly and the reflector at the degraded energy E'. The time required to travel this distance is designated as τ_4 and can be represented as follows:

$$\tau_4 = \frac{\int\limits_E \int\limits_{\vec{\Omega}} \int\limits_{r_r} \tau_4^*(\vec{r}, \vec{\Omega}, E)\, L_r(\vec{r}, \vec{\Omega}, E)\, P_{rc}(\vec{r}, \vec{\Omega})\, dr_r\, d\vec{\Omega}\, dE}{\int\limits_E \int\limits_{\vec{\Omega}} \int\limits_{r_r} L_r(\vec{r}, \vec{\Omega}, E)\, P_{rc}(\vec{r}, \vec{\Omega})\, dr_r\, d\vec{\Omega}\, dE} \tag{8}$$

where

$\tau_4^*(\vec{r}, \vec{\Omega}, E)$ = the time required for a neutron with coordinates in dr_r, $d\vec{\Omega}$, dE about $\vec{r}$, $\vec{\Omega}$, E to travel from the reflector to the fuel assembly.

$L_r(\vec{r}, \vec{\Omega}, E)$ = the number of neutrons escaping from the reflector with coordinates in dr_r, $d\vec{\Omega}$, dE about $\vec{r}$, $\vec{\Omega}$, and E per unit surface area per unit solid angle per unit energy.

$P_{rc}(\vec{r}, \vec{\Omega})$ = the probability that a neutron escaping from the reflector with coordinates $\vec{r}$, $\vec{\Omega}$ will reach the fuel assembly.

In order to facilitate the incorporation of τ_4 into the reflected kinetic equations, let τ_4^* and L_r be functions separable in space and energy. That is,

$$\tau_4^*(\vec{r}, \vec{\Omega}, E) = g(E)\, h(\vec{r}, \vec{\Omega}) \tag{9}$$

$$L_r(\vec{r}, \vec{\Omega}, E) = G(E)\, H(\vec{r}, \vec{\Omega}) . \tag{10}$$

Under these assumptions of separability τ_4 can be expressed as the product of an energy dependent function and a geometrical factor .

$$\tau_4 = \frac{\int_E \int_{\vec{\Omega}} \int_{r_r} g(E)\, h(\vec{r}, \vec{\Omega})\, G(E)\, H(\vec{r}, \vec{\Omega})\, P_{rc}(\vec{r}, \vec{\Omega})\, dr_r\, d\vec{\Omega}\, dE}{\int_E \int_{\vec{\Omega}} \int_{r_r} G(E)\, H(\vec{r}, \vec{\Omega})\, P_{rc}(\vec{r}, \vec{\Omega})\, dr_r\, d\vec{\Omega}\, dE}$$

or

$$\tau_4 = J \frac{\int_E g(E)\, G(E)\, dE}{\int_E G(E)\, dE} \qquad (11)$$

where

$$J = \frac{\int_{\vec{\Omega}} \int_{r_r} h(\vec{r}, \vec{\Omega})\, H(\vec{r}, \vec{\Omega})\, P_{rc}(\vec{r}, \vec{\Omega})\, dr_r\, d\vec{\Omega}}{\int_{\vec{\Omega}} \int_{r_r} H(\vec{r}, \vec{\Omega})\, P_{rc}(\vec{r}, \vec{\Omega})\, dr_r\, d\vec{\Omega}} \qquad (12)$$

For reasons which will become apparent later, the reflected neutron energy spectrum is divided into N - M distinct energy groups where M is defined as the number of delayed neutron groups which represent the bare reactor.

Let

$$\int_E g'(E)\, dE = \frac{\int_E g(E)\, G(E)\, dE}{\int_E G(E)\, dE} \qquad (13)$$

Then τ_{4_j} can be written as

$$\tau_{4_j} \quad = \quad J \int_{E_{j-1}}^{E_j} g'(E)\, dE \qquad\qquad j = M+1 \text{ to } N . \qquad (14)$$

After traversing the distance between the reflector and the fuel the neutrons re-enter the fuel assembly and are either absorbed or escape from the fuel again. The mean lifetime of these neutrons in the fuel is designated as τ_5 and is related to the relative effectiveness of the reflected neutrons causing fission.

To proceed with the representation of the time behavior of the rate term R, the following additional definitions are required.

L_c = the fraction of the neutrons produced in the core which ultimately escape from the core.

f_1 = the fraction of leakage neutrons from the core which enter the reflector.

L_j = the fraction of the neutrons entering the reflector which escape with energies in the j^{th} energy group.

f_{2_j} = the fraction of the j^{th} energy group neutrons escaping from the reflector which re-enter the core.

C'_j = the concentration of source energy neutrons in the reflector which ultimately appear as leakage neutrons of the j^{th} energy group.

The formal definitions of L_c, f_1, L_j, and f_{2_j} in terms of previously defined terms are as follows:

$$L_c = \frac{\int_E \int_{\vec{\Omega}} \int_{r_s} L(\vec{r}, \vec{\Omega}, E)\, dr_s\, d\vec{\Omega}\, dE}{\int_E \int_{\vec{\Omega}} \int_{\vec{r}} S(\vec{r}, \vec{\Omega}, E)\, d\vec{r}'\, d\vec{\Omega}\, dE} \tag{15}$$

$$f_1 = \frac{\int_E \int_{\vec{\Omega}} \int_{r_s} L(\vec{r}, \vec{\Omega}, E)\, P_{cr}(\vec{r}, \vec{\Omega})\, dr_s\, d\vec{\Omega}\, dE}{\int_E \int_{\vec{\Omega}} \int_{r_s} L(\vec{r}, \vec{\Omega}, E)\, dr_s\, d\vec{\Omega}\, dE} \tag{16}$$

$$L_j = \frac{\int_{r_r} \int_{\vec{\Omega}} \int_{E_{j-1}}^{E_j} L_r(\vec{r}, \vec{\Omega}, E)\, dr_r\, d\vec{\Omega}\, dE}{\int_{r_r} \int_{\vec{\Omega}} \int_{E} L(\vec{r}, \vec{\Omega}, E)\, P_{cr}(\vec{r}, \vec{\Omega})\, dr_r\, d\vec{\Omega}\, dE} \tag{17}$$

$$f_{2_j} = \frac{\int_{r_r} \int_{\vec{\Omega}} \int_{E_{j-1}}^{E_j} L_r(\vec{r}, \vec{\Omega}, E)\, P_{rc}(\vec{r}, \vec{\Omega})\, dr_r\, d\vec{\Omega}\, dE}{\int_{r_r} \int_{\vec{\Omega}} \int_{E_{j-1}}^{E_j} L_r(\vec{r}, \vec{\Omega}, E)\, dr_r\, d\vec{\Omega}\, dE} \tag{18}$$

The rate term $\gamma_r R$ can be represented as a summation of all the neutrons returned to the core weighted by the effectiveness in causing fission.

$$\gamma_r R = \sum_j R_j \gamma_j \qquad j = M+1 \text{ to } N \tag{19}$$

Where R_j is the number of neutrons returned to the core per unit time which are of the j^{th} energy group and γ_j is the effectiveness of the j^{th} group neutrons in causing fission.

Since the rate at which neutrons of the j^{th} energy group escape from the reflector is C_j' divided by the mean residence time of the j^{th} energy group neutrons in the reflector τ_{3_j}, the time dependent behavior of R_j is given by

$$R_j(t) = f_{2_j} \frac{C_j'(t-\tau_{4_j})}{\tau_{3_j}} \tag{20}$$

where

$C_j'(t-\tau_{4_j})$ is $C_j'(t)$ at time $t-\tau_{4_j}$.

The equations describing the kinetic behavior of the reflected core are then

$$\frac{dn(t)}{dt} = \frac{k(1-\gamma^* \beta^*)-1}{\ell} n(t) + \sum_i \gamma_i \lambda_i C_i(t) + \sum \frac{\gamma_j f_{2_j} C_j'(t-\tau_{4_j})}{\tau_{3_j}} \tag{21}$$

$$\frac{dC_i(t)}{dt} = \frac{\beta_i k}{\ell} n(t) - \lambda_i C_i(t) \qquad i=1, M \tag{22}$$

$$\frac{dC_j'(t)}{dt} = L_j f_1 L_c k \frac{n(t - \tau_2)}{\tau_{3_j}} - \frac{C_j(t)}{\tau_{3_j}}; \quad j = M+1, N \tag{23}$$

where $n(t - \tau_2)$ is the neutron level in the core at time $t - \tau_2$.

Consider first the steady state critical conditions

$$\begin{aligned} \frac{dn}{dt} &= 0 \\ \frac{dC_i}{dt} &= 0 \qquad i = 1, M \\ \frac{dC_j}{dt} &= 0 \qquad j = M+1, N \\ k &= 1 \end{aligned} \tag{24}$$

Under these conditions, equation (21) becomes

$$0 = (1 - \sum \gamma_i\beta_i - \gamma_r\beta_r - 1)\frac{n}{\ell} + \sum \gamma_i\beta_i \frac{n}{\ell} + \sum \gamma_j f_{2_j} L_j f_1 L_c \frac{n}{\ell} \tag{25}$$

or

$$\gamma_r\beta_r = \sum_j \gamma_j f_{2_j} L_j f_1 L_c = \sum_j \gamma_j \beta_j \tag{26}$$

where

$$\beta_j = f_{2_j} L_j f_1 L_c \tag{27}$$

Then, if

$$C_j = f_{2_j} C_j' , \tag{28}$$

the kinetic equations then become,

$$\frac{dn(t)}{dt} = \frac{k(1 - \gamma^*\beta^*) - 1}{\ell} n(t) + \sum \gamma_i \lambda_i C_i(t) + \sum \gamma_j \frac{C_j(t - \tau_{4_j})}{\tau_{3_j}} \qquad (29)$$

$$\frac{dC_i(t)}{dt} = \frac{k\beta_i n(t)}{\ell} - \lambda_i C_i(t) \qquad i = 1, M \qquad (30)$$

$$\frac{dC_j(t)}{dt} = \beta_j \frac{k}{\ell} n(t - \tau_2) - \frac{C_j(t)}{\tau_{3_j}} \qquad j = M + 1, N \qquad (31)$$

$$\gamma_r \beta_r = \sum \gamma_j \beta_j \qquad (32)$$

The reason for the definitions above now becomes apparent. Except for the lag time dependence, the terms accounting for the reflected neutrons have the characteristics of additional delayed neutron groups. This is a more convenient form because many solutions applicable to the bare reactor case may be carried over to the reflected model. Furthermore, the new terms which are introduced to the bare reactor model can be calculated using experimentally determined quantities.

It is of interest to find the solution of this set of linear differential equations for the special case where the neutron level is increasing with a constant period T. For this case, the solutions for C_i and C_j become:

$$C_i(t) = \frac{k\beta_i n(t)}{\ell\left(\frac{1}{T} + \lambda_i\right)} \qquad i = 1, M \qquad (33)$$

$$C_j(t) = \frac{k\beta_j n e^{-\frac{\tau_2}{T}}}{\ell\left(\frac{1}{T} + \frac{1}{\tau_{3_j}}\right)} \qquad j = M+1, N \qquad (34)$$

The integration is given in Appendix C. Substitution into equation (21) yields

$$\rho = \frac{\ell^*}{T} + \sum_i \frac{\gamma_i \beta_i}{1 + \lambda_i T} + \sum \gamma_j \beta_j \frac{\frac{\tau_{3_j}}{T} + 1 - e^{-\frac{\tau_2 + \tau_{4_j}}{T}}}{\frac{\tau_{3_j}}{T} + 1} \qquad (35)$$

where $\ell^* = \dfrac{\ell}{k}$. $\rho = \dfrac{k-1}{k}$

$$\rho(\$) = \frac{\ell^*}{\gamma\beta T} + \sum \frac{f_i}{1 + \lambda_i T} + \sum_j f_j \frac{\frac{\tau_{3_j}}{T} + 1 - e^{-\frac{\tau_2 + \tau_{4_j}}{T}}}{\frac{\tau_{3_j}}{T} + 1} \qquad (36)$$

where $\rho(\$) = \dfrac{\rho}{\gamma\beta}$ (37)

$$f_i = \frac{\gamma_i \beta_i}{\gamma\beta} \qquad (38)$$

$$f_j = \frac{\gamma_j \beta_j}{\gamma\beta} \qquad (39)$$

$$\gamma\beta = \sum_i \gamma_i \beta_i \tag{40}$$

One dollar is defined as that amount of reactivity which makes the reactor prompt critical and when expressed in terms of reactivity is equal to $\sum_i \gamma_i \beta_i$.

Equation (35) is the "inhour" equation for the reflected reactor and differs from the familiar inhour equation for a bare core only by the last term. It is to be noted that all of the previous definitions of the bare reactor parameters are preserved.

Application of Reflected Kinetic Model To A Godiva-Type Reactor

The effect of a reflector on the kinetics of a burst reactor depends on the relative magnitudes of the bare reactor parameters and the reflector parameters. The bare reactor parameters are fixed quantities for a given fuel assembly but the reflector parameters can vary widely since the reflector parameters are functions of the material of the reflector and the geometrical configuration of both the fuel assembly and the reflector. A moderating reflector has a much softer leakage spectrum than would a heavy non-moderating reflector which implies that the transit time τ_{4_j} would be more important for the moderating material.

A Godiva-type reactor has a prompt neutron lifetime on the order of 7×10^{-9} seconds [15]. The total fraction of delayed neutrons is approximately 6.6×10^{-3} and the shortest lived precursor group has a mean lifetime of approximately 0.264 seconds [16]. Using the results of the experimental work performed by R. L. Long [3], one estimates the time constants τ_3

and τ_4, of a moderating reflector to be on the order of 10^{-6} to 10^{-5} seconds. This number corresponds to the velocity of neutrons having energies above but near the cadmium cutoff. Time constants longer than this would be expected only for greater spacing between the core and the reflector than the 5 to 10 centimeter spacing of Long's experiment, since neutrons with energies below the cadmium cutoff would be unable to penetrate the cadmium shroud of the core and enter the fuel. In Appendix B it is shown that $\gamma_r \beta_r$ can be no greater than the measured worth of the reflector.

These parameters may be used as a guide to investigate the reflected inhour equation for various ranges of reactivity addition.

Small Reactivity Addition

Most reactivity measurements are made under conditions near delayed critical. The resulting periods in such cases are rarely less than 5 seconds. For periods greater than 5 seconds, two approximations can be made. These are:

$$\frac{\tau_{3_j}}{T} + 1 \simeq 1, \qquad j = M + 1 \text{ to } N$$

and

$$1 - e^{-\frac{\tau_2 + \tau_{4_j}}{T}} \simeq \frac{\tau_2 + \tau_{4_j}}{T}$$

The resulting reflected "inhour" equation is given by

$$\rho = \frac{\ell^*}{T} + \frac{1}{T} \sum_j (\tau_{3_j} + \tau_2 + \tau_{4_j}) \gamma_j \beta_j + \sum_i \frac{\gamma_i \beta_i}{1 + \lambda_i T} \tag{41}$$

or in "Dollar" notation as

$$\rho(\$) = \frac{\ell^*}{\gamma\beta T} + \frac{1}{\gamma\beta T} \sum_j (\tau_{3_j} + \tau_2 + \tau_{4_j}) \gamma_j \beta_j + \sum_i \frac{f_i}{1 + \lambda_i T} \tag{42}$$

For small reactivity additions, the observed effect of the reflected neutrons is an apparent change in prompt neutron lifetime, where the "new" lifetime is given by

$$\ell^*_r = \ell^* + \sum (\tau_{3_j} + \tau_2 + \tau_{4_j}) \gamma_j \beta_j . \tag{43}$$

For values of the parameters given above, ℓ^*_r is less than 10^{-6} seconds. The term $\frac{\ell^*_r}{T}$ can be shown to be negligible as compared to $\sum_1^6 \frac{f_i}{1 + \lambda_i T}$

for periods greater than or equal to 1 sec and the reflected inhour equation then becomes

$$\rho(\$) = \sum_i \frac{f_i}{1+ \lambda_i T} \tag{44}$$

which is identical to the "bare" inhour equation. This implies that period measurement made on the reflected assembly can be related to reactivity by use of the bare reactor kinetic parameters providing that the periods measured are relatively large as compared to ℓ^*_r.

Large Reactivity Addition

For larger reactivity insertions such that the resulting period is much shorter than the shortest time constant of the delayed neutron groups, the term $\lambda_i T + 1$ approaches unity. In this case the inhour relation becomes

$$\rho(\$) = \frac{\ell^*}{\gamma\beta T} + \sum f_i + \sum f_j \frac{\frac{\tau_{3_j}}{T} + 1 - e^{-\frac{\tau_2 + \tau_{4_j}}{T}}}{\frac{\tau_{3_j}}{T} + 1} \tag{45}$$

or

$$\rho_P(\$) = \frac{\ell^*}{\gamma\beta T} + \sum_j \frac{\frac{\tau_{3_j}}{T} + 1 - e^{-\frac{\tau_2 + \tau_{4_j}}{T}}}{\frac{\tau_{3_j}}{T} + 1} f_j \tag{46}$$

where $\rho_P(\$) = \rho(\$) - 1$ (47)

The periods that result at or near prompt critical conditions are on the order of 10^{-4} to 10^{-3} seconds. If the time constants τ_{3_j}, τ_2 and τ_{4_j} are on the order of 10^{-6} seconds less, equation (46) can be approximated by

$$\rho_P(\$) \simeq \frac{\ell^*}{\gamma\beta T} + \sum_j \left(\frac{\tau_{3_j} + \tau_2 + \tau_{4_j}}{T} \right) f_j \tag{48}$$

or

$$\rho_P(\$) \simeq \frac{\ell^*}{\gamma \beta T} \tag{49}$$

Thus, there would exist a linear relationship between prompt reactivity and reciprocal period for reactivity insertions near prompt critical. The results of R. L. Long's experiments indicated this linear relationship. One would therefore conclude that the reflector time constants encountered in his experiments were small as compared to the reactor period. In the case of metallic reflectors, the spectrum was undoubtedly "hard" and the important time constants were correspondingly small. The moderating materials apparently were too close to the core for the transit time to be large enough to cause a deviation from the linear relation.

As to whether this linearity persists for periods on the order of 10^{-5} seconds depends on the parameters τ_{3_j}, τ_2 and τ_{4_j}. Furthermore, if the parameters f_j are quite small, the effect of the reflected neutrons would not be observed in an experimental investigation. The region of large reactivity insertion is of special interest for it is a region in which the prompt neutron decay constant can be determined. The definition of prompt neutron decay constant at delayed critical is given as

$$a_{r_{DC}} = \frac{\gamma\beta}{\Lambda}$$

where Λ is the lifetime of neutrons in the entire system.

The prompt neutron decay constant for a reflected system can be a constant only if the approximations leading to equation (48) are valid. One concludes that the prompt neutron decay constant measured in the region of large reactivity insertion has meaning in the usual sense only if the reflector time constants are quite small as compared to the reactor period.

For reactor periods much less than the reflector time constants,

$$\lim_{\text{as } T \to o} \sum \frac{\frac{\tau_{3_j}}{T} + 1 - e^{-\frac{\tau_2 + \tau_{4_j}}{T}}}{\frac{\tau_{3_j}}{T} + 1} f_j \tag{50}$$

$$= \sum_j f_j = f_r \tag{51}$$

and

$$\rho(\$) = \frac{\ell^*}{\gamma\beta T} + f_r \sum_i \frac{f_i}{1+\lambda_i T} \tag{52}$$

or

$$\rho(\$) - f_r = \frac{\ell^*}{\gamma\beta T} + \sum_i \frac{f_i}{1+\lambda_i T} \tag{53}$$

The right side of equation (53) is identical to the bare reactor inhour relation. If one were using the normal delayed neutron parameters to describe the kinetics of a reflected reactor, the value of the dollar would appear to have changed. It would not be necessary for the time constants of all the reflected groups to be larger than the reactor period before this discrepancy appeared. Any group j with such a time constant and a measurable f_j would change the apparent value of the dollar. For example, suppose that the τ_4 of one energy group of reflected neutrons is large compared to T. Let this ~~be~~ the k^{th} energy group. Then

$$\rho_P(\$) \simeq \frac{\ell^*}{\gamma\beta T} + \sum_{j \neq k} \frac{\frac{\tau_{3_j}}{T} + 1 - e^{-\frac{\tau_2 + \tau_{4_j}}{T}}}{\frac{\tau_{3_j}}{T} + 1} f_j + f_k \tag{54}$$

or

$$\rho_P(\$) - f_k \simeq \frac{\ell^*}{\gamma\,\beta\,T} + \sum_{j \neq k} \frac{\frac{\tau_{3_j}}{T} + 1 - e^{-\frac{\tau_2 + \tau_{4_j}}{T}}}{\frac{\tau_{3_j}}{T} + 1} f_j \tag{55}$$

Furthermore, if τ_{3_j}, τ_2 and τ_{4_j} are all small compared to T for all j except $j = k$

$$\rho_P\,(\$) - f_k \simeq \frac{\ell^*}{\gamma\beta T} \quad \frac{1}{T} \sum_{j \neq k} (\tau_{3_j} + \tau_2 + \tau_{4_j})\, f_j \tag{56}$$

The effect would then manifest itself as an apparent change in both the neutron lifetime and the value of a dollar.

Another interesting feature associated with reflector time constants which are large is the possibility of decoupling the reactor from the reflector. If the approximations leading to equation (53) are met, then the burst characteristics of the reflected assembly should revert to the bare case. This effect can be achieved by positioning the reflector at such a distance that $\tau_{4_j} >> T$, $j = M + 1, N$. Under this condition equation (53) becomes

$$\rho_P(\$) = \frac{\ell^*}{\gamma\beta T} + f_r. \tag{57}$$

With the exception of the amount of reactivity required for a given initial period, all yield, burst width, and initial period relations revert to the relations of the bare core.

A technique which is used to determine the worth of a burst rod* is

* A burst rod is a movable fuel component normally having two static positions; either fully withdrawn from the system or fully inserted. In general a burst is initiated by the rapid insertion of the burst rod.

to plot prompt reactivity as a function of reciprocal period and to define prompt critical as that reactivity at which the resulting curve intercepts the abscissa. The displacement of this intercept upon addition of reflector may be interpreted as a change in the worth of the burst rod as indicated by equation (57).

Verification of the Small Reflected Reactor Kinetic Model

Several aspects of the reflected kinetic model developed in the preceding section may be implied with experimental data obtained by R. L. Long using the FBR [3]. The linear relationship between $\rho_p(\$)$ and $\frac{1}{T}$ was seen to apply for the non-moderating reflectors he used. The non-moderating reflectors led to small time constants compared to the reactor periods encountered and hence the conditions of equation (49) were met. The moderating materials were apparently near enough to the core that the transit times were small and again equation (49) applied. Taking 1 ev as the minimum energy of the reflected neutrons penetrating the cadmium shroud and 5 cm as the gap between reflector and core, one estimates a time constant on the order of 10^{-6} seconds.

In order to generate experimental data to accurately verify the reflected kinetic model, an experimental arrangement was chosen in the present investigation to emphasize the differences between the reflected and non-reflected assemblies. To insure that the greatest reflector effect exists, a moderating material was chosen as the primary reflector material to be investigated. A geometry was chosen that would be easy to describe analytically.

The various quantities defined in the development of the small reflected reactor kinetic model were calculated by Monte Carlo techniques. These calculations were performed using parameters of the SPR-I fuel assembly and of the particular reflector material chosen. The results of these calculations were inserted into the reflected inhour equation and the resulting relations were compared with experiment. The determination of the reflector parameters and the investigation of the reflected inhour equation was accomplished using the Control Data Corporation 3600 digital computer. An experimental investigation of the effect of the moderating material on the burst behavior was undertaken. Various geometrical configurations were investigated and the results compared with those predicted by the reflected kinetic model.

CHAPTER IV

CALCULATION OF THE REFLECTED GROUP PARAMETERS

Determination of the parameters γ_j, β_j, τ_{3_j}, τ_2, and τ_{4_j} can be achieved through various techniques common to reactor calculations. Each of the techniques possesses some advantages, but there are also distinct disadvantages. The more common approach to problems of this type would be to employ perturbation theory in conjunction with diffusion theory or some other approximation to the more rigorous Boltzman transport theory. Regardless of the model, this approach would require approximations other than those inherent in the model in order to arrive at a representation suitable for this study. Since the time constants and fractions discussed in the theoretical section have such a strong energy dependence, a multi-energy group diffusion model would require a relatively large number of groups. In addition to being cumbersome, a model of this type would require an exorbitant amount of computer time to arrive at suitably detailed neutron energy spectrums.

A more direct method is the Monte Carlo technique which is, in fact, a computer simulation of the physical neutron processes. The parameters of the reflected model are particularly suited to Monte Carlo calculations. This is evident in the form of the parameters which consist of either probability functions or mean lifetimes. The disadvantage of the Monte Carlo technique is that it can also require a large amount of computer time. The time consumed is not, however, directly proportional to the degree of rigor desired and certain simple and reasonable approximations can be made which greatly reduce the computer time required.

After weighing the advantages and disadvantages of the various techniques, it was decided that the Monte Carlo technique offered the greatest chance of success. This decision was aided by the presence of the high speed Control Data 3600 digital computer available at Sandia Laboratory. A brief description of the computer code and the approximations used is given in Appendix D. G. E. Hansen [39] has since supported the Monte Carlo approach as the preferred calculational method.

Calculation of Bare Reactor Parameters

The kinetic parameters of a bare system are generally well known for a given reactor, and when available, measured values were used in the calculations of this paper.

However several calculations of parameters pertaining to the bare assembly were performed in order to verify the Monte Carlo computer code used in calculating reflector parameters such as neutron effectiveness. In addition it was necessary to determine the energy distribution of the neutrons escaping from the fuel assembly in order to provide an energy dependent source term for the reflector calculations. A brief description of several of the parameter calculations is given.

Spatial Fission Distribution in the Fuel Assembly

The source term $S(\vec{r}, \vec{\Omega}, E)$ is given in equation (5) of the theoretical section. The Rosen-Cranberg fission energy spectrum [58] was used for the energy distribution of the fission neutrons. Although this distribution was measured for thermally induced fission, Grundl and Usner have indicated that this representation is applicable to a Godiva type reactor [10]. The angular distribution of the fission neutrons was assumed isotropic. The angular distribution is very slightly peaked in the direction of the incident neutron but the over-all effect is negligible.

The spatial distribution was calculated by iteration techniques. Two programs were used: the first assumed initially a uniform spatial distribution and the second assumed a spatial distribution inversely proportional to distance from the center in both axial and radial directions. The convergence required several runs; and the results and statistical variations are shown in Figure 1. The calculated distribution is seen to compare reasonably well with the measured flux distribution.

The reflector perturbation of the core spatial neutron distribution was assumed negligible. Since the percent of neutrons returned to the core is approximately 1 percent, any error introduced would be less than 1 percent. Figure 31 shows that the reflected neutrons do not appreciably alter the flux distribution in the core.

The mean lifetime of the neutrons in the bare fuel assembly is a function of the spatial, energy, and angular distributions of the neutrons at the time of fission. The average lifetime of neutrons in the dE, $d\vec{\Omega}$, $d\vec{r}$ interval of phase space is an inseparable function of energy, direction, and position of the neutrons. The Monte Carlo calculation of the neutron lifetime in the core consists of observing the time history of the source neutrons in a range ΔE, $\Delta\vec{\Omega}$, $\Delta\vec{r}$ about $(E, \vec{\Omega}, \vec{r})$ for the range of possible values of E, $\vec{\Omega}$, and $\vec{r}$. The distribution function for the source neutrons was $S(\vec{r}, \vec{\Omega}, E)$ given in equation (5).

The mean lifetime of the neutrons in the fuel assembly was then obtained by summing the time between all neutron interaction for all interactions occurring between fission and loss of the neutrons and dividing by the number of neutrons considered. The time between interactions was obtained by dividing the distance between interactions by the velocity corresponding to the energy possessed by the neutron. The prompt neutron lifetime in the core was calculated to be 5.36×10^{-9} seconds. While this lifetime is somewhat less than the experimentally determined value given in Chapter 6, it serves as a check of the Monte Carlo code. Where

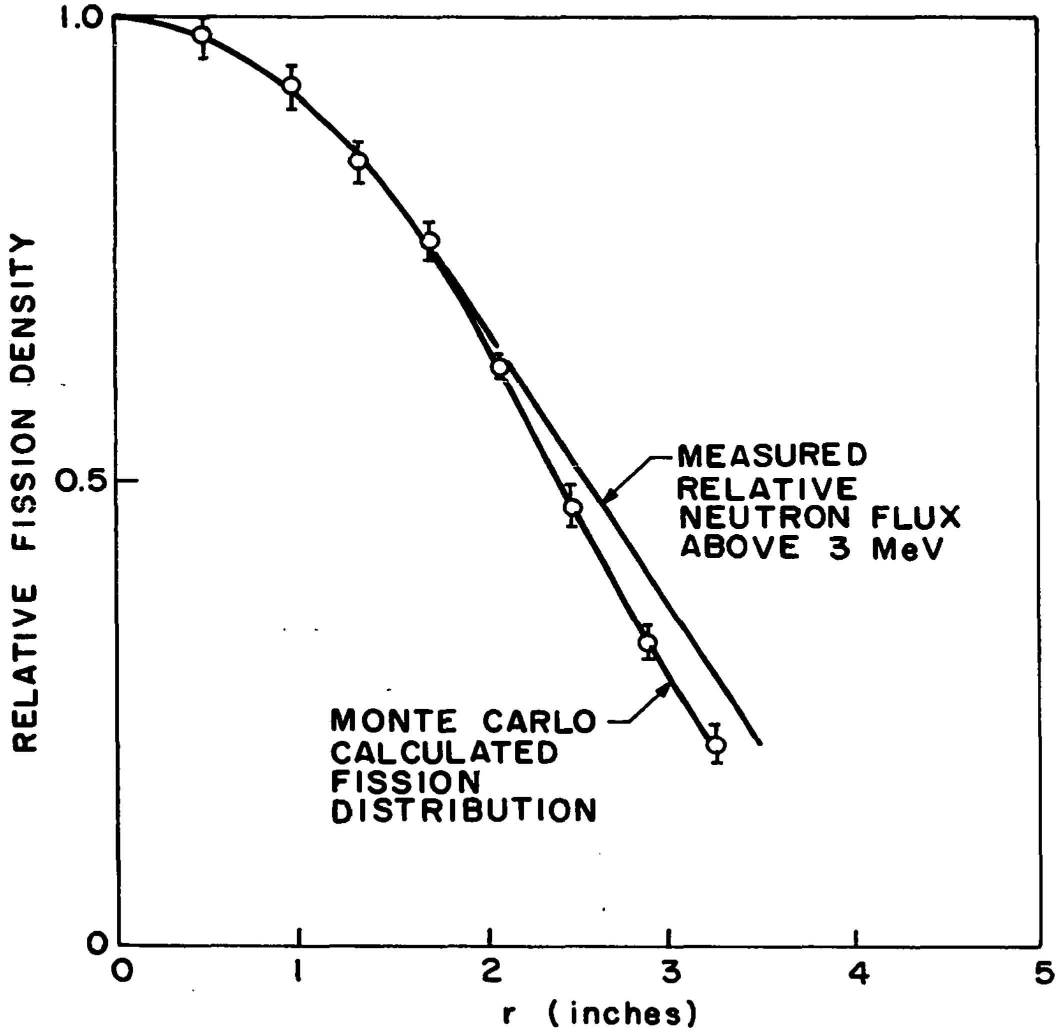

Monte Carlo calculated radial fission distribution in fuel

Figure 1

the lifetime is required for further calculations, the experimentally determined value has been used.

Multiplication Factor

The multiplication factor of the reactor is obtained as a natural consequence of the lifetime calculation. As each neutron is absorbed, the code adds the average number of neutrons produced per absorption at that energy to an accumulator. After the run the multiplication factor is calculated by dividing the total number of neutrons produced by the number of source neutrons used in the run. The value of k calculated for the SPR-I geometry was 1.0024 ± 0.002.

Fuel Assembly Leakage Spectrum

The leakage spectrum was obtained simultaneously with the other group which leaked from the system. The results of the calculated neutron leakage energy spectrum are shown in Figure 2 together with the measured leakage spectrum of the Godiva I reactor [40] and the fission neutron energy spectrum used as the neutron source energy [55] of the calculation. . It may be seen that the calculated and measured values agree very well and both represent a much softer energy spectrum than the fission spectrum. This represents an excellent test of the computer code since Godiva I and SPR I are essentially identical. Runs were made to compare the energy spectrum of side leakage with end leakage but no difference outside the limits of statistical variation was noted.

Calculation of the Reflector Group Parameters

In order for the small reflected model to be a useful tool to determine the burst behavior of a pulse reactor, the calculation of the reflector parameters must be reasonably simple and straightforward. A

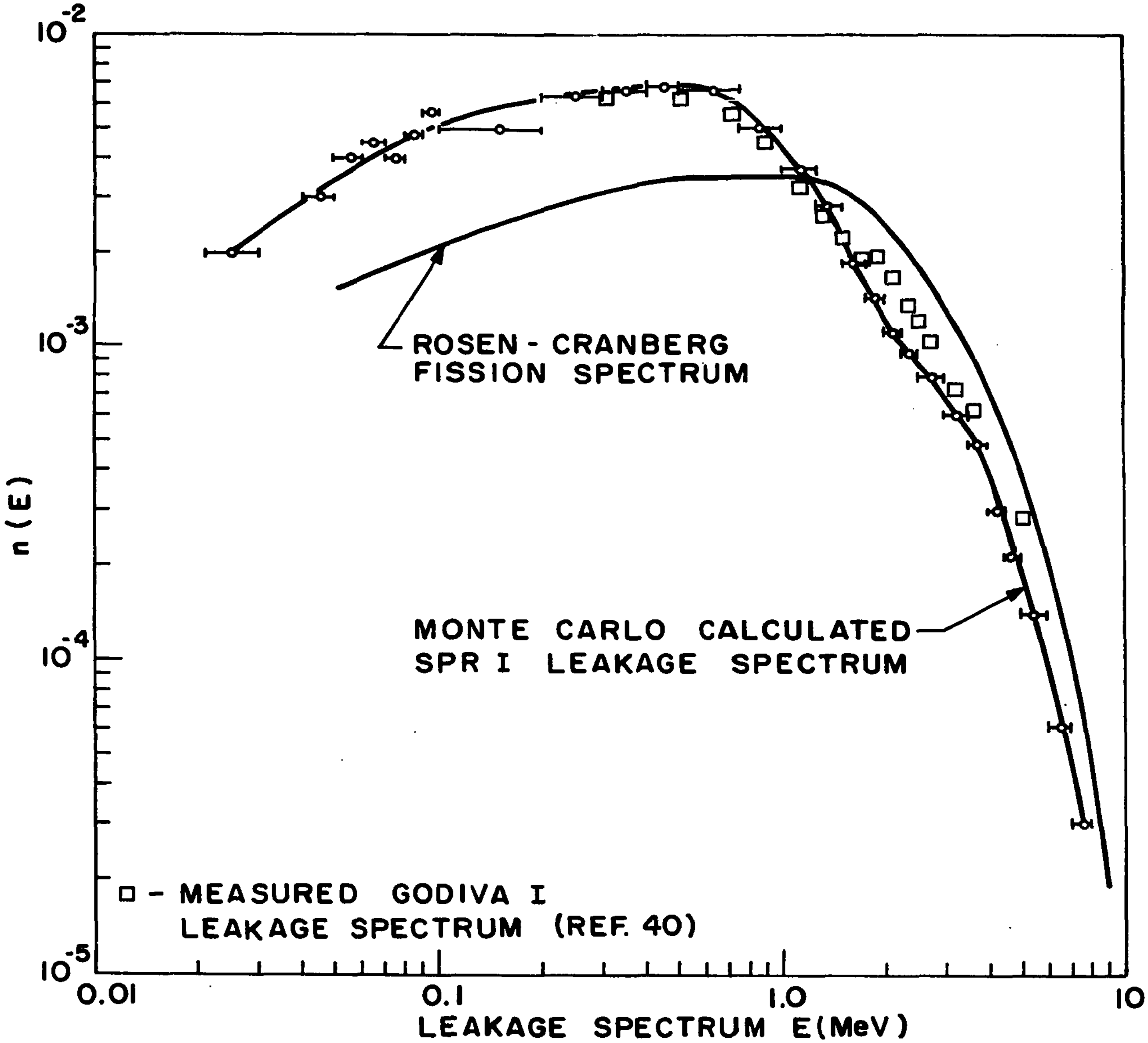

Monte Carlo calculated leakage spectrum for SPR-I geometry

Figure 2

rigorous integration of the complicated spatial, angle, and energy dependent formal definitions would defeat the purpose of the model. However, if the assumption is made that the energy dependence of the functions used in the formal definitions is separable from the geometric dependence, a useful set of equations results. The validity of this assumption is readily tested by experiment.

jth Reflector Group Effective Fraction

The fraction $\gamma_j\beta_j$ defined by equation (27) depends on the energy and geometrical coordinates of the neutrons. The formal definitions of L_c, f_1, L_j and f_2 are given in the theoretical section and from Appendix A we know that $\gamma_r\beta_r$ is equal to the measured worth of the reflector. Hence, from equation (26) we have :

$$\sum_j \gamma_j f_{2_j} L_j f_1 L_c = W$$

where W is defined as the measured worth of the reflector.

The term f_{2_j} is defined by equation (18). The function $L_r(\vec{r},\vec{\Omega}, E)$ used in the definition is a function of energy of the neutron and the spatial coordinates of the reflector. One would expect, for example, that the energy spectrum of the neutrons escaping from the exterior reflector surface would be somewhat different from the spectrum of the neutrons escaping from the interior surface. An internal surface is defined as one whose outwardly directed normal has a component in the direction of the fuel and an external reflector surface as one whose outwardly directed normal has no component in the direction of the fuel.

Since $P_{rc}(\vec{r}, \vec{\Omega})$ is zero for all surfaces whose outwardly directed normal has no component in the direction of the core, the integration of equation (18) over all surfaces yields:

$$f_{2_j} = \frac{\int_{r'_r} \int_{\vec{\Omega}} \int_{E_{j-1}}^{E_j} L_r(\vec{r}, \vec{\Omega}, E)\, P_{rc}(\vec{r}, \vec{\Omega})\, dr_r\, d\vec{\Omega},\, dE}{\int_{r'_r} \int_{\vec{\Omega}} \int_{E_{j-1}}^{E_j} L_r(\vec{r}, \vec{\Omega}, E)\, dE} \,. \tag{58}$$

where $\int_{r'_r}$ represents integration over interior surfaces only.

By assuming that the energy dependence can be separated from the spatial coordinates for all interior surfaces, L_r can be expressed for all interior surfaces as:

$$L_r(\vec{r}, \vec{\Omega}, E) = H(\vec{r}, \vec{\Omega})\, G(E).$$

This is equation (10) of the theoretical section. For all j groups f_{2_j} can then be expressed as

$$f_{2_j} = K,$$

$$K = \frac{\int_{r'_r} \int_{\vec{\Omega}} H(\vec{r}, \vec{\Omega})\, P_{rc}(\vec{r}, \vec{\Omega})}{\int_{r'_r} \int_{\vec{\Omega}} H(\vec{r}, \vec{\Omega})\, dr_r}\, d\vec{\Omega}\, dr_r. \tag{59}$$

By the preceding assumption, we can represent equation (26) by:

$$\sum_j \gamma_j K L_j f_1 L_c = W. \tag{60}$$

The terms K, f_1 and L_c are all independent of the reflected group neutron energies and can be removed from the summation. Hence,

$$L_c f_1 K = \frac{W}{\sum_j \gamma_j L_j} \tag{61}$$

β_j is defined by equation (27) as

$$\beta_j = L_j f_1 L_c f_{2_j}$$

or in terms of W

$$\beta_j = \frac{W L_j}{\sum_j \gamma_j L_j} \tag{62}$$

The combining of equations (17), (10), and (62) yields

$$\beta_j = W \frac{\int_{E_{j-1}}^{E_j} G(E)dE}{\sum_j \gamma_j \int_{E_{j-1}}^{E_j} G(E)dE} \tag{63}$$

which can be expressed as

$$\beta_j = \frac{W L_j^*}{\sum \gamma_j L_j^*}, \tag{64}$$

$$L_j^* = \frac{\displaystyle\int_{E_{j-1}}^{E_j} G(E)\, dE}{\displaystyle\int_0^\infty G(E)\, dE} \quad \text{which is the} \tag{65}$$

fraction of leakage neutrons from the reflector belonging to the j^{th} energy group.

The neutron effectiveness is also a function of the energy and geometrical coordinates of the neutron. The efficiency of the neutron in producing fission is dependent upon the energy of the neutron reaching the fuel. For SPR-I the neutron must penetrate a shield with an energy dependent cross section in order to reach the fuel. The efficiency of the neutron in producing fission is also dependent upon the point at which it enters the fuel and upon the angle of incidence. For the purposes of this paper, it is assumed that the effectiveness can be calculated by considering only neutrons which are incident upon the fuel along a normal to the fuel surface. The test of this assumption is the comparison of the experimental work with the calculated parameters.

The Monte Carlo code discussed previously was used to determine the effectiveness for each of 86 energy groups. The results of the calculation of reflected neutron effectiveness are given in Figure 3 as a function of energy for a 0.016 inch thickness of Cadmium shield. Second and third generation neutrons were considered in the calculation.

L_j^* was computed using a Monte Carlo code similar to that used for the fuel assembly, the only difference being the cross sections used and the geometry. The neutrons were assumed to enter the reflector surface with a direction normal to the reflector surface. The energy distribution of the incident neutrons was assumed to be that of the leakage spectrum from the fuel.

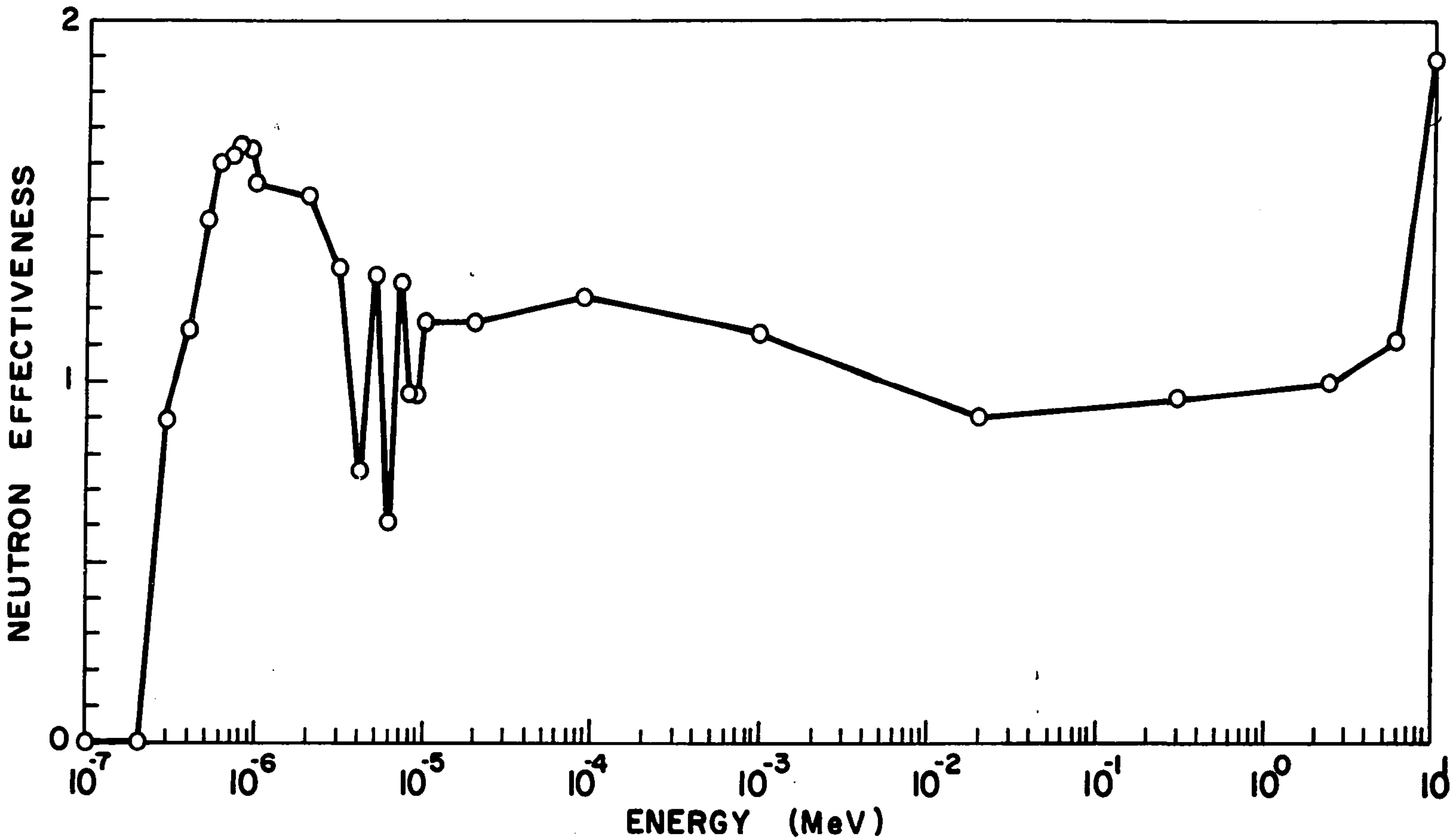

Monte Carlo calculated neutron effectiveness in
producing fission as a function of neutron energy

Figure 3

The number of neutrons of a given energy group which escaped from the reflector through the inner surface was determined for polyethylene reflectors of various thicknesses. The calculated energy spectrum was normalized to unity and is given in Figures 4 and 5.

T. F. Wimett performed a calculation using a diffusion theory with sixteen energy groups to determine the energy spectrum of neutrons escaping from a one inch thick shell of lucite in the direction of the fuel. Since lucite and polyethylene are similar in constituents, the energy spectrum of neutrons escaping from polyethylene should be similar to that of neutrons escaping from lucite. Wimetts computed data was normalized to 10 neutrons for convenient display and is also shown in Figures 4 and 5. The lucite data agrees quite well with that computed by the Monte Carlo code for polyethylene.

Reflected Group Time Constants

The reflected group time constants consist of τ_2, τ_{3_j}, and τ_{4_j} and are considered separately.

τ_{3_j} is computed using the reflector Monte Carlo code in the same manner as prompt neutron lifetime was calculated with the reactor code. The mean lifetime to leakage for each energy group was determined. Only neutrons which escaped through the inner surface were considered in the calculation of τ_{3_j}. The results of this calculation are shown as a function of energy for various thicknesses of polyethylene in Figure 6. The time constants τ_2 and τ_{4_j} are functions of both energy and average distance a neutron must travel in crossing the gap between the reflector and the core. The rigorous representation of this transit distance is a complicated expression depending on the spatial coordinates of both the reflector and the fuel.

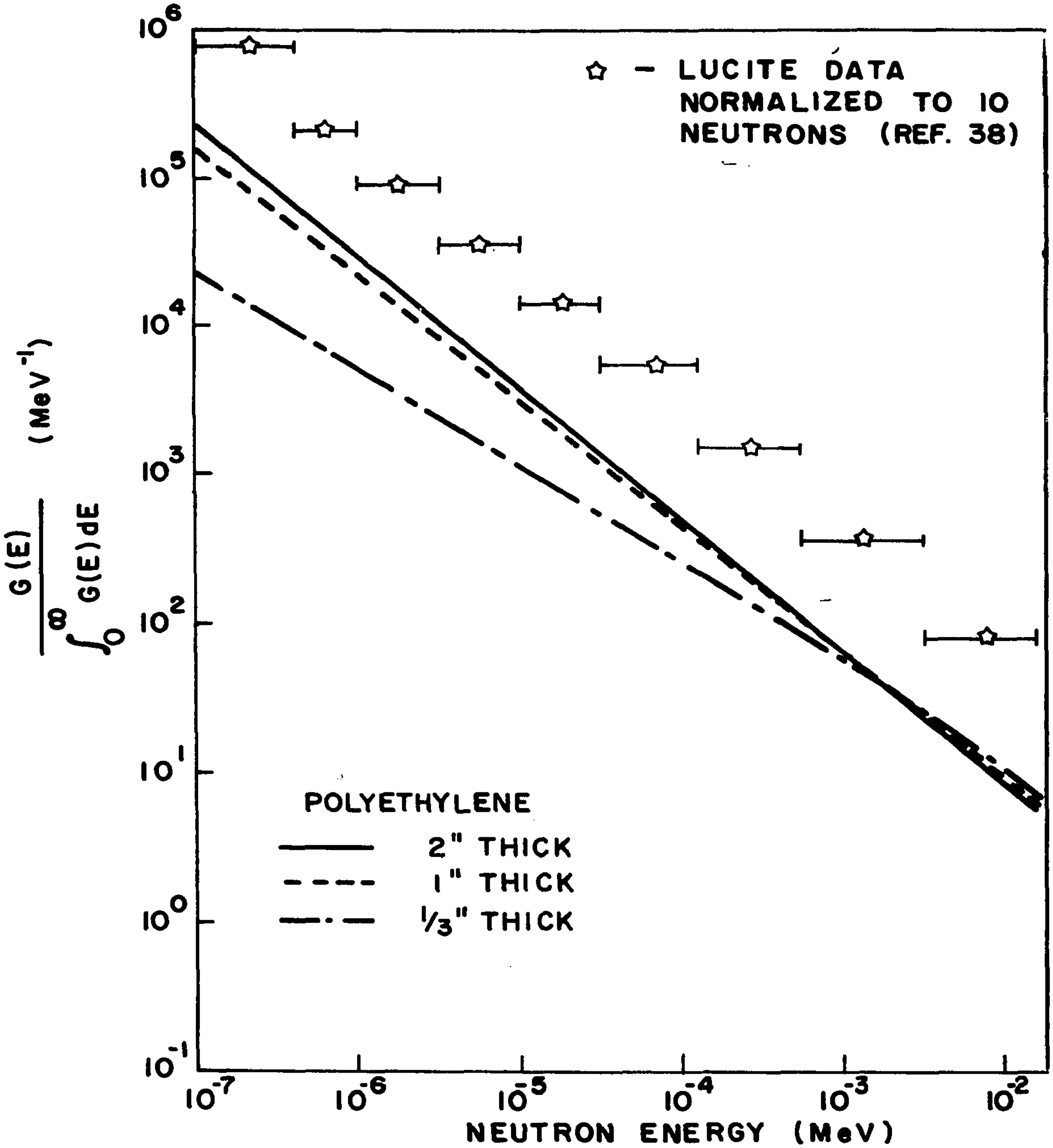

Monte Carlo calculated spectrum for reflector leakage through inner surface

Figure 4

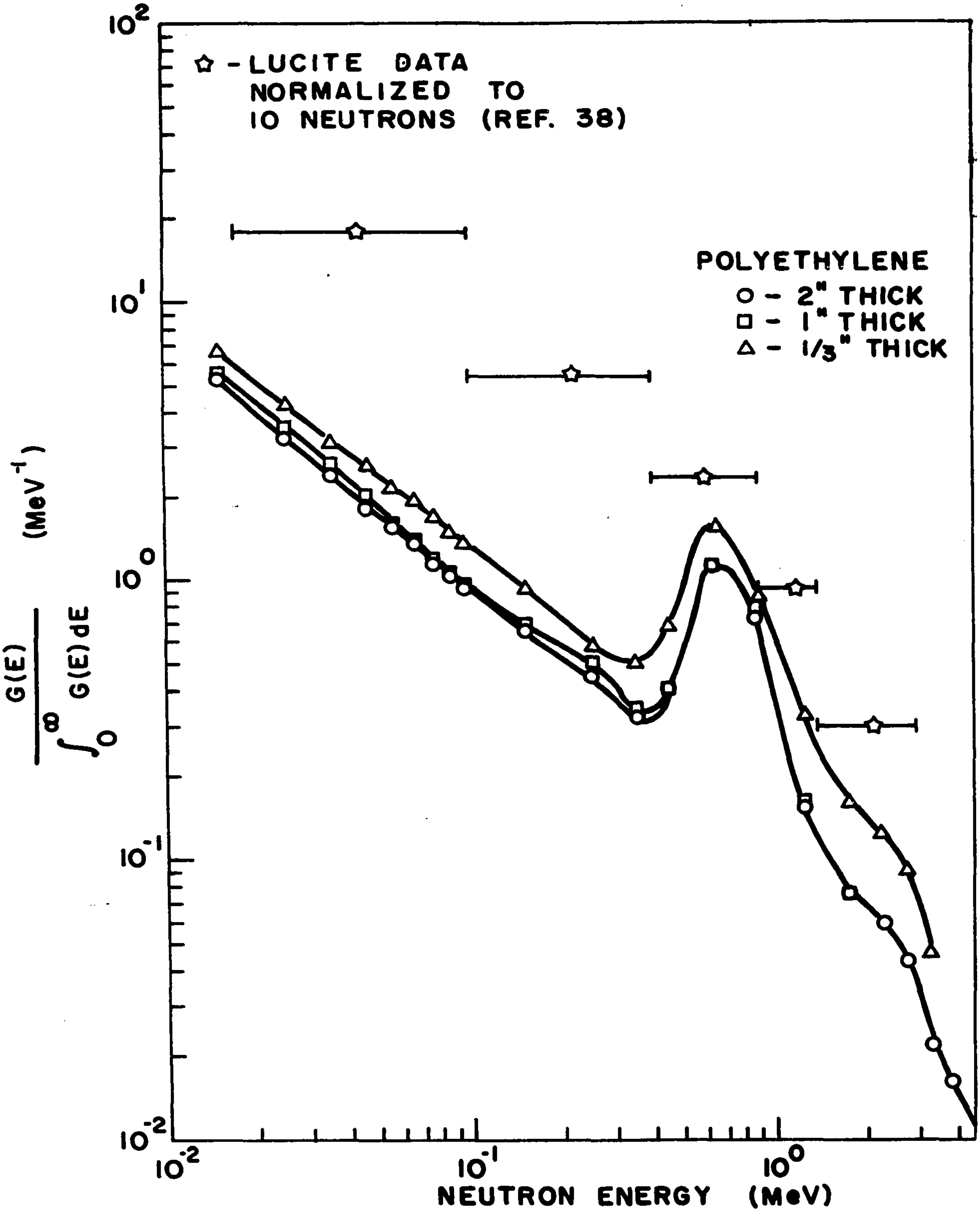

Monte Carlo calculated spectrum for reflector leakage through inner surface

Figure 5

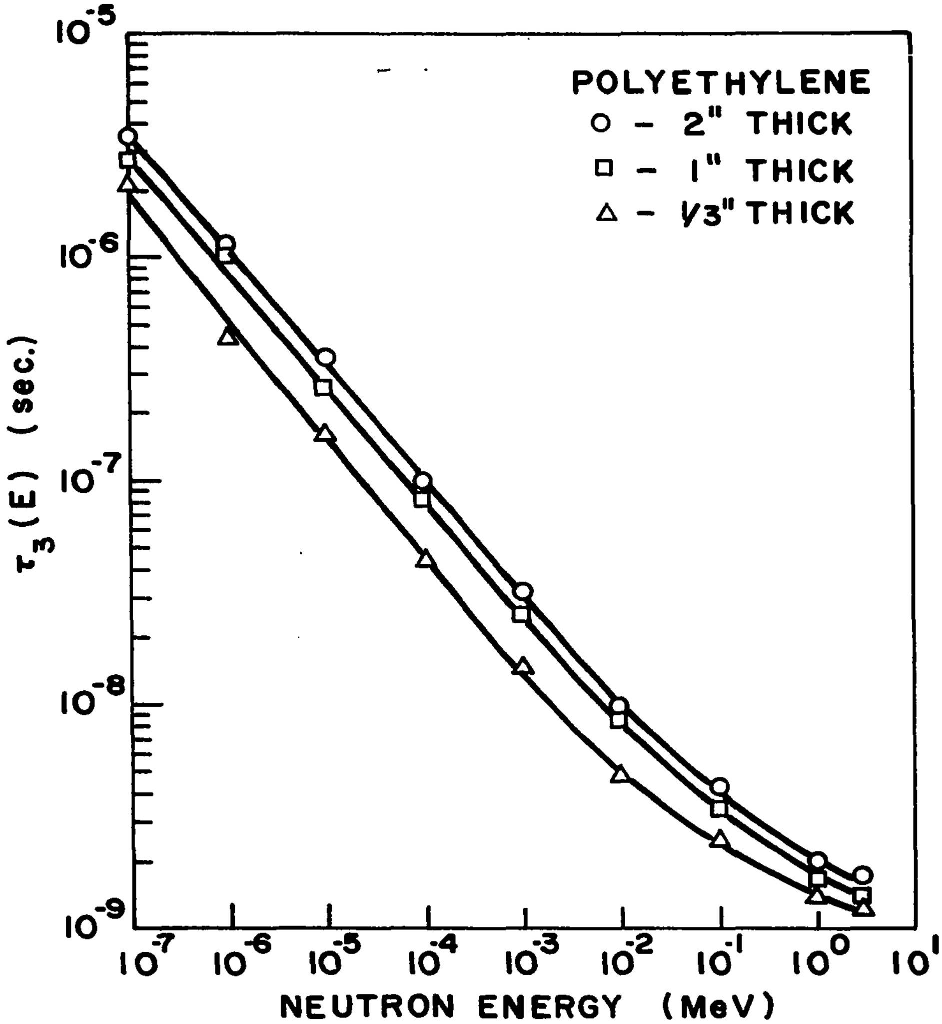

Monte Carlo calculated mean residence time neutrons in polyethylene reflector as a function of neutron energy

Figure 6

An investigation of the calculated leakage spectrum indicated that τ_2 was negligible compared with the time constants for all of the reflected groups with the exception of the high energy groups which were expected to have a negligible contribution. Hence, τ_2 was ignored in this analysis.

The formal expression for τ_4 is given by equation (14) of the theoretical section

$$\tau_{4_j} = J\, g^* = J \int_{E_{j-1}}^{E_j} g'(E)\, dE \tag{14}$$

where

$$g^* = \int g'(E)\, dE = \frac{\int g(E)\ G(E)}{\int G(E)\, dE}\, dE\ ;$$

and g(E) is given simply by

$$g(E) = \frac{m}{2E}$$

where m is the mass of a neutron.

By the formal definition G(E) pertains to the leakage over all surfaces but since $P_{rc}(\vec{r}, \vec{\Omega})$ is zero for all exterior surfaces, it suffices to say that G(E) is the energy distribution of the neutrons escaping from the inner surface of the reflector. Thus, once the energy distribution of the reflected neutrons is known the integral expression in equation (14) can be evaluated. Using the reflector leakage spectrums calculated for the various polyethylene thicknesses g^* was evaluated. The deviation from $\frac{1}{v}$ dependence was very slight and g^* could be represented as $\frac{m}{2E}$ for all reflectors. Small corrections based on the rigorous evaluation of g^* were incorporated when τ_{4_j} was calculated.

The quantity J defined in equation (12) depends on the geometrical configuration of the reflector. J is zero for zero distance between the fuel and the reflector and approaches the separation distance r, as r becomes large compared to the dimensions of the fuel. The representation of J for small non-zero separation distance is quite complicated and the evaluation is difficult.

A calculation was performed for the particular geometry of the experiment shown in Figure 7. This calculation assumed that the leakage from the reflector inner surface was uniform and that each point on the inner surface was an isotropic neutron emitter. The integrations were performed numerically. The calculated values of J used in this study are given in Table I.

TABLE I

EFFECTIVE TRANSIT DISTANCE, J

Inner Radius of Cylinder (inches)	Effective Transit Distance (inches)
6.25	3.69
7.06	4.56
8.37	5.62
11.37	8.65
13.13	10.60

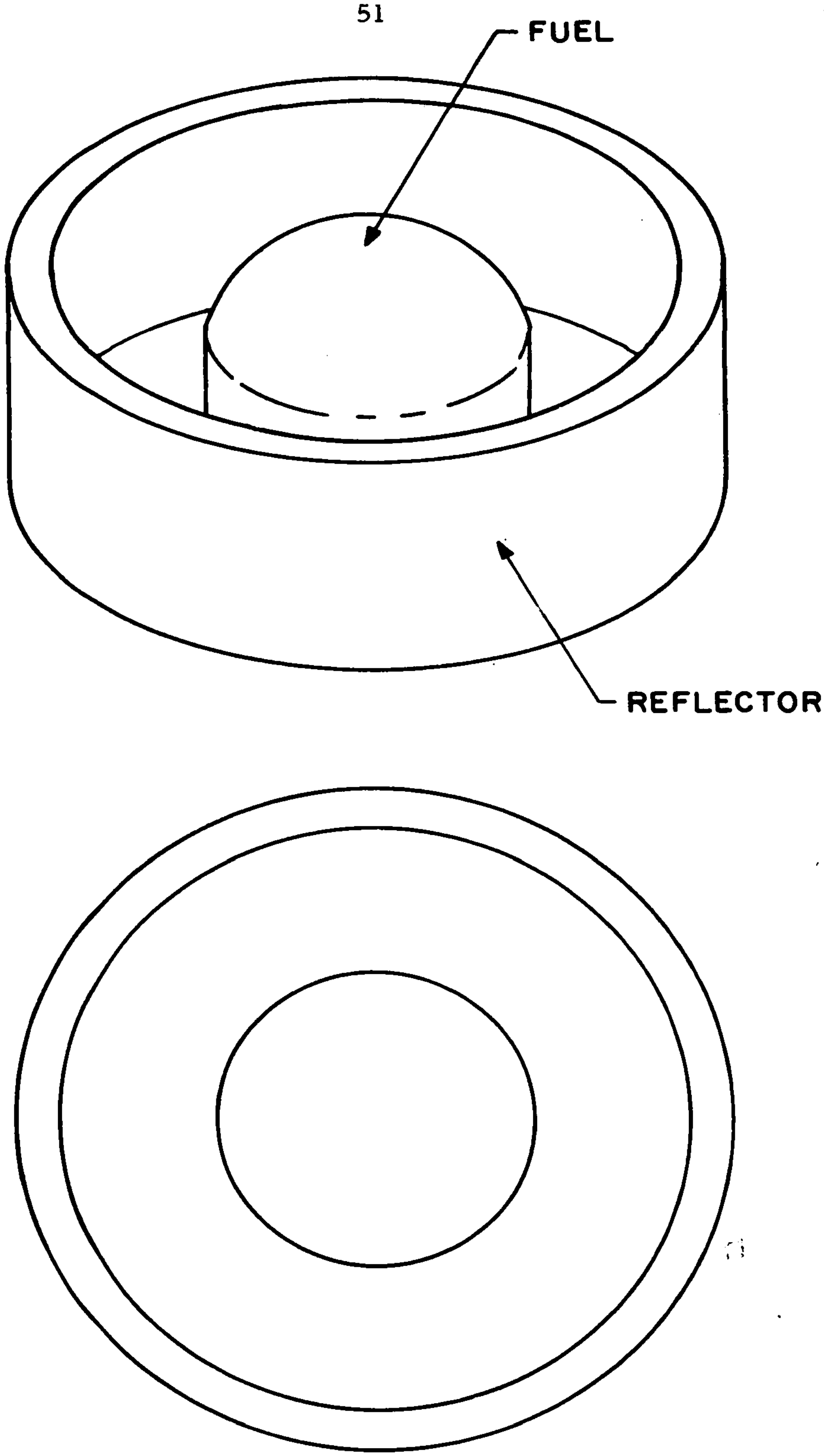

Typical reflector-fuel configuration

Figure 7

CHAPTER V

OBJECT OF EXPERIMENTAL INVESTIGATION AND EXPERIMENTAL EQUIPMENT

The object of the experimental investigation was the verification of the small reflected reactor kinetics model.

The experimental investigation was primarily directed toward verification of the reflected inhour equation in the vicinity of prompt critical. This choice was based on several considerations which are as follows:

1. The most important characteristics of a burst reactor are those associated with super prompt critical conditions.
2. The inhour expression is a convenient tool for comparison of the reflected and bare fuel assembly.
3. The time constants of interest are of the same order or magnitude as the reactor period in the prompt critical region and thus have the greatest visible effect on reactor period.
4. By limiting the investigation to the inhour relation variables such as safety block and burst rod position as a function of time during the burst and the dynamic shutdown coefficient of the assembly need not be studied in detail. The description of safety block position during a burst would, for example, be quite difficult without continuously monitoring the position. This is due to the fact that the expansion of the core following a burst apparently forces the safety block out of the core momentarily. This movement is only a few mils but represents

a considerable reactivity change. The incorporation of this movement into the reflected kinetics equations, while possible, would be quite tedious.

In addition, an experimental investigation of the neutron yield, burst width and peak fission rate for the reflected assembly was undertaken. This investigation was performed using the Sandia Pulsed Reactor, SPR-I, shown in Figure 8.

Description of SPR-I Fuel Assembly

The SPR-I is an unreflected, cylindrical, enriched uranium assembly based on the design of the Los Alamos Scientific Laboratory's Godiva II [2].

The stationary fissionable components consist of three cast oralloy rings and one cast oralloy domed cap. The oralloy is enriched to 93.2% U^{235} with an average density of 18.75 gm/cm^3.

Assembled, the stationary oralloy components form a right circular cylinder with a domed cap. The diameter of the cylinder is 7 inches and the over-all height is 5-5/8 inches; the domed cap has a 4-3/4 inch radius. The bottom of the stationary assembly is flat to permit rigid mounting to the steel support plate; three steel bolts fasten the oralloy to the support plate. Four cylindrical cavities opening at the bottom accommodate the safety block, the two control rods, and the burst rod. The safety block is concentric with the stationary section and provides an 0.060 inch radial clearance for the safety block. Cavities for the control and burst rods are displaced at 120° on a 2-11/16 inch radius, measured from the axis of the assembly. The safety block, control rods and burst rod also are composed of cast oralloy with an enrichment of 93.2% U^{235} and a density of 18.75 gm/cm^3.

Figure 9 shows the fissionable components of the SPR-I fuel assembly. All external surfaces of the assembled reactor are coated with

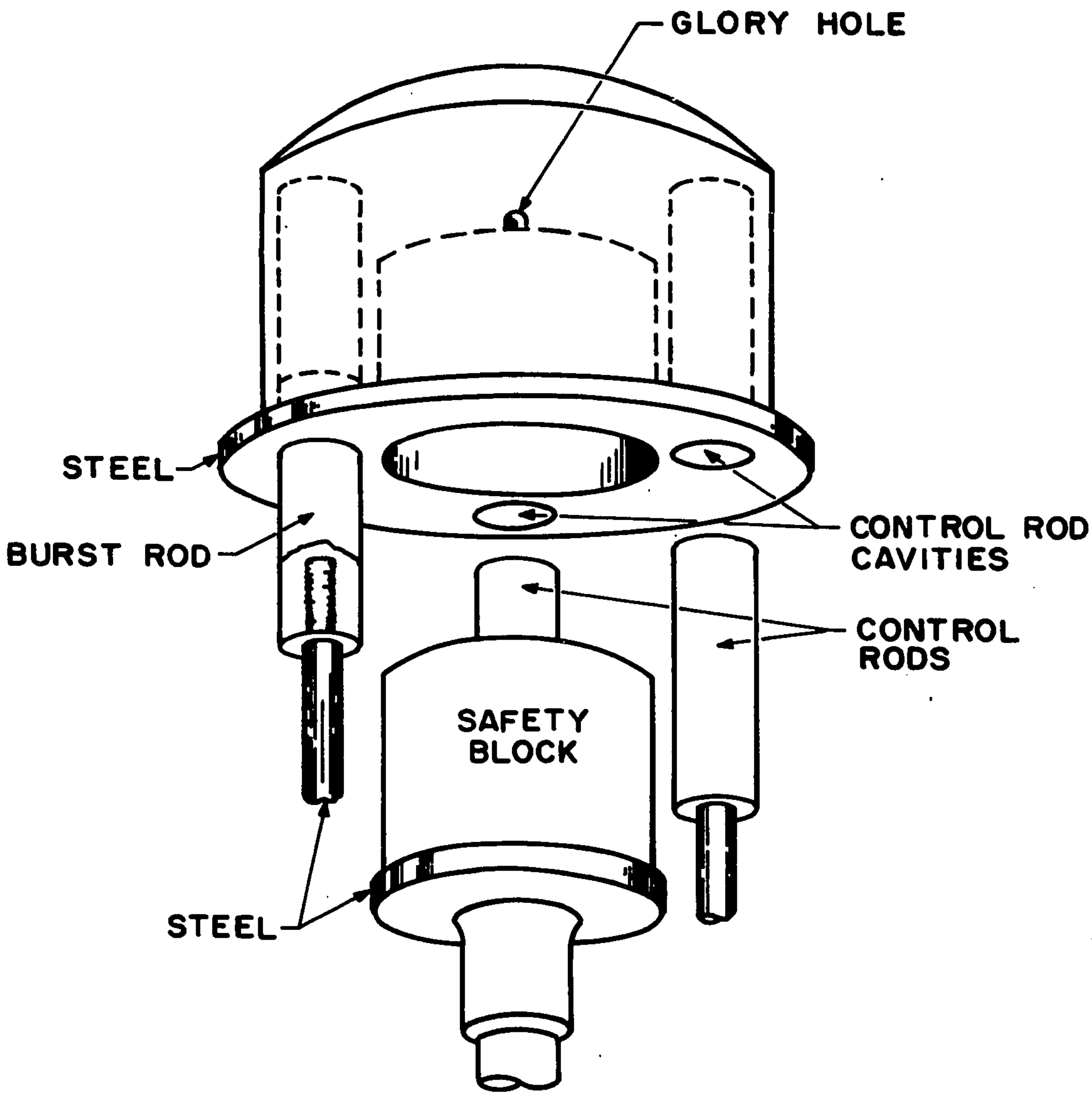

Fissionable components of the SPR-I

Figure 9

1 to 2 mils of aluminum which reduces the possibility of contamination. The masses of the components are as follows:

Part	Oralloy Mass Kg.
(Stationary parts)	
Cap	13.096
Top cylindrical section	10.146
Center cylindrical section	9.535
Lower cylindrical section	10.338

Part	Oralloy Mass Kg.
(Movable parts)	
Safety Block	11.620
Control Rod 1	1.053
Control Rod 2	.911
Burst Rod	.979
Total	57.728

A domed Cadmium shroud covers the fissionable components. The Cadmium shroud is 0.016 inches thick and is supported by perforated aluminum shroud 0.031 inches thick. The purpose of the Cadmium shroud is to prevent reflected thermal neutrons from returning to the fuel assembly and to decrease possible contamination of the kiva* in which the reactor is housed.

The fuel assembly and control rod drive mechanisms are mounted on a rigid stand which is supported by an elevator. The entire assembly can be lowered below floor level and shielded so that experimenters may work in the kiva between bursts.

* A kiva is a Pueblo Indian ceremonial structure usually round and located just beneath the ground. Due to the similarity in shape between a Pueblo kiva and the room in which the reactor is located, the word has been adopted by burst reactor facilities.

The reactor is remotely operated from the SPR-I control room located about 200 feet from the kiva and instrumentation is provided in a building adjacent to the kiva. Figure 10 shows the relative locations of the reactor kiva, the instrument building, and the SPR-I control room.

Reflectors

Since the theoretical work of Chapter 3 indicated that the greatest reflector effect occurs when moderating materials are used as reflectors, polyethylene was chosen as a primary material to be studied. An investigation of the effect of steel reflectors was also made in order to compare a non-moderating reflector with a moderating reflector.

To facilitate the comparison between calculated and measured quantities, a reflector geometry was chosen which could be easily handled in calculations based on the theoretical equations. The reflectors were constructed as cylinders 6 inches high with various inner diameters and thicknesses.

An aluminum stand shown in Figure 11 was constructed to support the reflectors. Aluminum was chosen for the stand since aluminum was expected to have very little effect on the measurements. In addition, the stand was constructed in such a manner as to insure that the aluminum was at the greatest possible distance from the fuel assembly.

To insure that the position of the reflector with respect to the fuel assembly did not change between bursts, the reflector stand positioned on and was supported by the reactor stand. In addition to insuring the reproduction of location between bursts, the construction allowed the reflector stand to be removed from the reactor and replaced at a later date without change of position of the reflector with respect to the fuel assembly. The stand was also designed to provide the maximum versatility for experiments. A view of the reflector when mounted on the reactor stand is given in Figure 12.

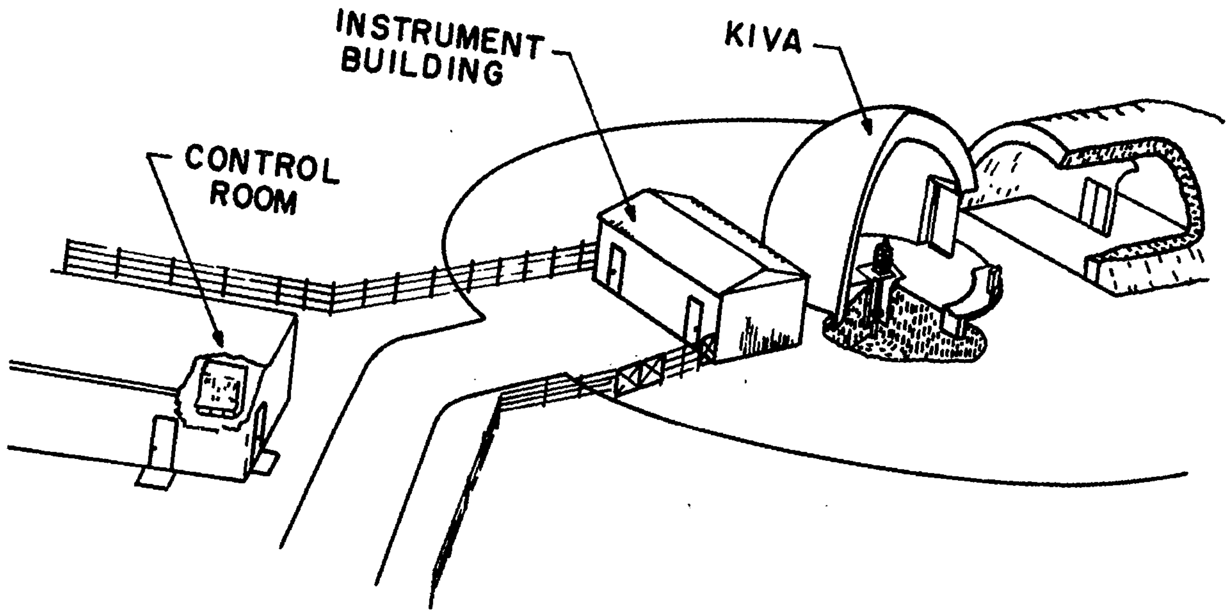

SPR-I burst facility area.

Figure 10

Instrumentation

The quantities measured in this investigation are basically as follows:

1. fissionable component position
2. temperature of the assembly
3. neutron level as a function of time
4. integrated neutron dose

Position Measurements

A display of the position of the safety block and the control rods was continuously available at the reactor console shown in Figure 13. Litton linear potentiometers were used to provide a voltage signal proportional to the displacement of the control rods from a reference position. This signal was used to drive a Gilmore mechanical readout at the console. A similar arrangement was used to indicate safety block position although operation was always with the safety block fully inserted. A microswitch provided a signal which indicated full insertion.

The burst rod which was driven pneumatically had static positions of either fully withdrawn or fully inserted. Insertion time of the burst rod was 150 milliseconds and microswitches provided signals indicating the position of the burst rod.

Temperature Measurements

Two iron-constantan thermocouples provided continuous signals proportional to the fuel temperature in the region of the thermocouples. One thermocouple was located near the center of the fuel while the other was located near the fuel surface. The outputs of the thermocouples were recorded on strip chart recorders located at the reactor console.

Intrinsic thermocouples were also employed in connection with dosimetric work. These are described in the dosimetry section.

The iron-constantan thermocouples were used to indicate stability of the temperature when establishing critical and to indicate total energy release for a given burst. For a given temperature profile the energy released will be directly proportional to the change in temperature as indicated by the thermocouples. The location of the thermocouples afforded a check on the temperature profile. The voltage output of the center thermocouple for a 100° burst was 4.82 mv. while the output from the one located near the edge was 2.83 mv.

Neutron Level Instrumentation

The neutron level measurements made can be divided into two classes: those made under near delayed critical conditions and those performed under near prompt critical conditions. The instrumentation for each of these classes, by the nature of the reactor response must be different, and each class is discussed.

Delayed Critical. Measurements made under delayed critical conditions consisted primarily of period and material worth measurements. These measurements require observation of the neutron level as a function of time. In addition, temperature was also monitored to permit corrections for change in reactivity due to temperature changes.

Three separate channels were employed to monitor the neutron level. Channel 1 D and Channel 2D used Westinghouse WL-8074 compensated ionization chambers as detectors embedded in a polyethylene geometry 15 feet from the fuel assembly. The amplified signals from these detectors were recorded on separate Westronics strip chart recorders. The time required for full-scale deflection on the recorder was one-half second. One recorder provided start and stop signals to a Hewlett Packard digital timer. The levels at which the signals were generated were separated by a factor of e, thus providing a digital display of reactor period.

Channel 3D was employed when the reactor period became so small that neutron level could not be followed by Channels 1D or 2D. This channel employed a fission chamber which was located in a polyethylene assembly for low neutron level measurements and was left bare for high neutron level measurements. The chamber was located about 3 feet from the fuel assembly.

The linearity of the fission chamber output was confirmed by comparison with the compensated ion chambers. The signal from the detector after amplification provided an input to a discriminating circuit which gave start and stop signals to a Hewlett Packard digital timer. The start signal was generated when the amplified signal reached .5 volts and the stop signal was generated when this signal reached 1.36 volts, thus, providing digital display of the reactor period from this channel also.

A block diagram of the three instrumentation channels are given in Figures 14 and 15. The recorders and timers are built into the reactor console, Figure 13.

Prompt Critical. Three separate channels provided detection and display of the neutron level as a function of time during prompt critical operation.

Channel 1P was used to provide a photographic record of the reactor burst pulse shape and amplitude. The system consisted of a plastic scintillating crystal and photodiode combination, a high voltage power supply for the photodiode and a dual beam oscilloscope equipped with a Polaroid camera. The crystal was a right circular cylinder 2 inches by 2 inches composed of a clear plastic doped with diphenal-stilbine manufactured by Pilot Chemicals, Inc. The photodiode was a type FW-114 manufactured by the International Telephone and Telegraph Company. The output of the photodiode system was used as the input to a type 565 dual beam Tektronix oscilloscope. The upper beam of the oscilloscope was used to display the

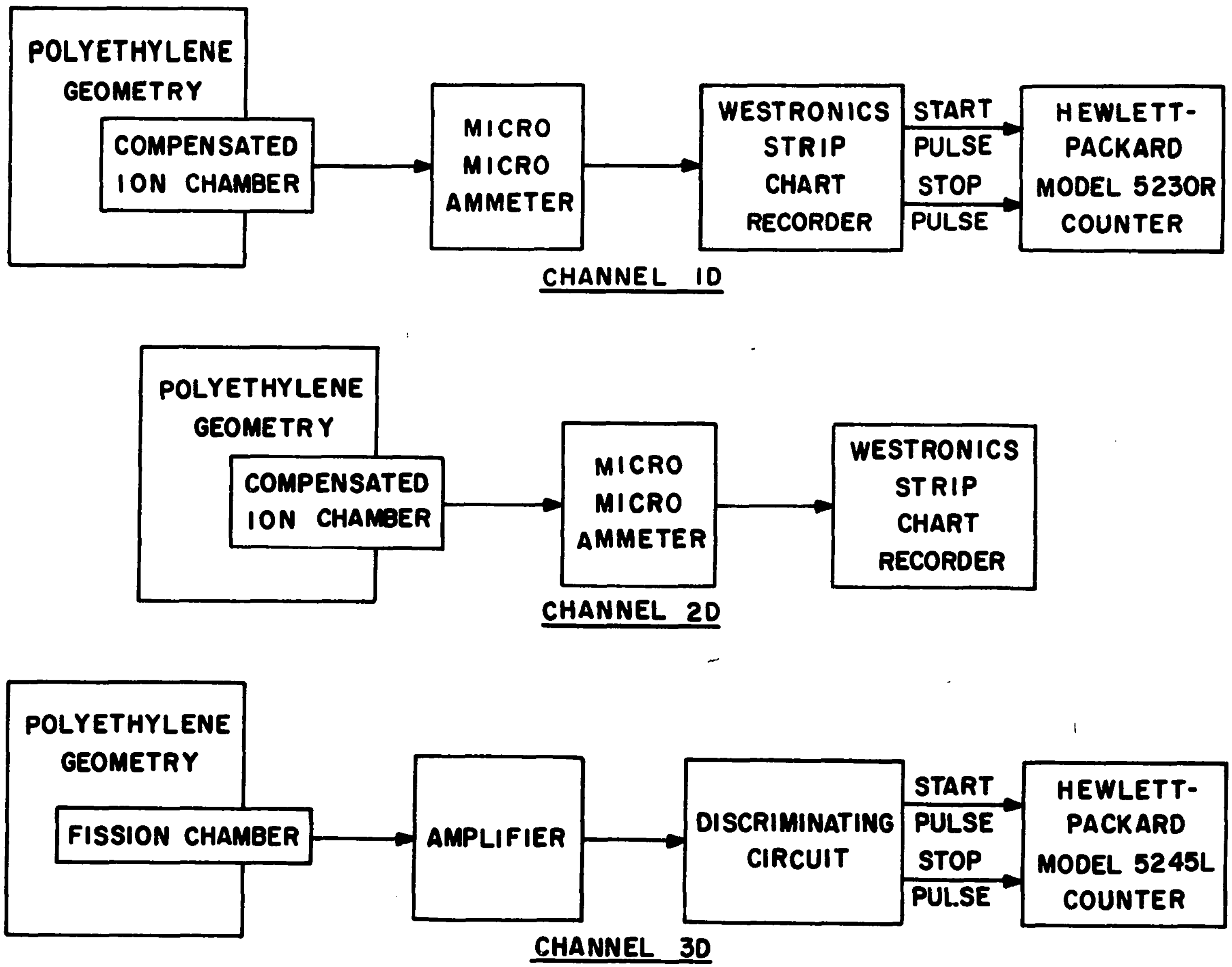

Block diagram of channels, 1D, 2D, and 3D

Figure 14

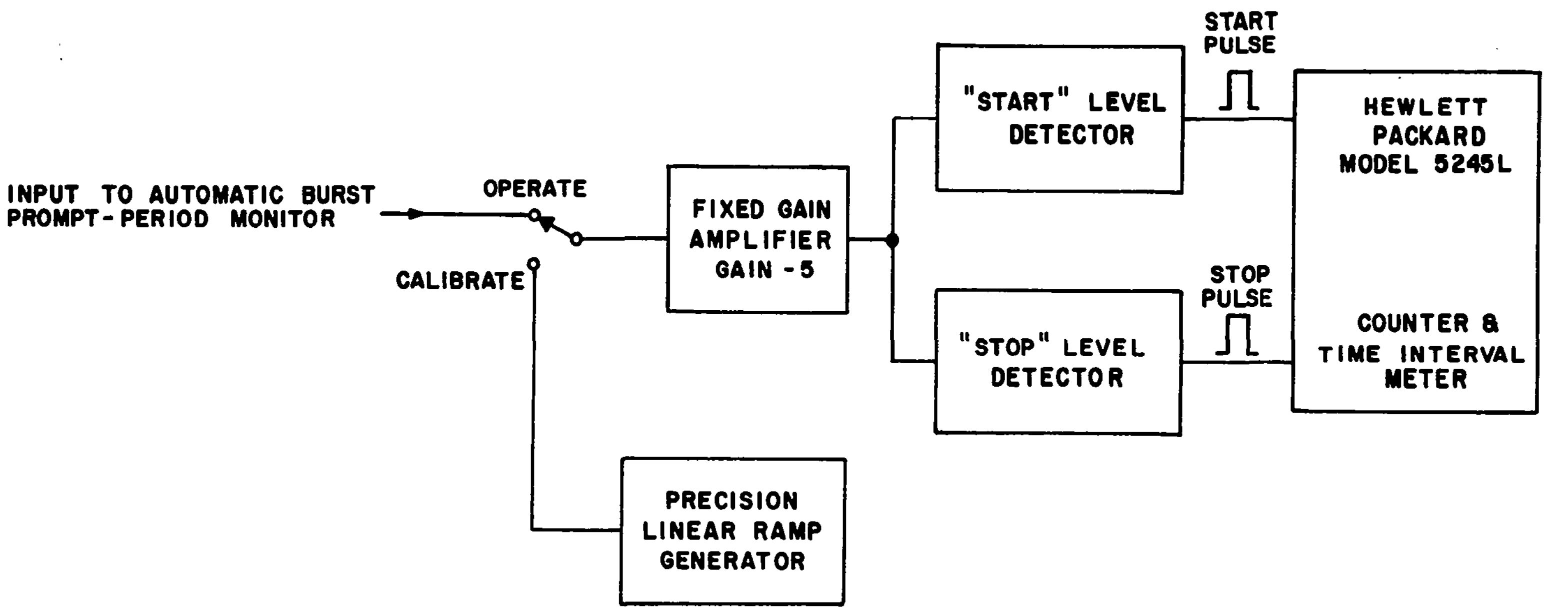

Block diagram of period meter circuit

Figure 15

of the burst pulse, and the lower beam of the oscilloscope was used to display the burst plateau. A sweep trigger signal was provided by a discriminator circuit driven by a sensitive photomultiplier detector system.

The linearity of the photodiode system over the range of measurement was confirmed by measuring the period of a given burst over a wide range of detector outputs.

The recording equipment for Channel 1P was located in the SPR-I control room as an intregral part of the SPR-I control system [35]. A more detailed description of such a system is available in reference [33].

Channel 2P was used to provide a signal to the automatic burst, prompt-period monitoring system which indicates reactor period during prompt burst operations. This system consisted of a plastic scintillation crystal and photodiode combination, a high voltage power supply, a discriminating circuit and a 10 megacycle time mark generator and associated counter.

The crystal was a 1/2 inch thick disc, 5 inches in diameter composed of the same plastic material as the crystal used in Channel 1P and the photodiode was an ITT FW-127. The photodiode output was used as the input of a discriminator which gave a start to a Hewlett Packard Molel 5245L counter when the photodiode output reached 0. 5 volts. A stop signal was generated when the photodiode output reached 1. 36 volts. An automatic measurement of the initial period was thus available. To insure that the 1. 36 volt level was reached before heating occurred in the fuel assembly, an additional stage of amplification was used for small bursts.

To insure that the amplifier did not saturate, and the voltage input to the discriminator circuit was sufficient, the amplifier output was used as an input to a type 555 dual beam Tektronix oscilloscope. When no amplifier was used, the output of the photodiode was used as the input to the 555 oscilloscope. A polaroid camera was used to provide a permanent record of the trace.

A block diagram of this system is given in Figure 16. This system is also an integral part of the SPR-I control system, and the discriminator circuit, the counter, and the oscilloscope are located in the SPR-I control room.

Prior to this work there was very little quantitative experience as to the effect of the reflectors on the burst shape of the SPR-I reactor and, since only a few bursts were possible per day, back up for Channels 1P and 2P was necessary lest the information concerning a given burst be lost due to improper oscilloscope or amplifier settings. Channel 3P served as a back-up for Channels 1P and 2P. A crystal-photodiode combination identical to that of Channel 1P was used as the detector. Other components of the system were a high voltage power supply and two type 555 dual beam Tektronix oscilloscopes. One oscilloscope was used to record the initial rise of the pulse, thus affording a means of measuring the period. The other oscilloscope recorded the pulse shape. The output of both oscilloscopes was recorded with Polaroid cameras. The information from Channel 3P was superior to that from Channels 1P and 2P in about 30 percent of the shots.

Integrated Neutron Dose

A limited dosimetric investigation was undertaken. Of particular interest were the flux profile of the reflected reactor as compared to the bare reactor and the energy spectrum of the neutrons between the reflector and the fuel assembly.

Strips of Nickel, 7.5 inches long, .375 inches wide and .016 inches thick, were irradiated in the glory hole of the SPR-I fuel assembly for

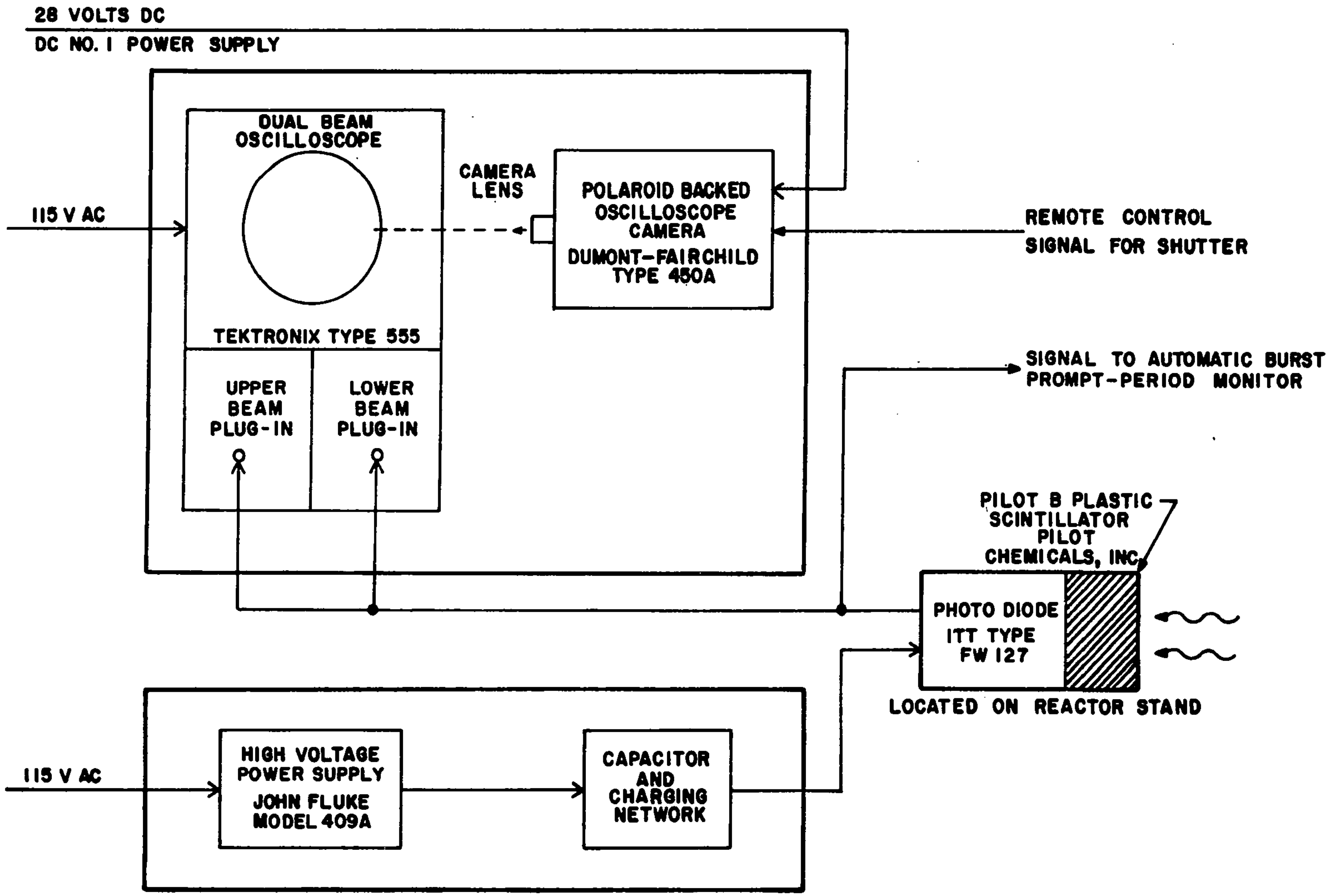

Block diagram of channel 3P

Figure 16

each of three reflector configurations. The strips were cut into several pieces each of which was counted using a scintillation counter. The activity per unit mass was then determined and related to absolute neutron flux by the use of standard relations developed by this Sandia dosimetry section. This resulted in a radial flux map of the core for energies greater than 3 Mev.

A detailed investigation of the spectrum would require an elaborate dosimetry program much as that given in reference [10]. The investigation here was merely to provide insight as to the spectral shift resulting from the addition of reflectors to the bare core. To provide an indication of the spectral shift, cadmium ratios were taken with indium foils and were compared for the bare and reflected systems. Sulfur was also irradiated to serve as another basis for comparison.

In addition, an instantaneous indication of spectral shift was afforded by the use of intrinsic thermocouples [31]. The intrinsic thermocouple consisted of alumel chromel leads on opposite sides of a U^{235} bead which served as the hot junction. The Uranium bead, when exposed to a neutron flux field, increases in temperature due to internal fissions. The voltage developed across the chromel alumel junction was photographically recorded from a 555 dual beam oscilloscope with a Polaroid camera.

Two thermocouples were used. One thermocouple was wrapped with cadmium and the other was left bare. A ratio of fissions due to the whole energy spectrum and the fissions due to epi-cadmium energy was obtained.

CHAPTER VI

EXPERIMENTAL PROCEDURE, DATA REDUCTION AND EXPERIMENTAL RESULTS

Delayed Critical Measurements

Rod Calibrations

The experimental investigation of the reflected inhour equation required a detailed knowledge of the integral and differential control rod worth in both the bare and the reflected cases. For the bare case, the rods were calibrated over the full length of travel by period measurements. The results are given in Figures 17 and 18. Rod shadow studies were also made, and the conclusion was made that any rod shadow effect was negligible. This property is unique to this type of fuel assembly and for a detailed account of this study, the reader is referred to reference [36].

In the reflected case, the control rods were calibrated over their expected range of movement when adjusting for a given reactivity insertion prior to a burst. This provided a means to investigate the effect of the reflectors on the differential control rod worth. No significant change was noted in this study that could not be attributed to errors in the parameters of the bare inhour relation. R. L. Long [37] has indicated that any error introduced by use of the bare reactor differential rod worth for the reflected cases would be quite small. The validity of using the bare inhour relation for reactivity measurements was justified in the theoretical section of this paper.

The worth of the burst rod was calculated for various reflector configurations using period measurements. The calculated worth was

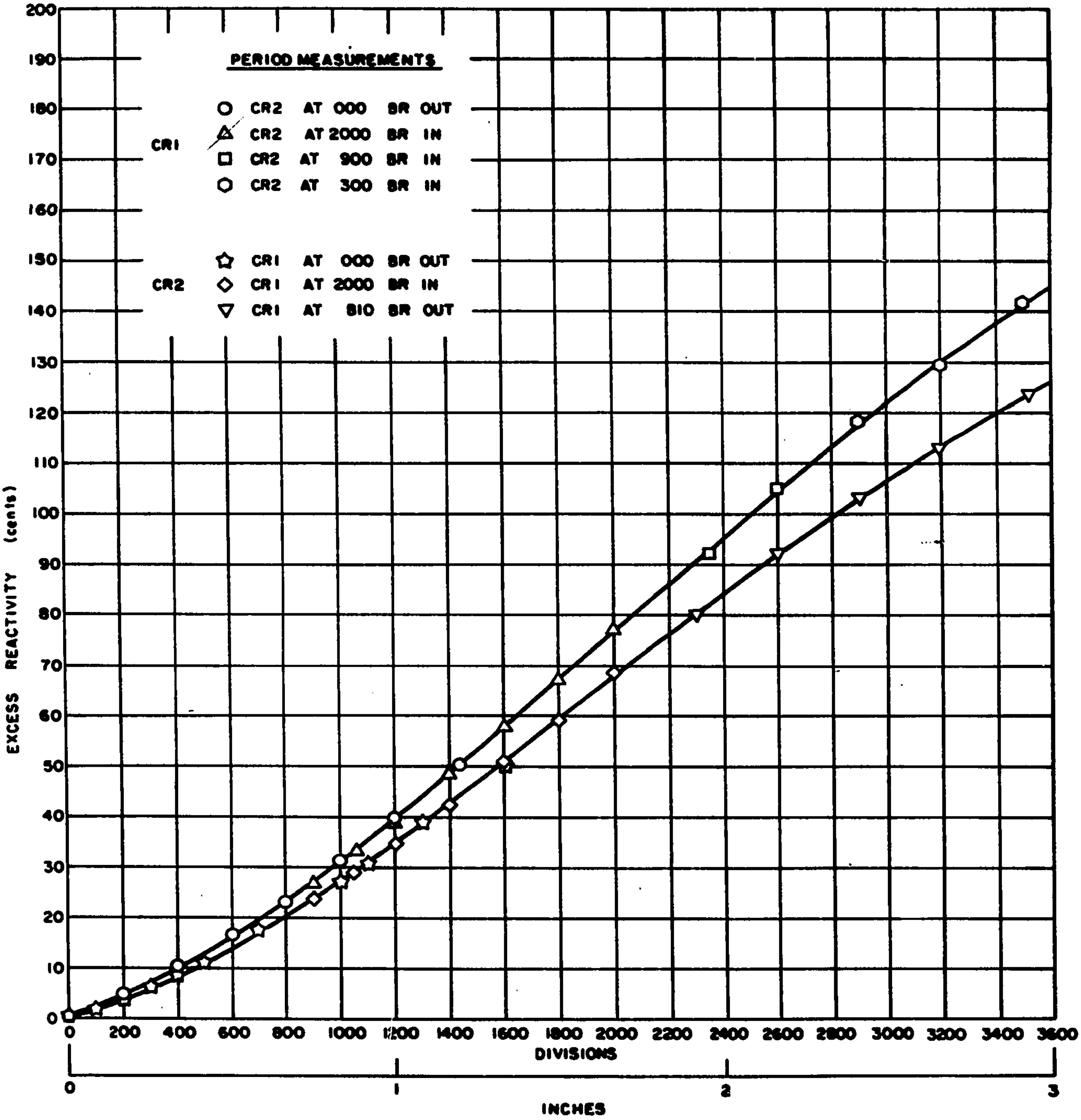

Calibration curves of SPR-I control rods

Figure 17

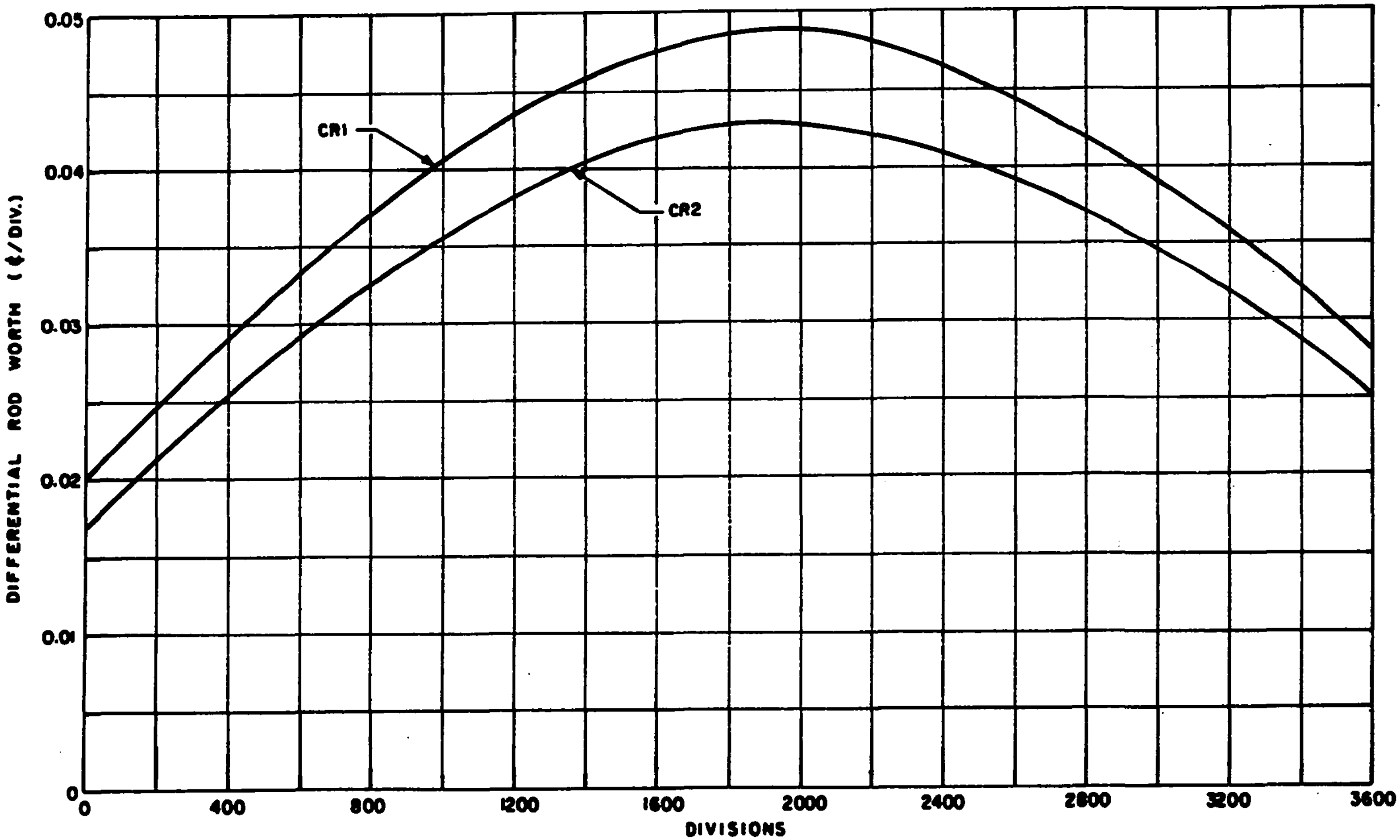

Differential worth of SPR-I control rods

Figure 18

estimated to be accurate to within 0. 5 percent for the parameters used in the inhour equation. Indications are, however, from the work performed here and from the work of R. L. Long that a discrepancy of approximately three percent exists between worth calculations made at prompt critical and those made at delayed critical. Since this discrepancy is independent of reflector configuration, the calculations made at delayed critical yield an estimate of the change in the burst rod worth upon addition of a reflector, but do not provide a good quantitative value to be used in burst analysis.

The instrumentation used for the rod calibrations consisted of Channels 1D and 2D. Period measurements taken from the period meter were compared with those obtained by measuring the time between two power levels with a stop watch. The minimum period encountered was 1. 4 seconds, which is still within the range of validity of the bare reactor inhour equation.

Temperature Coefficient

The temperature coefficient was measured under static conditions for a uniform temperature profile across the fuel assembly. The temperature range covered included the range of delayed critical operation. The results of the original measurements were checked daily as more data accumulated. The value obtained was . 34 cents per degree centigrade. The estimated error is $\pm$ .01 cents per degree centigrade.

Reflector Worth Measurements

The worth of the individual reflectors was determined by establishing the critical position of the control rods for the bare and the reflected case. Using the rod calibration for the bare reactor, the reactivity worth of the reflectors was determined. The error in using the bare reactor calibration curve was estimated to be less than two percent, while the experimental error was estimated to be less than 1.3 percent. This method was used rather than period measurements, since prohibitively small periods would result. The results of these measurements are given in Table 2. The reactivity contribution of the reflectors as a function of distance from the core and as a function of thickness is given in Figures 19 and 20. The reactivity worth of the reflector stand was measured and found to be 1.9 $\pm$ .5 cents. All measurements have been corrected by this amount to provide net reflector worths.

Prompt Critical Measurements

Measurements of the initial prompt reactor period, burst yield, peak fission rate and burst width all took place under burst conditions, which required prompt critical operation. The general procedure followed to generate a burst with the SPR-I fuel assembly is described below. For a description of the time dependent characteristics of a burst the reader is referred to Appendix A.

1. The reflector to be studied was arranged in the desired manner with respect to the fuel assembly.

2. The delayed critical condition was obtained by inserting the control rods into the core. The burst rod was in the out position during this operation.

3. The control rods were withdrawn a certain distance, such that when the burst rod was inserted, the system would have the desired prompt reactivity.

4. The safety block was withdrawn and the neutron level in the fuel assembly was allowed to decay. This wait period was 15 minutes.

5. Fifteen seconds before the burst rod was inserted, the safety block was seated inside the core. The reactor was still in a subcritical state after this insertion.

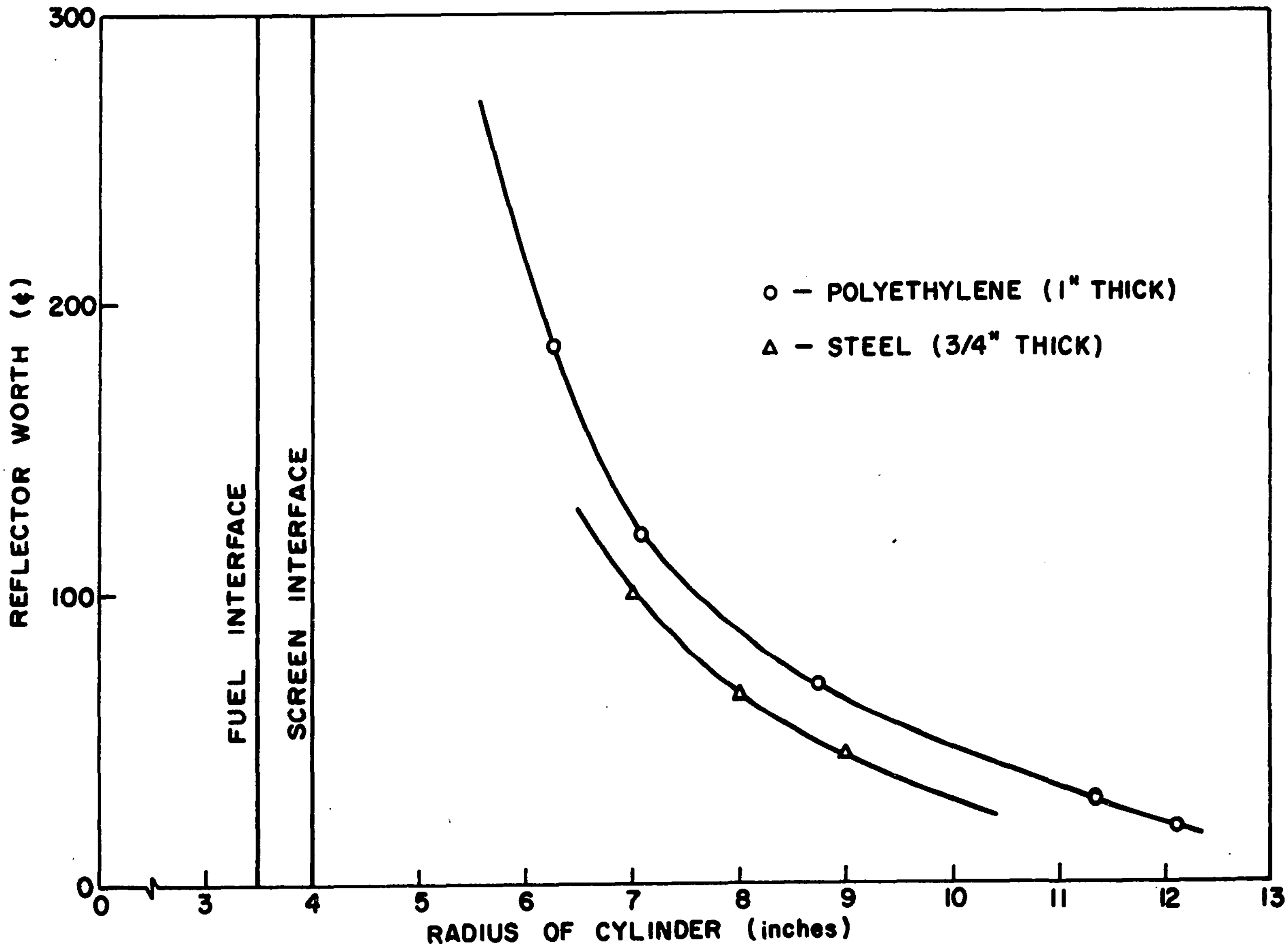

Reactivity worth of reflectors as a function of
distance of inner surface from the fuel center line
Figure 19

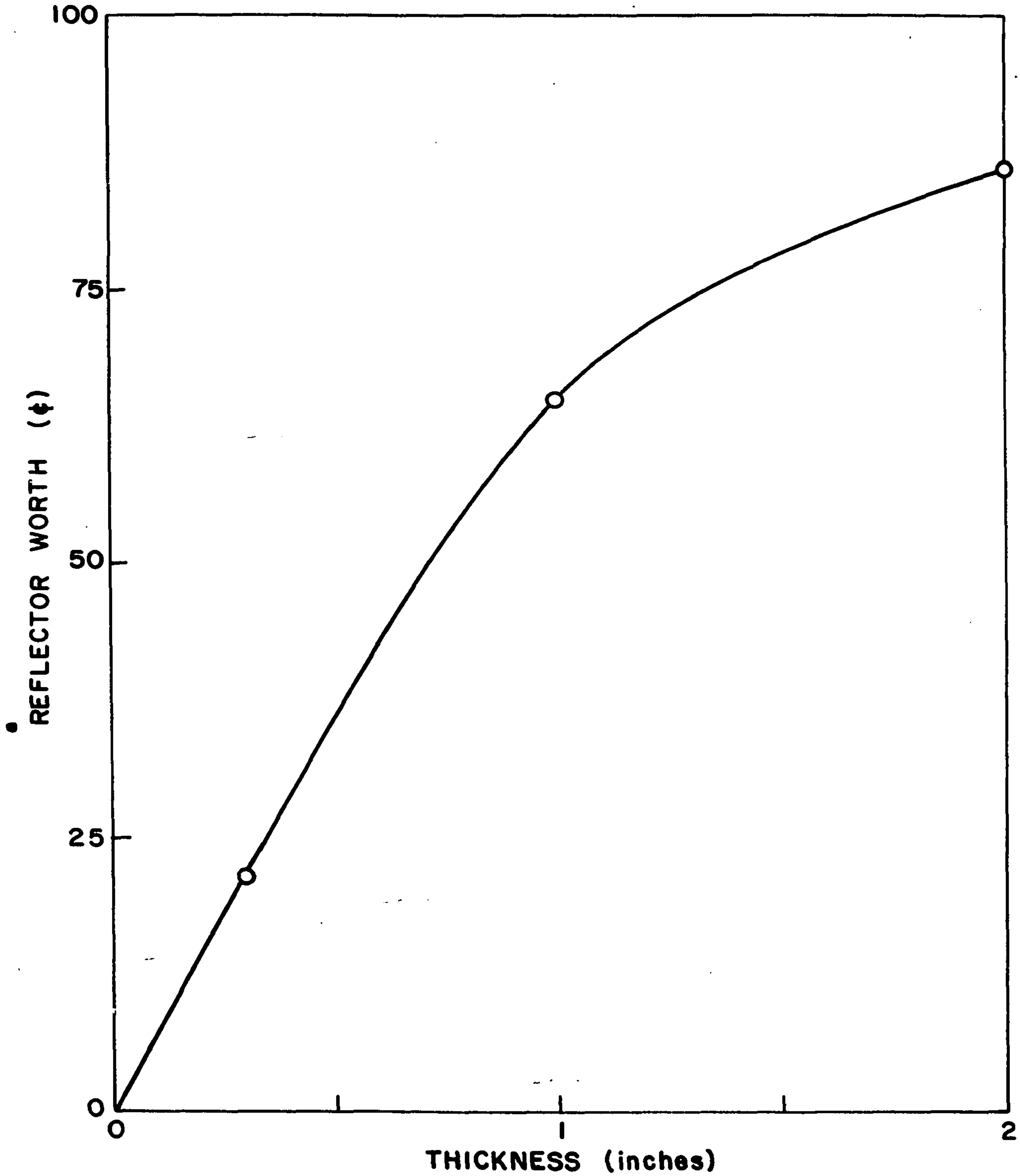

Reactivity effect of a polyethylene reflector of 8 3/4 inch inside radius as a function of reflector thickness

Figure 20

TABLE 2

REACTIVITY EFFECT OF REFLECTORS

Material	Thickness inches	Inner Diameter inches	Reflector Worth Cents	Apparent Change In BRW
Poly-ethlene	1/3	17 1/2	21. 2	+. 36 ± . 1
	1	17 1/2	64. 1	+. 86 ± . 1
	2	17 1/2	85. 7	+. 1. 11 ± . 1
	1	14 1/8	121. 3	+. 1. 51 ± . 1
	1	12 1/2	185. 2	+. 1. 86 ± . 1
	1	22 3/4	30. 2	+. 60 ± . 1
	1	26 1/4	18. 9	+. 55 ± . 1
Steel	3/4	18	46. 31	+ 1. 2 ± . 1
	3/4	16	66. 51	+ 1. 85 ± . 1
	3/4	14	99. 9	+2. 65 ± . 1

6. At burst time the burst rod was inserted, placing the reactor in a prompt critical condition. An automatic relay system initiated a pulse of neutrons from a neutron generator. This provided control over the time the burst began; and the automatic timing system could be set to provide a scram at any given time.

7. When the power level reached 2 KW, a scram signal was initiated and a trigger signal was provided for the oscilloscopes used in the experimental system. The burst is terminated by the negative reactivity feedback due to the thermal expansion of the fuel assembly. The scram causes the safety block and the burst rod to move out of the core and reduce heating in the plateau.

Initial Period Measurements

As previously mentioned, Channel 2P and Channel 3P provided information concerning the initial period. The oscilloscope in Channel 3P had settings such that the period could be obtained at least four decades below peak power so that there would be no negative reactivity feedback due to a temperature rise. Other oscilloscopes were set to perform the functions described in the equipment sections. The information from these channels was compared and the best estimate of the initial period was obtained. The error in the initial period measurement was estimated to be less than three percent.

The reciprocal period data was then plotted as a function of the reactivity withdrawn by the control rods. (see step 3 above) This reactivity was calculated using the known distance the rods were withdrawn and the best estimate of the differential rod worth in that region. The error in the reactivity calculated in this manner was estimated to be less than two percent. The intercept of the resulting curve with the reactivity axis was noted, and all curves were translated to the intercept of the free field curve. The displacement of the intercepts of the reflector curves from the free field intercept was taken to the change of burst rod worth less any j^{th} fractions of reflected neutrons satisfying the conditions of equation (55). The intercept displacements are given in Table 2. The translated reciprocal period curves are given in Figures 21, 22, and 23. These curves are plotted as functions of the amount of reactivity above that point where the curve intercepts the reactivity axis. This reactivity can be called $\Delta k_p'$ and if the intercept is the prompt critical point, then $\Delta k_p'$ is the amount of reactivity above prompt critical. It will be shown later that the intercept is the prompt critical point. Table 2 gives the intercept in terms of reactivity as determined from the control rod calibration. If the intercept is truly the prompt critical point, this amount of reactivity should be equal to the worth of the burst rod above one dollar.

The extension of the initial period measurement to the region below prompt critical required the use of Channel 3D. Measurements were made for periods ranging from several seconds to 3 milliseconds. The results are given in Figure 24. The burst rod worth determined above was used in determining the amount of reactivity present at each point of measurement.

The polyethylene curves in Figures 21 and 22 show a definite departure from linearity. This departure could be predicted on the basis of the parameters calculated in Chapter 5. The relatively soft energy spectrum of neutrons escaping from the polyethylene increases the importance of the energy groups which have the largest time constants τ_3 and τ_4. As the reactor period decreases the approximation that

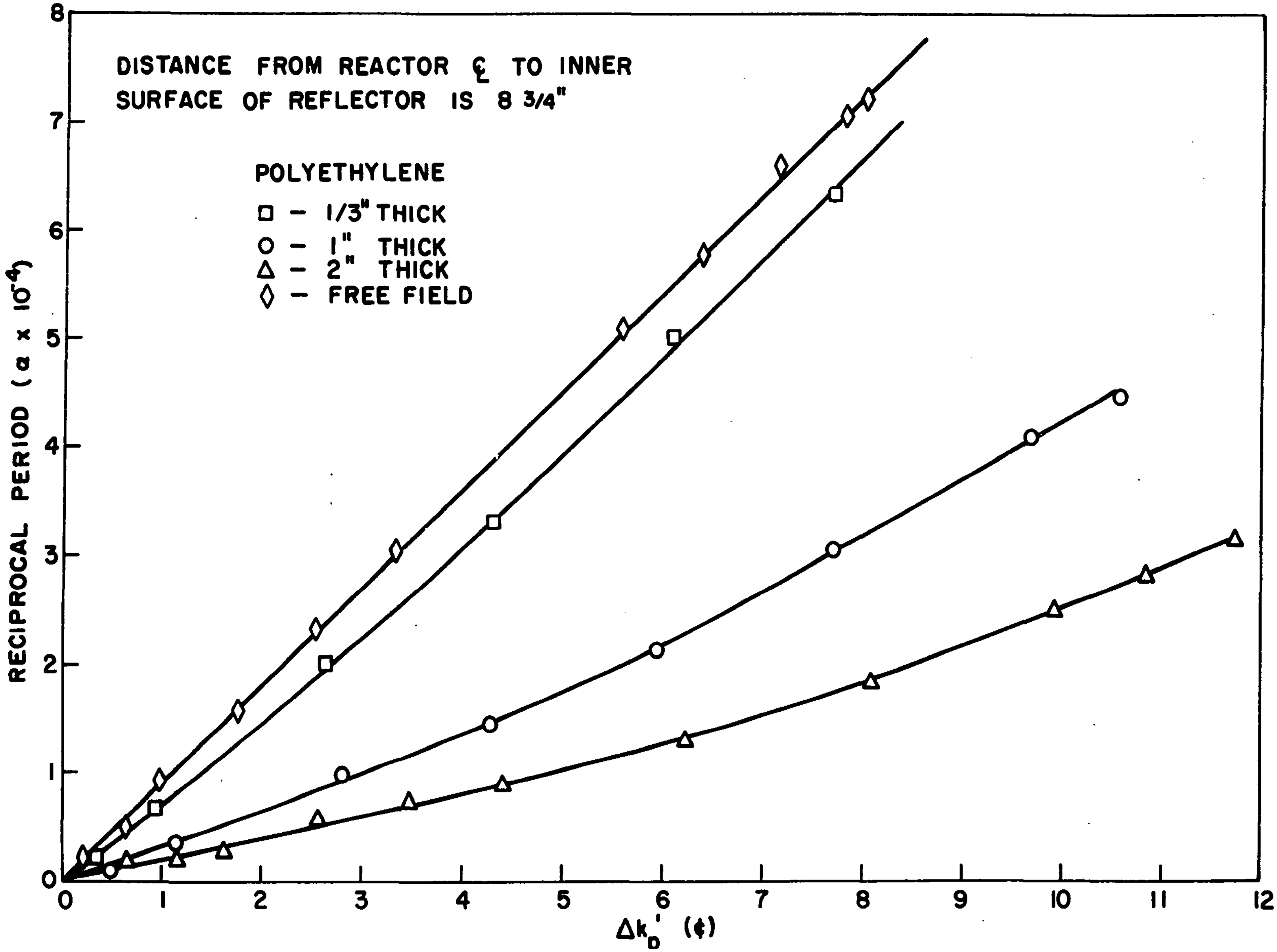

Reciprocal period as a function of prompt reactivity for various polyethylene reflectors at a fixed position

Figure 21

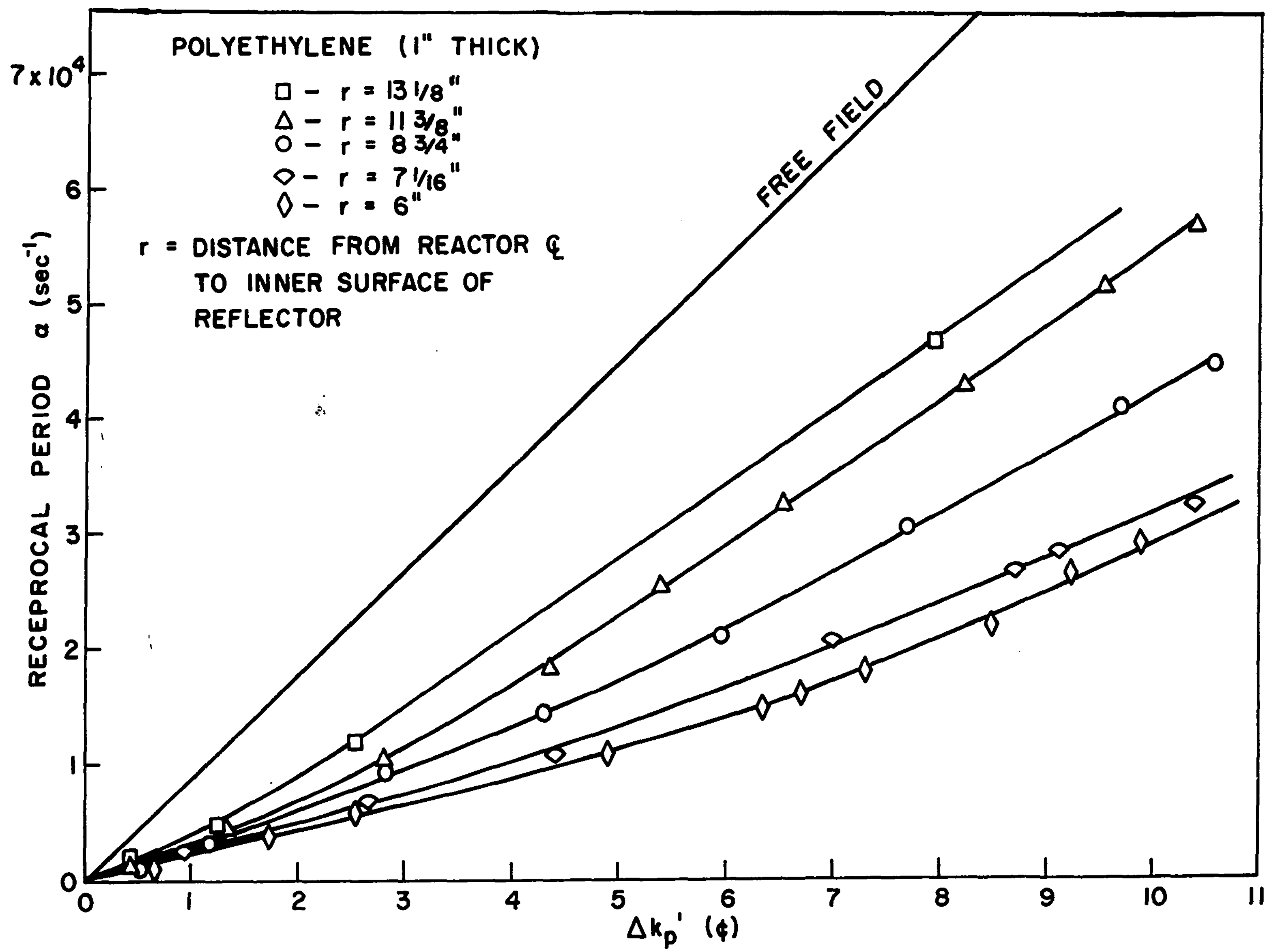

Reciprocal period as a function of prompt reactivity for various polyethylene reflectors of uniform thickness

Figure 22

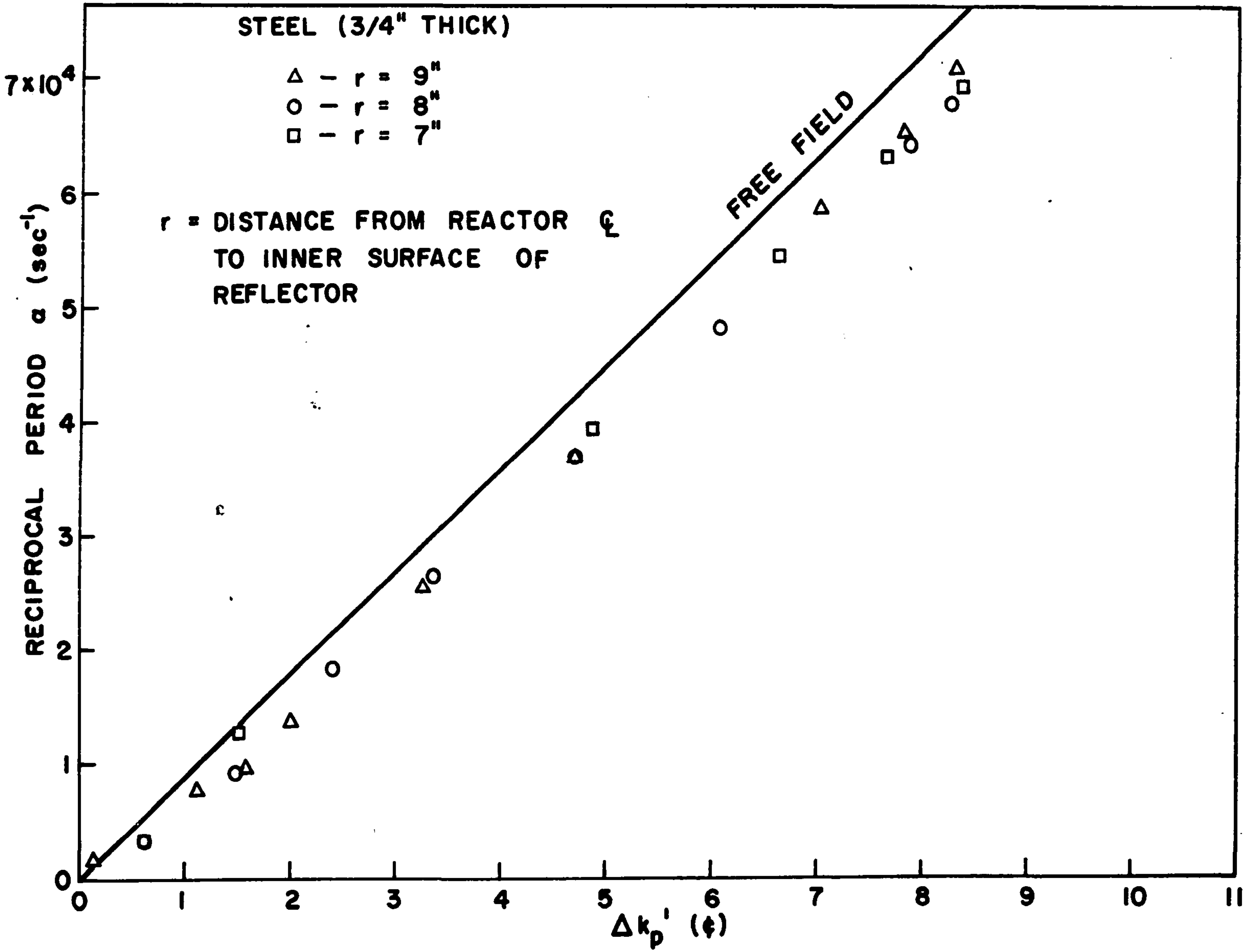

Reciprocal period as a function of prompt reactivity for various steel reflectors of uniform thickness

Figure 23

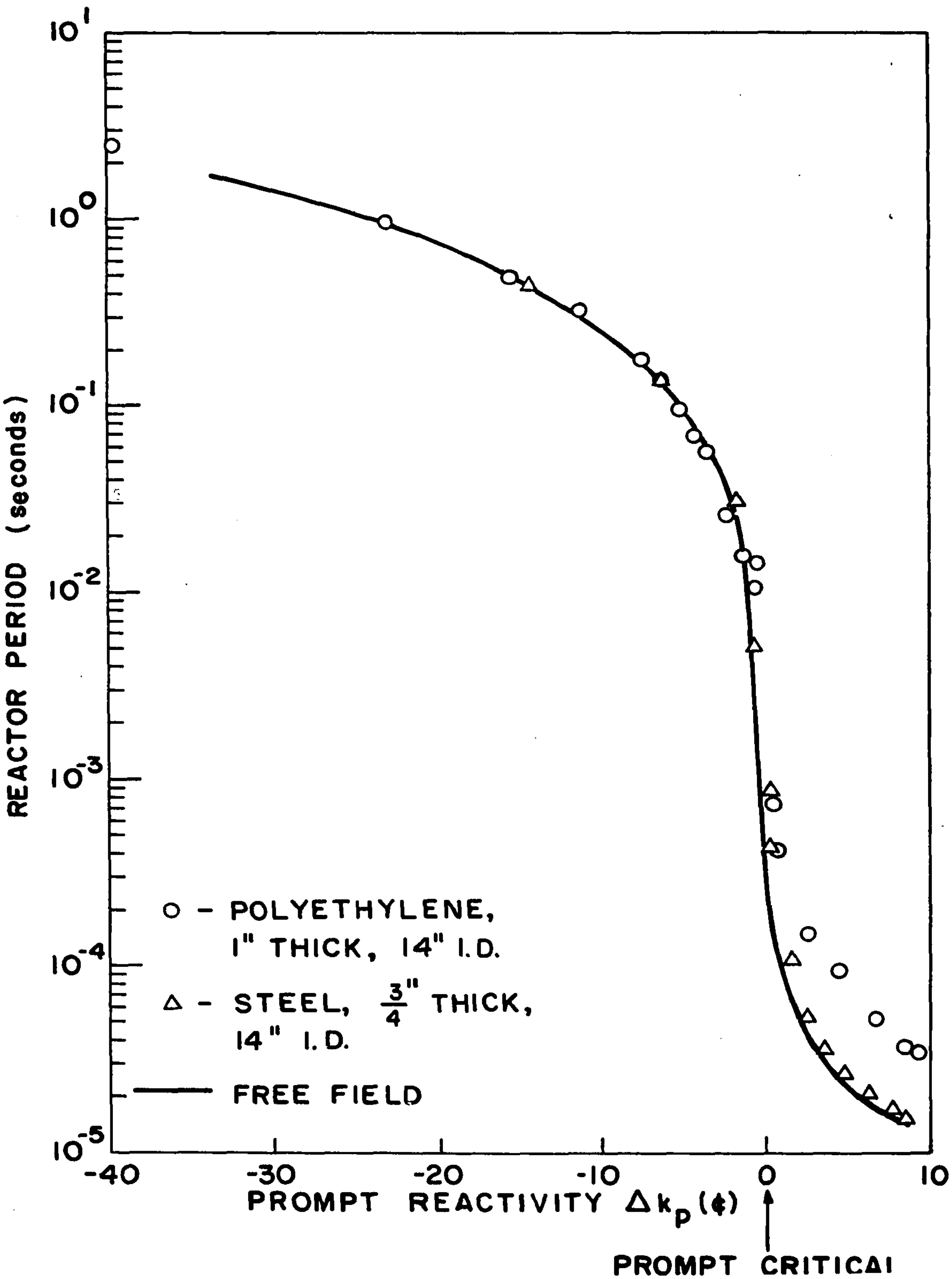

Reactor period as a function of prompt reactivity

Figure 24

$$e^{-\frac{\tau_4 + \tau_2}{T}} \simeq 1 - \frac{\tau_4 + \tau_2}{T}$$

used in arriving at the linear expression, equation (48), is not valid for the low energy groups and a non-linear curve results if there is a significant number of neutrons in the low energy groups.

The linear relation between prompt reactivity and initial period shown in Figure 23 results from the relatively hard energy spectrum of neutrons escaping from the steel reflector. The fractions β_j for the low energy groups are insignificant and the application of equation (48) is valid.

A least squares analysis was made for free field data in Figure 21 and the 14 inch diameter steel data in Figure 23 to determine the prompt neutron decay constant (page 29).

The results are given in Table 3 and show a decrease in the prompt neutron decay constant which implies an increase in neutron lifetime as would be expected on the basis of equation (43). Using 0.0065 for $\gamma\beta$ the free field prompt neutron lifetime is calculated to be 7.08×10^{-9} seconds.

TABLE 3

Inner Diameter of Reflector	Reflector Worth	Prompt Neutron Decay Constant (10^6/seconds)
14	99.9	$.845 \pm .020$
16	66.51	$.860 \pm .020$
18	46.31	$.910 \pm .020$
free field	free field	$.918 \pm .010$

Figure 24 shows that there is very little effect on the relation between reactor period and reactivity for relatively large periods for either the polyethylene or the steel reflector. Since the time constants τ_3 and τ_4 are insignificant compared to large reactor periods for all reflected neutron groups, there should be no observable effect.

Burst Yield Measurements

The total yield of the burst was obtained indirectly using the iron constantan thermocouples discussed previously. For a given fission distribution throughout the fuel assembly, the total yield of the burst is directly proportioned to the change in temperature indicated by the thermocouples. The change in the spatial fission profile for the reflectors used in this experiment was estimated to produce an error of no greater than two percent in the determination of yield. The temperature as recorded on the strip chart recorder could be read to within 0.5 °C. Thus an error of from five percent for a 10°C burst to 0.5 percent for a 100°C burst was possible due to temperature reading error.

The programmed timer was set such that a scram occurred before significant heating took place in the plateau region of the burst. The setting was chosen in such a way as to allow only a very small portion of the plateau to appear on the oscilloscope trace of Channel 1P. The observation of this plateau region insured that the safety block did not move out during the burst and invalidate the data. This procedure was quite successful and the temperature rise due to the plateau was estimated to be no more than 2.5°C for all reflector configurations.

The yield data is plotted in terms of the temperature rise as a function of initial period in Figures 25, 26, and 27. Figures 25 and 26

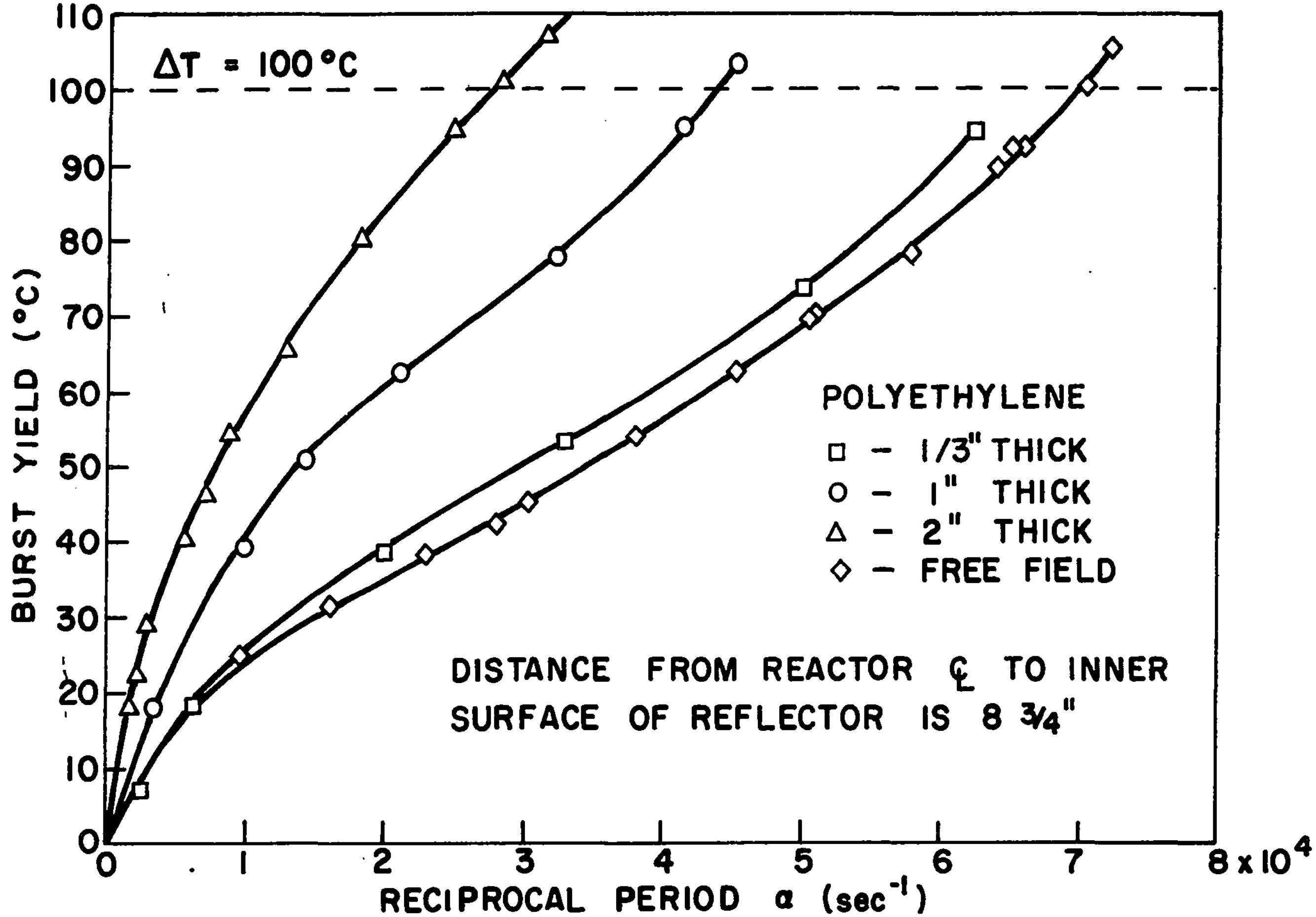

Energy release per burst as a function of reciprocal period for various polyethylene reflectors

Figure 25

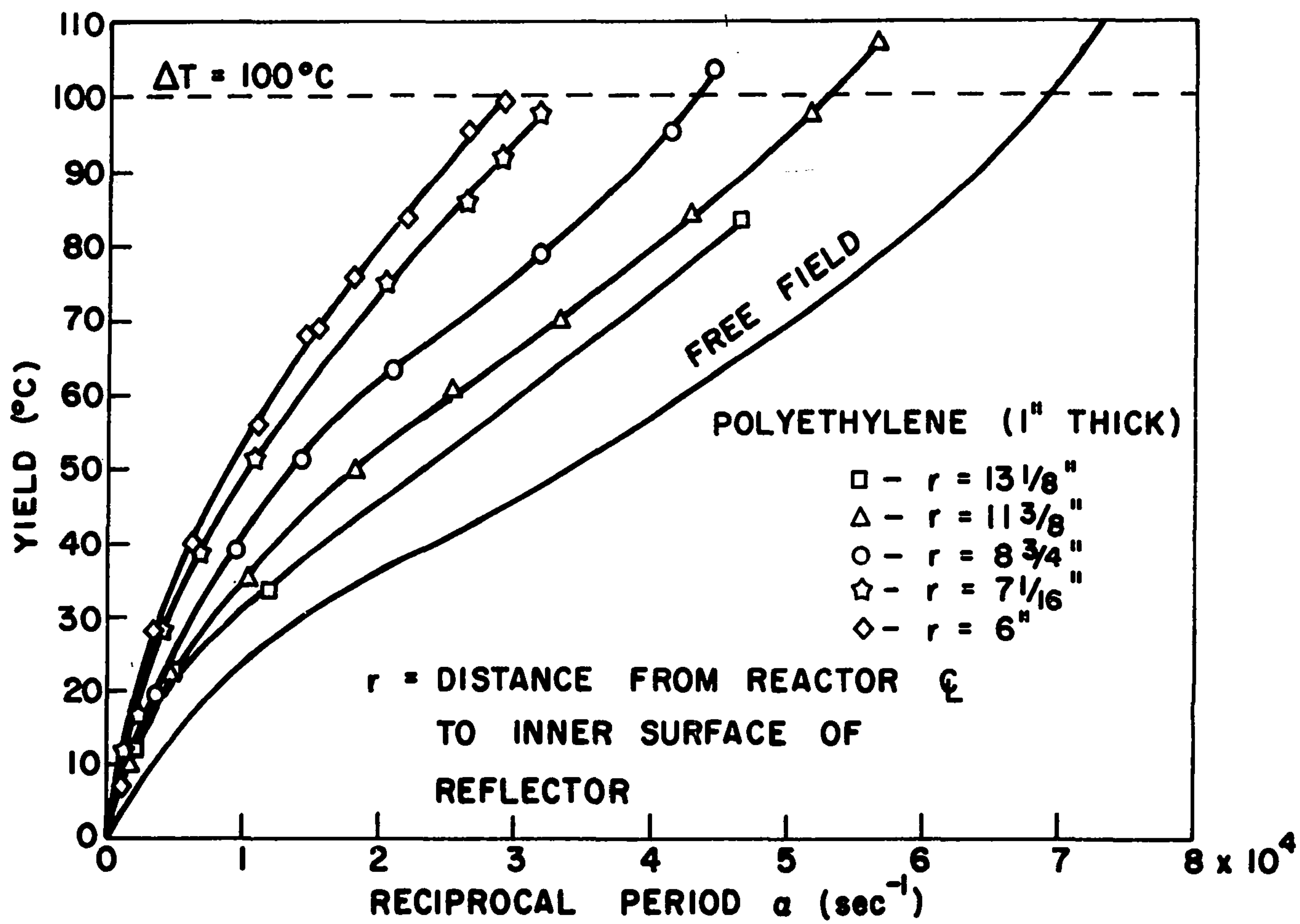

Energy release per burst as a function of reciprocal period for various polyethylene reflectors

Figure 26

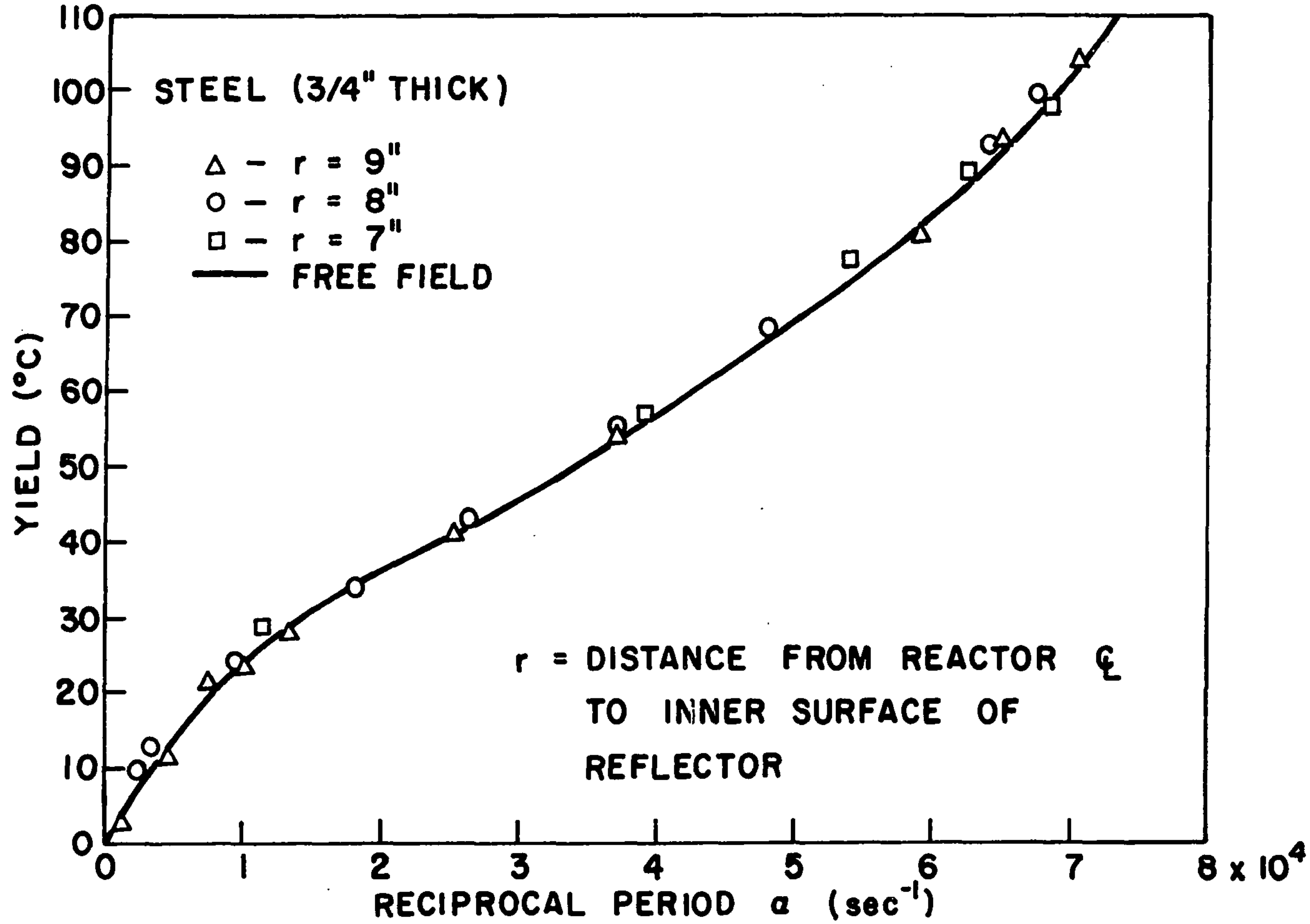

Energy release per burst as a function of reciprocal period for various steel reflectors

Figure 27

show that the energy released for a given initial period increases considerably when polyethylene is used as a reflector. The yield for a given initial period was increased by about a factor of 2.5 over that of the free field when the two inch thick reflector was used. The relative increase in yield lessened however as the reactor period decreased. This effect could be attributed to the relatively slow response of the lower energy reflected neutrons. The reactor is in effect "running away from" the lower energy reflected neutrons. The steel had no significant effect on the yield for a given initial period. Most of the data points for steel were above the free field line as shown in Figure 27, which is to be expected since the slight increase in lifetime implied by Table 3 would have a broadening effect on the burst shape.

The yield and fission rate data can be related to fissions and fissions per unit time using the conversion factor of $1.82 \times 10^{14} \frac{\text{fissions}}{^{\circ}\text{C}}$ [2] which was obtained for Godiva II.

Burst Width and Peak Fission Rate Measurements

The determination of the width of the pulse at half maximum and the peak fission rate was accomplished using the photographs of the oscilloscope traces from Channels 1P and 3P. The burst width at half maximum power was obtained directly from the photograph. The maximum error in this determination was from resolution in the photograph of the oscilloscope trace. The error varied depending on the ability of the experimenter to perdict the oscilloscope settings which would give the best resolution. In general the results were accurate to within $\pm$ 5 percent; on occasion, however, the errors reached $\pm$ 10 percent. Results of burst width measurements are shown in Figures 28 and 29.

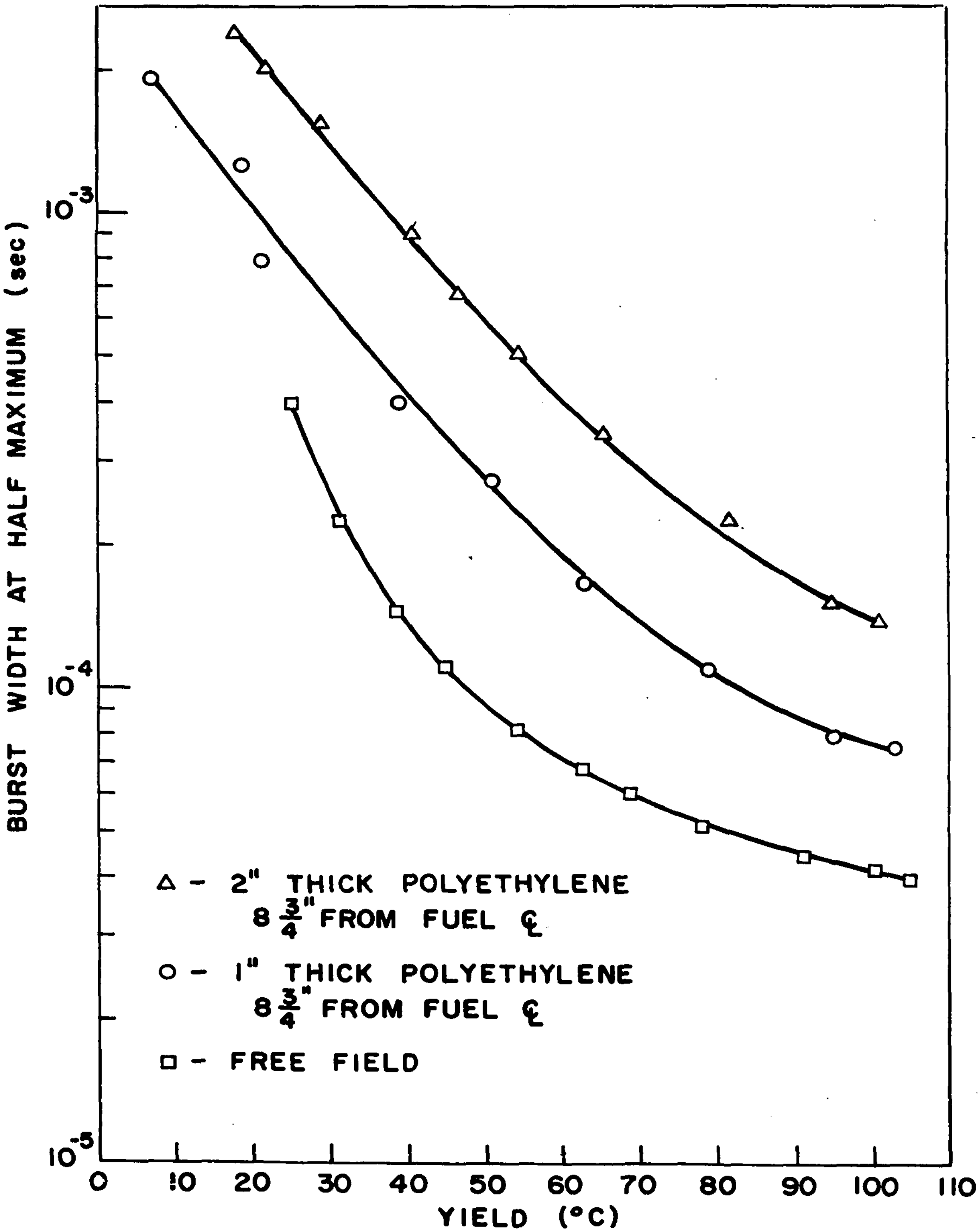

Burst width at half maximum fission rate as a function of burst yield for various polyethylene reflectors

Figure 28

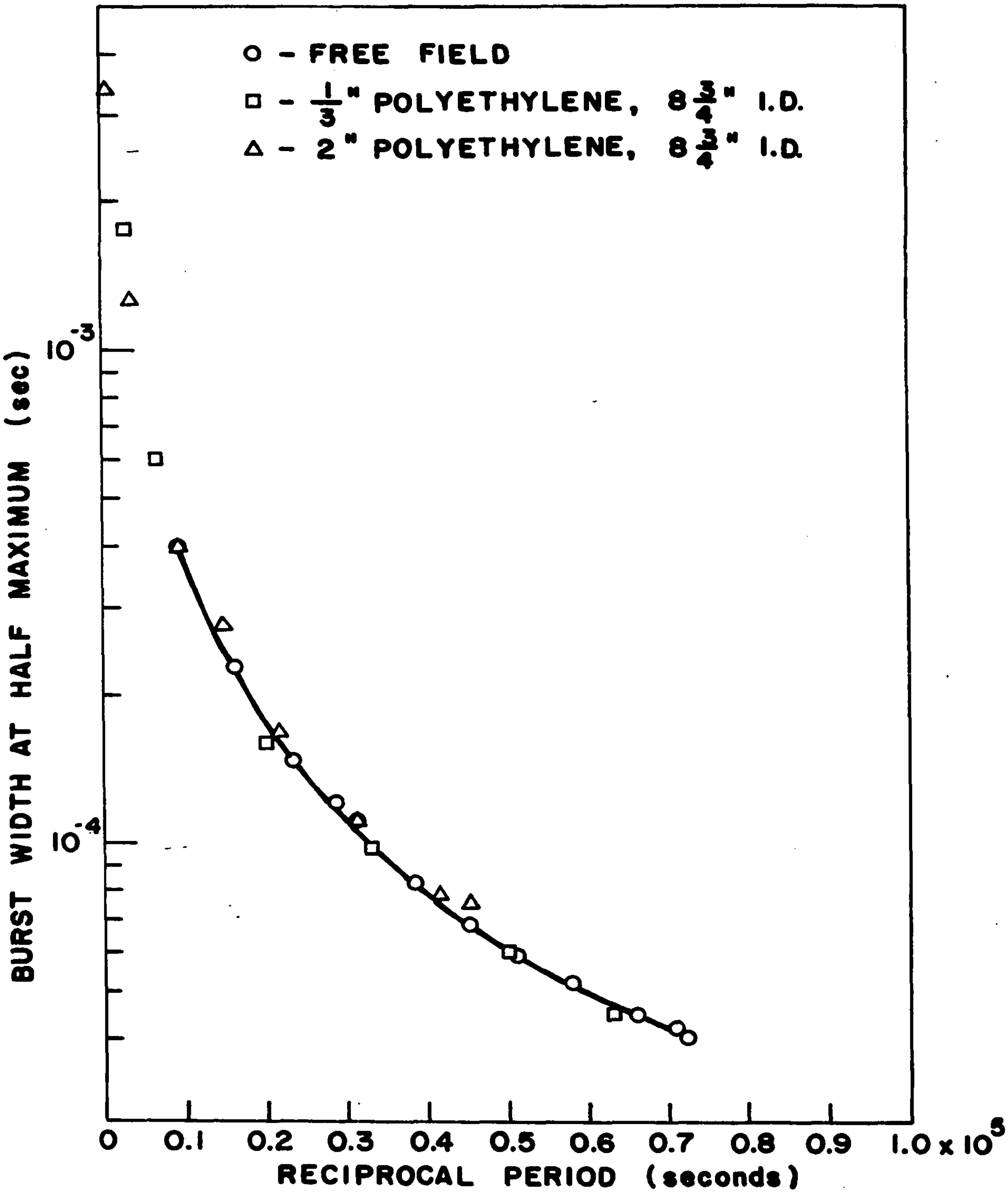

Burst width at half maximum fission rate as a function of reciprocal period for various polyethylene reflectors

Figure 29

The peak fission rate was determined by integrating under the pulse curve with a planimeter and setting the result equal to the burst yield to obtain a calibration of the vertical axis of the oscilloscope trace. Again the error in general was estimated to be less than 3 percent. Results of these measurements are shown in Figure 30.

Figures 28 and 30 exhibit the broadening effect moderating reflector has on the burst shape.

For a given yield there is a considerable increase in the burst width and a considerable decrease in the peak fission rate.

Firgure 29 indicates that the relation between burst width and initial reactor period is independent of the reflector. T. F. Wimett [15] using a bare kinetics model has shown that the relation between burst width and initial period is independent of the neutron lifetime. If the reflector effect is treated as a change in the prompt neutron lifetime then the results shown in Figure 29 are in agreement with the relation developed by Wimett.

Dosimetry

A limited amount of dosimetry was performed. This work consisted of neutron flux mapping and determining the relative "hardness" of the neutron flux at the inner surface of the reflector.

Flux Mapping. The neutron flux along a horizontal radial line was determined by irradiating nickle strips in the "glory hold" with a relatively high yield burst. The nickle strips were cut into segments, each of which was weighed and the activity determined. The activity per gram per °C of burst yield was then obtained. The results are given in Figure 31. The standard deviation in the data was less than one percent.

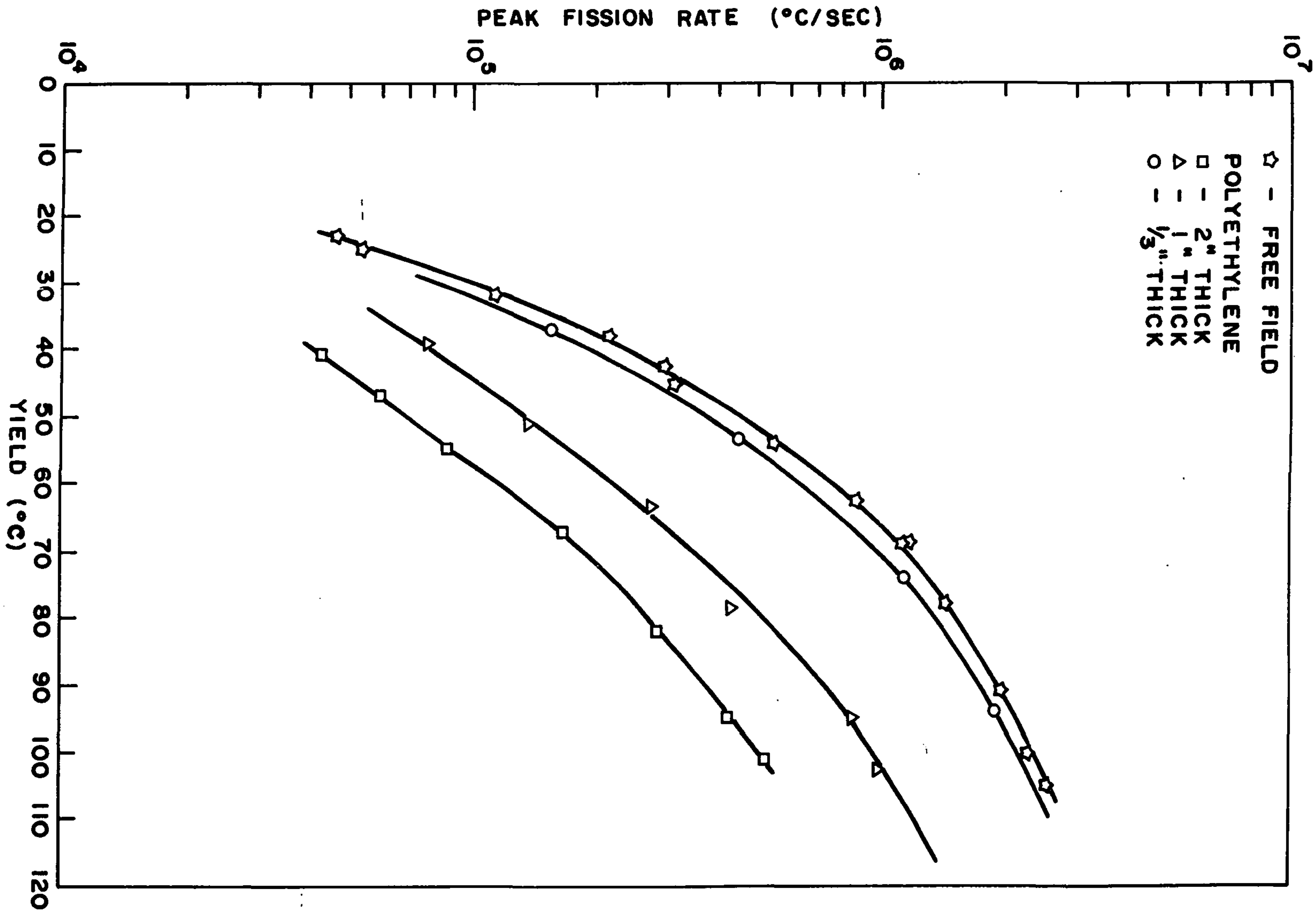

Peak fission rate as a function of burst yield for various polyethylene reflectors

Figure 30

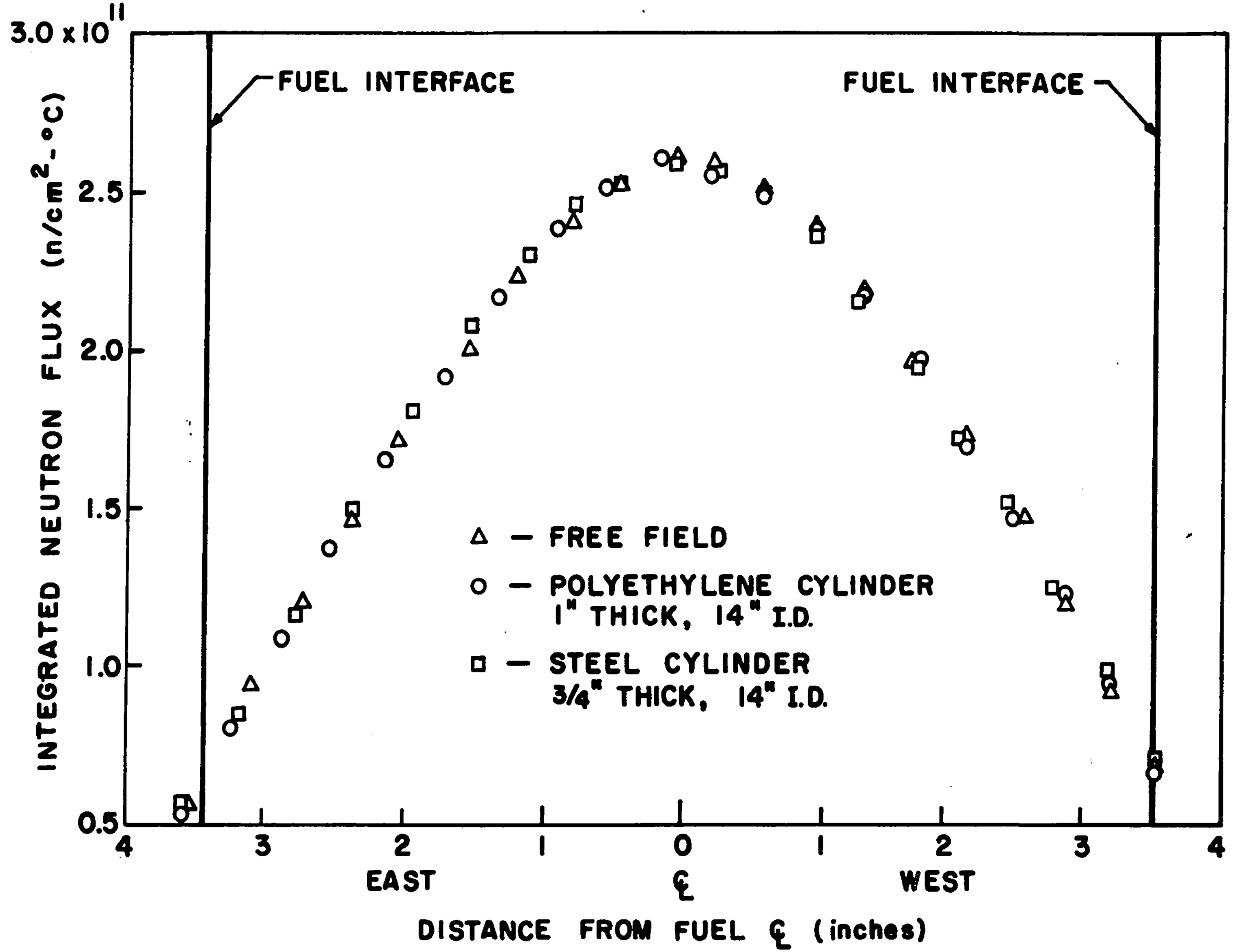

Integrated neutron flux in fuel above 3 mev as a function of radial position

Figure 31

The neutron flux between the reflector and the fuel assembly was also mapped. Sulfur pellets were used for this determination. The spectral dependence for sulfur and nickle activation is essentially the same. The sulfur data was normalized to activity per gm. per °C and the results are given in Figure 32. The standard deviation in the data was less than one percent.

Spectral Investigation. An indication of the relative "hardness" of the neutron flux between the reflector and the fuel assembly was obtained by comparing the activation of sulfur pellets, indium foils, and cadmium covered indium foils located at the inner surface of the reflector. As a further indication of this "hardness," intrinsic thermocouples were placed on the inner surface of the reflector. One thermocouple was wrapped with cadmium. The ratio of the two voltages as obtained from the oscilloscope trace provided an indication of the "hardness" of the neutron spectrum. The ratio of the bare thermocouple output to the output of the cadmium covered thermocouple was $4.0 \pm .2$ for 1 inch thick polyethylene and $1.0 \pm .2$ for 3/4 inch steel.

Unfortunately, drift in the instruments used to determine the activity of the indium foils rendered the data quantitatively unuseful. The data indicated an increase in the lower energy neutron flux with increasing thickness of the moderator, but the variation in the data was such that no conclusions could be drawn with confidence.

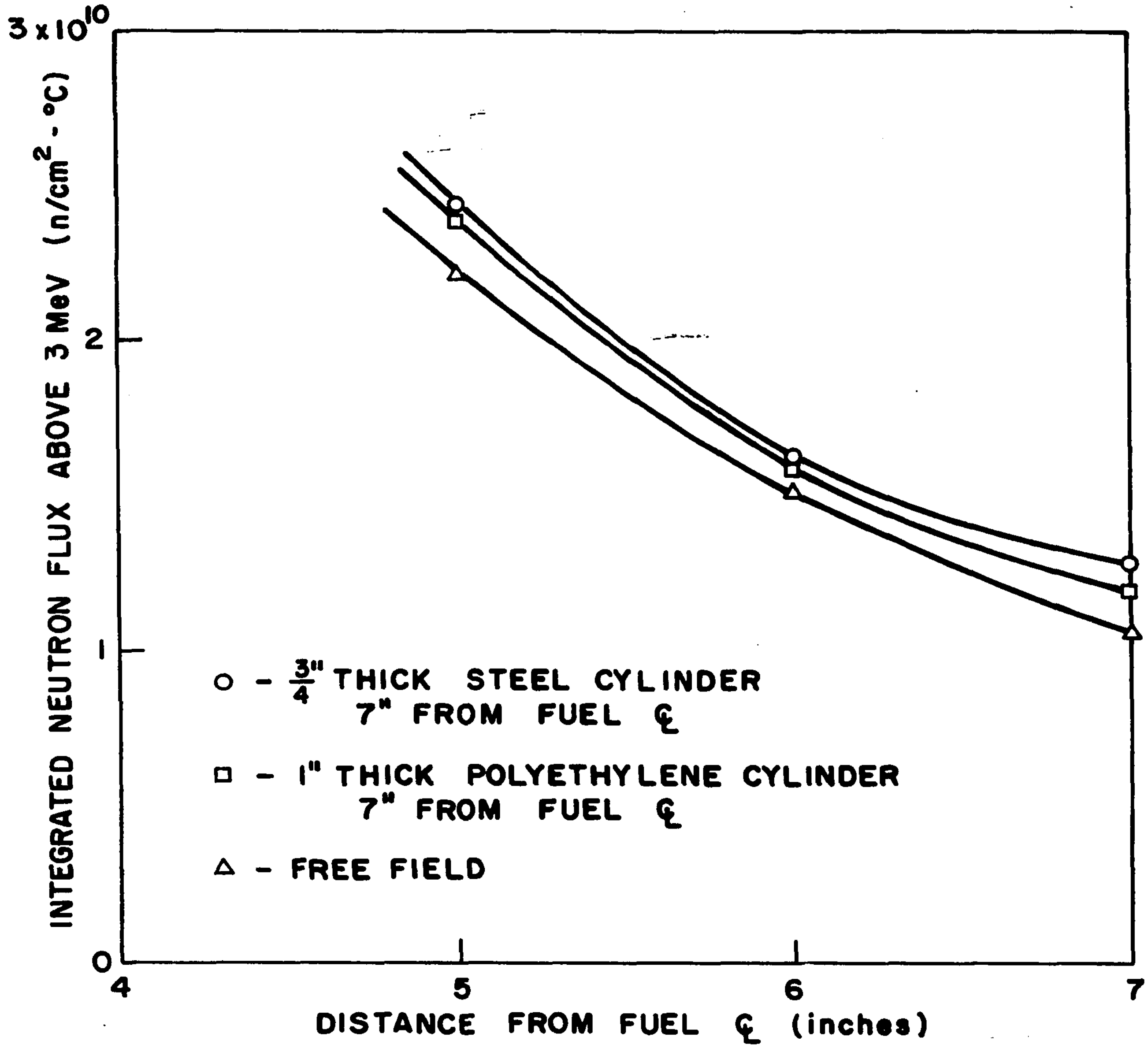

Integrated neutron flux above 3 mev between fuel and reflector

Figure 32

CHAPTER VII

DISCUSSION OF RESULTS

Calculations

In general the results of the calculations described in Chapter IV were in good agreement with those measured values which are available in the literature. Each of the calculations is discussed below.

The radial fission distribution calculated for the SPR I differed from the measured flux distribution near the surface of the core. The calculations consumed considerable computer time which was protortional to the number of spatial points used in the calculations, the statistics required for a given point and the degree of convergence desired. Although a better agreement with the measured value may have been reached by further operations the results indicated in Figure 1 were felt to be adequate.

The neutron lifetime calculated differed from the measured value of 7.1×10^{-9} seconds by 20 percent. This is a characteristic common to all calculations of neutron lifetime. Calculated prompt neutron lifetimes are invariably lower than the measured values by 15 percent to 30 percent. This difference could be attributed to, as Brunson [19] suggests, uncertainty in the effective delayed neutron fraction, or to uncertainties in the cross sections used in the calculations. The calculated value was sufficiently close to the measured value to substantiate the validity of the Monte Carlo calculation.

The neutron multiplication factor was calculated to be essentially unity for the SPR I geometry. This again serves to substantiate the validity of the Monte Carlo calculations.

The SPR I leakage spectrum calculated by the Monte Carlo code agrees reasonably well with that measured by Rosen, et. al. [40]. The only significant difference between the two assemblies is that Godiva I has a spherical geometry as opposed to the cylindrical geometry of the SPR I. The differences in the spectra can be attributed to uncertainty in the reported values for cross sections, particlarly the inelastic cross sections in the high neutron energy range, and the statistical uncertainty in Rosen's measurements. The agreement between the calculated leakage spectrum and the leakage spectrum measured for Godiva I is shown in Figure 2.

It is practically impossible to accurately measure the leakage spectrum from the reflector since it represents only a small percentage of total spectrum in the space between the core and the reflector. However, the calculated leakage spectrum from the reflector shown in Figures 4 and 5 appears to be reasonable for a moderating reflector since a higher fraction of the returned neutrons will be at lower energies due to scattering in the reflector. The peak in the spectrum at about 0.6 mev shown in Figure 5 may be attributed to the nearly direct return of fuel leakage neutrons by 180° scattering with carbon in the polyethylene.

Calculated values of the time constant τ_3 are shown in Figure 6. The time constants τ_3 and τ_4 are dependent on both the reactor leakage spectrum and the reflector leakage spectrum. The decrease in average neutron energy between the reactor leakage spectrum and that of the reflector results in the relatively high value of τ_3 for low energy neutrons while the fact that τ_4 is proportional to the reciprocal of neutron velocity of the returning neutrons accounts for the high values of τ_4 at the lower energies. These time constants also depend upon the geometrical configuration of the system. If the leakage spectra are accurately determined as indicated above, then the values of the time constants are valid since the geometrical dependence is easily evaluated.

The calculation of neutron effectiveness as a function of energy is strongly dependent upon the measured scattering, fission and capture cross sections of Uranium 235 and Uranium 238 over the entire energy spectrum of the reflector leakage neutrons. Since appropriate values for the fission and capture cross sections, particularly in the resonance region, are hard to determine, it is felt that considerable error could exist in the effectiveness value calculated for some of the energy groups. Before better information concerning the cross sections is available these calculations must suffice.

It is to be noted in Figure 3 that the calculated effectiveness falls off sharply for the lowest energy groups, This is due to the increase in the absorption cross section of cadmium with decreasing energy.

It is evident from the calculated reflector leakage spectra that the neutrons returned to the core represent a continuum in energy and it would be difficult to represent this return of neutrons by single group time constants τ_3 and τ_4. The calculations indicate that the principle time constant for the geometrical configurations of this study was τ_4, which becomes increasingly more important as the distance between the reactor and the reflector increases.

Experiment

In general the experimental results agreed quite well with the predictions of the reflected kinetics model developed in Chapter III. The effect of moderating reflectors on the burst characteristics is quite pronounced while the steel reflectors appeared to have little effect. This is evident from an inspection of the burst data given in Chapter VI. One would expect that the effect of the steel reflectors would be quite small since little degradation of the neutron energy occurs upon scatter of the neutron from a heavy nucleus. Since there is little degradation of the neutron energy, the time constants τ_{3_j} and τ_{4_j} would be quite small for all effective neutron groups and hence would have little effect on the burst behavior of the reactor. The most significant effect of the reflectors is shown in Figure 21 which shows a significant departure from the linear relationship between reciprocal period and prompt reactivity that has characterized all previous burst investigations.

The discussion of results of previous investigations the reflector effect has invariably been described as a change in the prompt neutron lifetime. In view of the departure from linearity for moderating reflectors this representation is invalid. This departure from linearity is predicted by the reflected kinetics model developed in Chapter III.

Implications of the Kinetic Model

The purpose of the preceding work was to develope and substantiate a model which would describe the effect of reflecting systems on the burst behavior of a burst reactor. The focal point of the following discussion is the reflected inhour equation (35) and its application to the description of the kinetic behavior of the SPR-I fuel assembly when surrounded by polyethylene reflector.

Period and Worth Measurements

Calculations which were performed to determine each of the parameters necessary for the model described in Chapter VI. The results of these calculations are indicated in the various tables and figures of that section.

The presence of a cadmium shield prevents the return to the core of reflected neutrons having energies less than .2 ev. Taking .2 ev as a lower limit on the energy of the reflected neutrons returning to the fuel, one determines that τ_{4_j} is less than 5×10^{-5} seconds for the greatest separation of core and reflector investigated. The maximum τ_{3_j} was determined from Figure 6 to be less than 4×10^{-6}. τ_2 was determined to be much less than 1×10^{-7} seconds using the calculated SPR-I leakage spectrum, Figure 2.

Since $\gamma_r \beta_r$ must be less than or equal to the measured worth of the reflector it can be shown on the basis of the calculations that the reflector term in equation (35) for periods greater than 0.1 second is much less than the effect of delayed neutrons. That is:

$$\sum_j \gamma_j \beta_j \frac{\frac{\tau_{3_j}}{T} + 1 - e^{-\frac{\tau_2 + \tau_{4_j}}{T}}}{\frac{\tau_{3_j}}{T} + 1} << \frac{\gamma_i \beta_i}{1 + \lambda_i T} \quad ; \quad \begin{array}{l} i = 1, M \\ j = 1+M, N \end{array}$$

Thus, the model implies that for the geometrical configurations of the experiments reported in this paper, the bare reactor inhour relation was applicable to the reflected case providing the reactor periods were greater than .1 second. .

For values of T greater than 10^{-4} seconds, none of the time constants of the reflected groups is greater than T and equation (55) is not applicable. The approximations used in obtaining equation (49) are valid, however, and the conclusions drawn from this equation that there would exist a linear relationship between prompt reactivity and reciprocal period for reactivity insertions near prompt critical may be utilized. By measuring the reactor period for reactivity values slightly above prompt critical where T is greater than 10^{-4} seconds, equation (49) may be used to predict the value of the prompt critical reactivity. When reciprocal period is plotted as a function of reactivity in this region, the linear extropolation of the resulting curve intercepts the reactivity axis at the prompt critical reactivity value. A displacement of this intercept with reflector from the intercept without reflector is equivalent to a change in the worth of the burst rod. The value of the reactivity above the intercept of this curve is the prompt reactivity , $\Delta k'_p$, used in the presentation of experimental data in Chapter VI.

To substantiate these arguments for period measurements and burst rod worth measurements an experimental inhour relation was obtained for the free field and for the reflected cases. The results are given in Figure 24. The reactivity determinations were based on the arguments above and the results of Figures 18 and Table 2 were used in the determination of the reactivity. The fact that the data points fall on the free field curve of Figure 24 in the regions below prompt critical is sufficient support for the above arguments and represents a significant point of agreement between the model and experiment.

Prompt Critical Measurements

In order to correlate the measured results with those predicted by the model it is convenient to express the inhour relation in the following form:

$$\Delta = \frac{T}{\sum_j \gamma_j L_j^*} \sum_j^1 \frac{\gamma_j L_j^* \left(\frac{\tau_{3_j}}{T} + 1 - e^{-\frac{\tau_{4_j}}{T}} \right)}{\frac{\tau_{3_j}}{T} + 1} \tag{66}$$

where

$$\Delta = \frac{\rho\,(\$) - \frac{\ell^*}{\beta T}}{W(\$)}\ T$$

and τ_2 has been ignored as negligibly small.

Consider the case where a given thickness of reflection material is maintained but the distance between core and reflector is allowed to vary. Then for a given reciprocal period the only change in Δ is through the time constant τ_{4_j}. Thus Δ is represented as

$$\Delta^* = \Delta\,(J, \frac{1}{T})$$

For zero separation Δ^* is given by

$$\Delta^*\Big|_o = \frac{1}{\sum_j \gamma_j L_j^*} \sum_j \frac{\gamma_j L_j^* \ \tau_{3_j}}{\frac{T_{3_j}}{T} + 1}$$

And for eactor periods which are large compared to T;

$$\Delta^*\Big|_o \doteq \frac{1}{\sum_j \gamma_j L_j} \sum \gamma_j L_j^* \ T_{3_j}$$

Thus $\Delta^*\Big|_o$ for large periods is merely the weighted mean residence time of the neutrons in the reflector.

For periods which are large compared to the time constants τ_{4_j}, e.g. $T > 10^{-4}$ seconds,

$$\Delta^* = \frac{\sum_j \gamma_j L^*_j \left(\tau_{3_j} + \tau_{4_j} \right)}{\sum_j \gamma_j L^*_j}$$

$$\text{and} \quad \left(\frac{\partial \Delta^*}{\partial J}\right)_T = \frac{1}{J} \frac{\sum_j \gamma_j L^*_j \tau_{4_j}}{\sum_j \gamma_j L^*_j} \tag{68}$$

Therefore $J\left(\frac{\partial \Delta^*}{\partial J}\right)_T$ is the mean transit time of neutrons returning from the reflector.

Using the experimental data of Figure 21, Figure 22 and Table 2 $\Delta^*\Big|_{T=const}$ was determined as a function of J. The values of $\Delta^*\Big|_{T=const}$ were obtained by least squares analysis of the points in Figures 21 and 22 for which the period was greater than 10^{-4} seconds. A second least squares analysis was performed to fit these values to a straight line. From this analysis it was determined that the mean residence time of the neutrons in the reflector is less than 3×10^{-7} seconds which is consistant with the calculated value of 1.04×10^{-7} seconds. The slope of the straight line obtained indicates that the mean value of $\frac{\tau_{4_j}}{J}$ is $2.27 \times 10^{-7} \pm .35 \times 10^{-7}$ sec / cm. This compares reasonably well with a calculated value 1.14×10^{-7} sec /cm. and demonstrates that as the separation distance increases the effect becomes more pronounced. Thus agreement between the experimental results and the theoretical model is demonstrated in the prompt critical region for periods much greater than the calculated values τ_{3_j} and τ_{4_j}.

According to the reflected inhour relation Δ should be independent of reactor period in the range of periods large compared to the reflector time constants. For small periods, however, the model indicates that Δ is a function of the reactor period and that the change in Δ with decreasing periods is negative and is greatest for those reflectors located at the greatest distance from the fuel.

To demonstrate that the experimental data supports this view, Δ was evaluated for several values of the period. The results are given in Table 4 and show that the greatest change in Δ occurs for large separation distance and that the change is negative.

As further evidence of the agreement equation (35) was evaluated using the constants calculated for the one inch thick polyethylene cylinder located 8 3/4 inches from the fuel center line. The results are given in Figure 33 in addition to the points measured for this geometry. It is noted that the model predicts the amount of reactivity required to produce a given reciprocal period to within 13 percent of the measured value. Considering the uncertainty in the published cross sections used in determining the effectiveness and in the approximations made to calculate the reflector parameters this represents good agreement between the model and experiments.

The neutron effectiveness calculation is most likely the greatest single contributor to the differnece between the results calculated from the model and the experimental results. Another source of error is the estimation of the effective transit distance. A larger value of the effective distance would give better agreement for the curves in Figure 33 and for the weighted mean transit times.

Softer calculated reflector leakage spectra would also improve the agreement between the theoretical and experimental results. The

TABLE 4

Δ as a Function of Reciprocal Period for Various One Inch Thick Polyethylene Reflectors

Inner Diameter of Reflector (inches)	Reciprocal Period (seconds)	Δ (seconds)
26.25	1×10^{4}	5.9×10^{-6}
22.75		4.85×10^{-6}
17.50		3.1×10^{-6}
14.13		2.45×10^{-6}
12.50		1.8×10^{-6}
26.25	2×10^{4}	4.9×10^{-6}
22.75		3.95×10^{-6}
17.50		2.65×10^{-6}
14.13		2.0×10^{-6}
12.50		1.5×10^{-6}
26.25	3×10^{4}	3.9×10^{-6}
22.75		3.2×10^{-6}
17.50		2.25×10^{-6}
14.13		1.75×10^{-6}
12.50		1.25×10^{-6}
26.25	4×10^{4}	3.1×10^{-6}
22.75		2.7×10^{-6}
17.50		2.0×10^{-6}

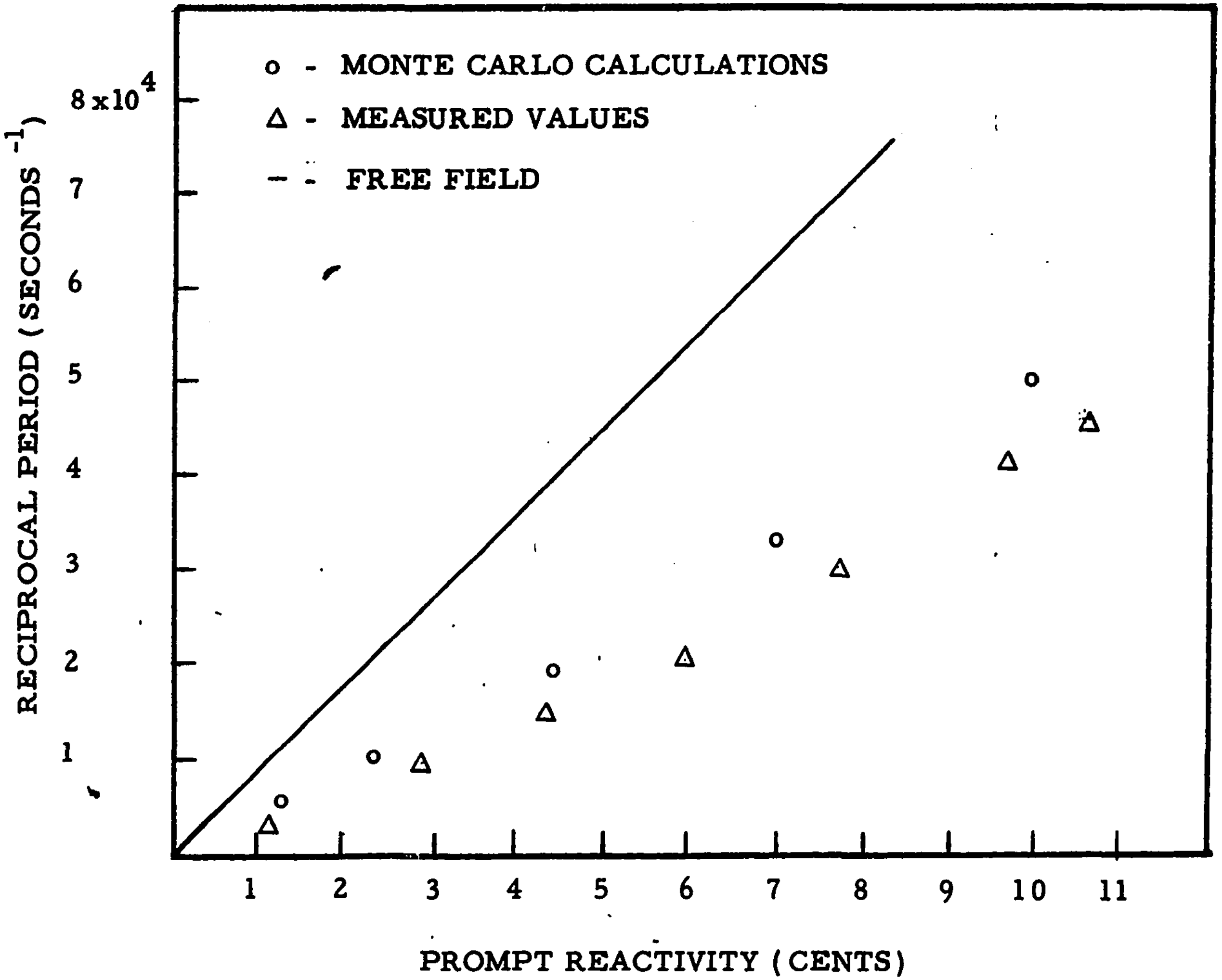

Solution to the reflected inhour equation using the calculated parameters for a one inch thick polyethylene reflector with inner surface 8 3/4 inches from the fuel center line.

FIGURE 33

statistical variation would be reduced by further calculations and could possibly lead to a softer spectrum.

The effect of multiple reflection which has been neglected in this study, could possibly account for a slight portion of the difference between experimental and theoretical results. Including the effect would undoubtedly imporve the agreement since a softer spectrum and longer time constants would result, but the percentage of neutrons undergoing multiple reflection is estimated to be very small. The Monte Carlo code used in the present investigation could be modified to adequately account for multiple reflection.

In summary the following points are to be emphasized:

1. A reflector has a large affect on the burst characteristics of a pulse reactor. The effect is most pronounced for moderating materials. This supports R. L. Long's conclusions (3).

2. The model proposed is adequate to describe the effect of reflectors on the kinetic behavior.

3. The effect of a reflector separated from the core is strongly dependent on the transit time of the reflected neutrons in returning to the fuel.

4. The model successfully provides an explanation for the anomalies that have occured in previous investigations.

As an extension of this work, the calculated reflector parameters could be used with the reflected kinetic equations presented here to predict the burst behavior of a reflected system in regions of reactivity insertion not encompassed by the experiments of Chapter V.

An experiment program could then be initiated which would allow extension of the experimental data of Chapter VI into regions of greater initial reactivity. This should serve as further verification of the reflected kinetic model. The question of decoupling discussed on page 30 has not been completely answered. This could be resolved by the programs suggested above.

APPENDIX A

DESCRIPTION OF A TYPICAL NEUTRON PULSE

A pulse in the neutron level of a burst reactor is initiated by the insertion of a large amount of reactivity such that the reactor is super prompt critical. In this condition the reactor is super critical on the basis of prompt neutrons alone and its neutron level will increase at a rate such that the delayed neutron contribution can be neglected.

Initially the time dependent behavior of the neutron level can be represented by;

$$n(t) = n(t_o)\ e^{\frac{t - t_o}{T}}$$

where $n(t_o)$ is some reference level and T is the reactor period for that reactivity insertion.

When the fission rate becomes large enough to result in significant heating of the fuel the core will undergo thermal expansion. This thermal expansion represents a negative reactivity input due to the increase of neutron leakage from the fuel and results in a net reactivity below prompt critical. Since the system is then subscritical on the basis of prompt neutrons alone the fission rate will decrease at a rate dictated by the decay of the delayed neutron precursors produced during the initial part of the pulse and by the negative reactivity being added to the system due to heating.

Since the decay constants of the delayed neutrons are long compared to the time scale of a typical pulse, a region of relative stable fission rate will result. This is called the plateau or "tail" of the burst. Although the magnitude of the fission rate in this region is several orders of magnitude below the peak fission rate, significant heating can take place since the condition can persist for relatively long times. In order to eliminate this heating the scram system can be programmed in such a manner as to cause the safety block to be withdrawn at any given time. This will result in a termination of the power excursion. A graphical description of a typical burst is given in Figure 34.

The quantities by which a burst is characterized are initial period, burst width at half maximum fission rate, peak fission rate, and burst yield. The initial period is determined by the initial amount of reactivity inserted into the system; and has the units of time. The burst width also has the units of time. The burst yield is simply the total numbers of fissions occurring during the power excursion.

Since the fission rate is not a directly measurable quantity, the peak fission rate and the total yield are determined in terms of the temperature increase of the system. The fission rate which is given in this report in terms of degrees centigrade per second can be related to fissions per second through calibrations based on dosimetry.

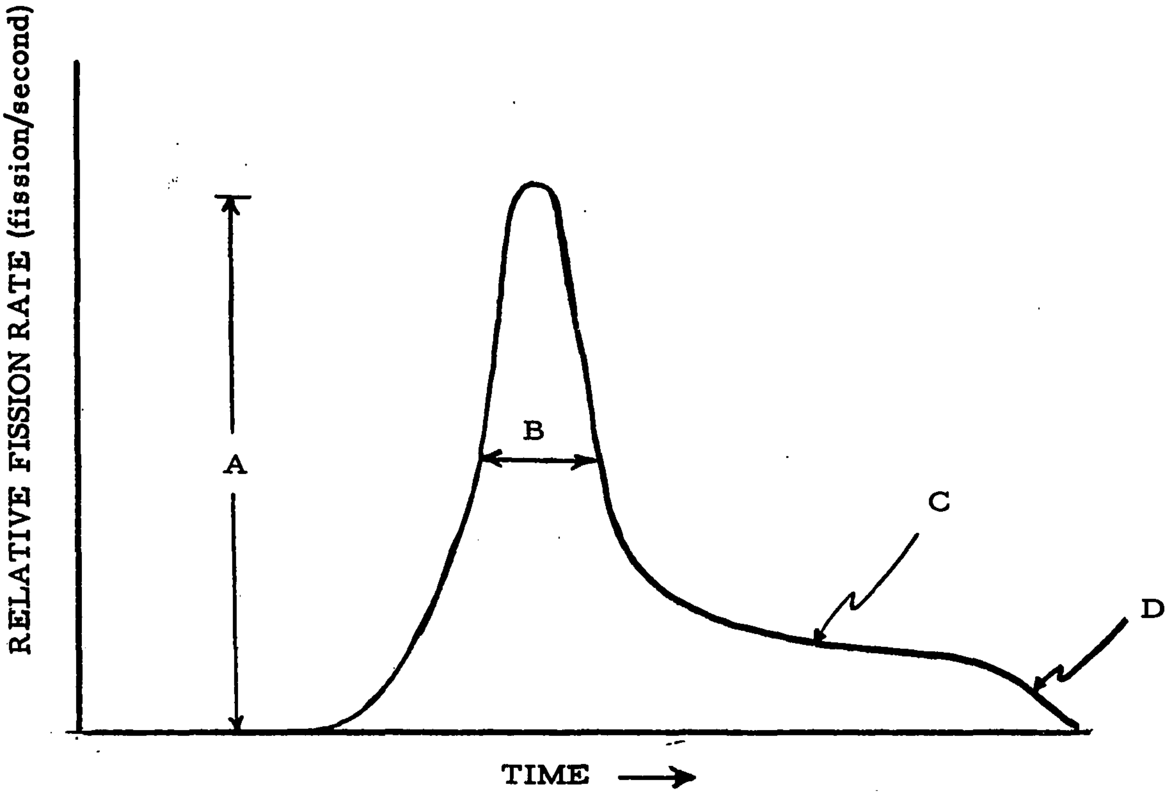

A - Peak fission rate

B - Burst width at half maximum fission rate

C - Plateau (or tail) region

D - Region of safety block withdrawal

Relative fission rate as a function of time for a typical burst.

FIGURE 34

APPENDIX B

NEUTRON BALANCE FOR A REFLECTED FUEL ASSEMBLY

The usual representation for the neutron balance when an external source of neutrons is present is given by

$$\frac{dn(t)}{dt} = [k(1 - \gamma\beta) - 1]\frac{n(t)}{\ell} + \sum_i \gamma_i \lambda_i C_i(t) + \gamma_s S \qquad (1B)$$

where C_i is given by

$$\frac{dC_i(t)}{dt} = k\beta_i \frac{n(t)}{\ell} - \lambda_i C_i(t) \qquad (2B)$$

These equations and the definitions of the terms are given in the introduction.

The conditions for critical steady state are as follows:

$$\frac{dn}{dt} = 0$$

$$\frac{dC_i}{dt} = 0$$

$$\frac{dS}{dt} = 0$$

$$k = 1$$

Equation (1B) can not simultaneously meet all of these conditions in its present form unless the source term is zero.

In most cases the source term S is independent of the neutron level. In the case where S is to represent the return of neutrons to the core from a reflecting material, S should be related to the neutron level in the core. Under steady state conditions, the number of neutrons returned to the fuel assembly by reflection should be some time independent fraction of the neutron leakage from the fuel and hence should be directly proportional to the neutron level in the core.

Let the relation between S and n be as follows:

$$S = \beta_r \frac{n}{\ell} = R$$

where β_r represents the fraction of the fission neutrons which are returned to the core after reflection.

The term $\gamma\beta$ is replaced by $\gamma^* \beta^*$, and it is required that the resulting neutron balance satisfy the four steady state conditons.

In the case where S is composed of reflected neutrons, equation (1B) can be expressed as

$$\frac{dn(t)}{dt} = [k(1 - \gamma^* \beta^*) - 1]\frac{n(t)}{\ell} + \sum_i \gamma_i \lambda_i C_i(t) + \gamma_r R \tag{3B}$$

where

γ_r = the reflected neutron effectiveness in causing fission

R = the rate at which reflected neutrons are returned to the core.

By imposing the steady state critical conditions, equation (3B) becomes

$$-\gamma^* \beta^* + \sum_i \gamma_i \beta_i + \gamma_r \beta_r = 0$$

Therefore, in order to meet the conditions for critical steady state the following requirement is necessary:

$$\gamma^* \beta^* = \sum_i \gamma_i \beta_i + \gamma_r \beta_r \tag{4B}$$

The representation for the neutron balance is then as expressed in equation (3B).

Relation of $\gamma_r \beta_r$ to Measured Reflector Worth

The equations describing a reflected reactor system are equations (2B), (3B) and (4B). The steady state critical conditions for such a system are simply

$$\frac{dn}{dt} = 0$$

$$\frac{dC_i}{dt} = 0$$

$$\gamma_r \beta_r \frac{n}{\ell} = \gamma_r R \tag{5B}$$

$$k = 1$$

I f the reflector is removed reactivity must be added to the system in order to re-establish the critical condition. Let Δk be the change in k of the system by movement of the control rods.

Equations (2B) and (3B) for the new delayed critical condition are

$$\frac{dn(t)}{dt} = 0 = [(1+\Delta k)(1-\gamma^*\beta^*) - 1]\frac{n(t)}{\ell} + \sum_i \gamma_i \lambda_i C_i(t) \tag{6B}$$

$$\frac{dC_i(t)}{dt} = 0 = (1+\Delta k)\beta_i \frac{n(t)}{\ell} - \lambda_i C_i(t) \tag{7B}$$

or

$$\Delta k = (1+\Delta k)\sum_i \gamma_i \beta_i - (1+\Delta k)\gamma_r \beta_r - \sum_i (1+\Delta k)\gamma_i \beta_i$$

or

$$\frac{\Delta k}{(1+\Delta k)} = \gamma_r \beta_r \tag{8B}$$

Hence, the term $\gamma_r \beta_r$ is simply equal to the reactivity measured between critical conditions for the reflected and unreflected cases. The alternate approach of adding a reflector to the system yields the same result.

APPENDIX C

SOLUTION OF PRECURSOR AND REFLECTOR EQUATIONS

The delayed neutron precursor equations are given by

$$\frac{dC_i(t)}{dt} = \frac{k\beta_i}{\ell} n(t) - \lambda_i C_i(t); \qquad i = 1, M \tag{1C}$$

The general solution of equation (1B) is

$$C_i(t) = e^{-\lambda_i t} \int_{-\infty}^{t} \frac{k\beta_i}{\ell} n(\xi)\, e^{-\lambda_i \xi}\, d\xi\ ; \qquad -\infty \leq \xi \leq t \tag{2C}$$

where the precursor concentration is assumed to be zero at t -∞

For the special case where n is given by

$$n(\xi) = n_o e^{\xi/T} \qquad -\infty \leq \xi \leq t$$

we have

$$C_i(\bar{t}) = \frac{k\beta_i n(t)}{\ell\left(\frac{1}{T} + \lambda_i\right)} \qquad i = 1, M \tag{3C}$$

The reflector equations are given by

$$\frac{dC_j(t)}{dt} = k\beta_j \frac{n(t - T_2)}{\ell} - \frac{C_j(t)}{T_{3_j}} \qquad j = M+1, N \tag{4C}$$

The general solution of equation (4C) is given by

$$C_j(t) = e^{-t/\tau_{3j}} \int_{-\infty}^{t} \frac{k\beta_j}{\ell}\, n(\xi - \tau_2)\, e^{\xi/\tau_{3j}}\, d\xi\,, \qquad -\infty \le \xi \le t \tag{5C}$$

where the j^{th} group neutron concentration in the reflector is assumed to be zero at $t = -\infty$.

For the special case where n is given by

$$n(\xi) = n_o e^{\xi/T} \qquad -\infty \le \xi \le t$$

we have

$$C_j(t) = e^{-t/\tau_{3j}} \int_{-\infty}^{t} \frac{k\beta_j}{\ } \; e^{(\xi - \tau_{2j})/T}\; e^{\xi/\tau_{3j}}\, d\xi \tag{6C}$$

$$C_j(t) = \frac{k\beta_j}{\ell} \; \frac{e^{-\tau_2 T}}{\left(\frac{1}{T} + \frac{1}{\tau_{3j}}\right)} \; n_o e^{t/T}$$

or

$$C_j(t - \tau_{4j}) = \frac{k\beta_j}{\ell} \; \frac{e^{-(\tau_2 + \tau_{4j})/T}}{\frac{1}{T} + \frac{1}{\tau_{3j}}} \; n_o\, e^{t/T} \tag{7C}$$

for $j = M+1,\ N$

APPENDIX D

M 2687-A GENERAL PURPOSE NEUTRON MONTE CARLO CODE

M 2687 is a general purpose Monte Carlo computer code developed for the specific problems presented in this paper. The code is designed for use with a high speed digital computer such as the Control Data 3600. Certain approximations have been incorporated into the code to increase the speed of calculations over conventional Monte Carlo techniques. These approximations deal only with dividing $(E, \vec{r}, \vec{\Omega})$ phase space into discrete intervals. Each of the approximations is discussed below. The basic characteristics of M 2687 are

1) 87 Energy groups
2) 26 Angular flux groups
3) LxMxN geometric cells
4) The following reactions are included
   a) anisotropic and isotropic scattering
   b) elastic and inelastic scattering
   c) absorption with fission
   d) (n, 2n) (n, 3n) reactions

The time required per neutron depends on the information desired. A typical value for a 25 x 25 x 25 lattice using the Control Data 3600 digital computer is 3 millisec per 2 mev neutron.

The discussion of the techniques is broken into various parts, each of which covers a physical aspect.

A. Neutron Energy

The initial energy of the neutron can be specified by either a particular choice or a choice made by random sampling for a given energy distribution. The energy of the neutron is calculated after each collision and is not quantized. The purpose in quantizing the energy spectrum is to use measured cross sections for which there are no analytical expressions describing their energy dependence. The selection of 87 energy groups is arbitrary and the extension to a greater number is possible with minor alteration of the code. The time required per neutron, however, increases with the number of energy groups.

B. Neutron Location

The most time-consuming feature of most Monte Carlo codes is the location of the neutron. Upon each collision, a new direction must be assigned by calculation and then a calculation using the new direction must be made to locate the particle. A less rigorous but much less time-consuming method is employed in M 2687.

The space covering a multi-region medium consists of a three-dimensional array of lattice points. The boundary of a given region is determined by analytic functions describing the region surface. If the lattice point lies within the space enclosed by these functions, the point is assigned cross sections and other parameters characteristic to that region. The neutron is assumed to exist in a finite cell around each lattice point. If that lattice point is in the region, the cell is considered wholly within the region.

This permits easy location of the particle with respect to the many regions which make up the whole assembly. For example, if a neutron penetrates a region surface by traveling to a lattice point outside the boundary of the region, a new set of parameters is used in determining the future of that particle. Thus, a heterogeneous system can be readily studied. The loss in rigor will not be significant if a large number of lattice points are chosen. If the number of lattice points is such that the distance between adjacent lattice points is much less than the mean free path of the neutron, the accuracy should be quite good. This implies that the required number of lattice points is dependent on the neutron energy spectrum which results.

C. Neutron Direction of Travel

The neutron direction can be selected by random sampling for a given distribution. The number of possible directions have been restricted to twenty-six. These directions correspond to the possible paths a neutron may take in going from one lattice point to another where only the points in the immediate vicinity of the neutron can be a destination. In addition to conforming with lattice requirements this restriction eliminates the need for a transcendental calculation upon each neutron collision. This results in a considerable savings in computer time and leads to no significant error. A 26 x 26 scattering matrix for both isotropic and anisotropic scattering is used to determine the neutron direction scattering. The manner of handling the energy dependence of this matrix is discussed later.

D. Neutron Penetration

For a neutron at some lattice point with a known energy and direction, the code must determine if the neutron travels to the next lattice point in its path. In order to do this the code determines the energy group to which a neutron of this energy belongs and calls from storage the appropriate probability (P), that the neutron will penetrate to the next point. This probability has been previously calculated for each combination of energy and direction. The information is stored in a 58 x 26 array. A direction tag is continuously carried with the neutron.

A random number is then chosen. If the number R is less than P, the neutron is said to penetrate to the next point without collision and the process is repeated. If $R \geq P$ the neutron is said to undergo a collision within the cell covering the first lattice point.

If the neutron penetrates to the next point, its spatial coordinates are changed and the code determines if the neutron has penetrated a region boundary. If so the neutron is governed by a new set of probabilities. If the boundary of the multi-region medium was crossed, the neutron is counted as a leakage neutron and the information desired is stored.

If $P \ll 1$ a considerable error can result in both lifetime and multiplication factor calculations. The number of lattice points should be chosen such that P is only slightly less than 1.

E. Neutron Interaction

Assuming that the neutron undergoes a collision, the code determines the type of interaction the neutron undergoes by comparison of random numbers with cross section ratios previously computed for that lattice point and that neutron energy. Each of the possible reactions is discussed separately.

1) Fission

If fission occurs, the code determines the number of neutrons released by using the value of γ for that energy. The information is stored and a new neutron cycle is initiated.

2) (n, γ) Reaction

If the code determines that the neutron undergoes the (n, γ) reaction, the desired information is stored and a new neutron cycle is initiated.

3) <u>(n, 2n), (n, 3n) Reaction</u>

The energy spectrum in a reactor is such that the (n, Nn) reactions make very little contribution. For this reason simplification by treating the reactions as fissions is justified. Although the energy of the resulting neutrons differ considerably from a fission spectrum, the resulting neutrons are counted as fission neutrons. The cycle is considered terminated and a new cycle is commenced.

4) <u>Elastic Scattering</u>

The angular distribution of the neutron direction after a collision is a strong function of energy. Below 50 Kev the distribution is essentially isotropic in the center of mass system and since the mass numbers of the materials considered in the fuel assembly are very large as compared to the neutron mass, the scattering is essentially isotropic in the laboratory system. Above 50 Kev, however, the scattering angle distribution becomes progressively more peaked in the forward direction as energy increases.

In order to account for the anisotropic and isotropic properties at each energy group, an M x 26 x 26 matrix must be formed, where M denotes the number of energy groups. However, since many of the matrix elements are identical, the matrix can be broken into several two-dimentional matrices.

The energy of the neutron after collision is calculated upon each collision once the scattering angle is determined. The calculation is based on the energy and momentum balance of the scattering process. However, it has been found that virtually no difference in calculated quantities occurs if the neutron is assigned the average energy loss for each elastic scattering event.

5) Inelastic Scattering

The angular distribution of the neutron after undergoing an inelastic scattering collision is assumed to be isotropic. A review of cross section data indicated that this was true. References are given in the discussion of the cross section data.

The energy of the neutron after a collision is determined by a much more involved process than that for elastic scattering. Seven distinct energy levels of the uranium nucleus are included along with an evaporation spectrum to account for energy levels in the continuum.

6) Other Reactions

All other reactions have such low probability of occurrance that they are neglected.

Cross Sections

U-235 . The fission, absorption, and inelastic scattering cross sections for the first 58 energy groups which extend from 15 mev to 1 kev are taken from reference [21]. Reference [59] provided fission cross sections for the range . 1 ev to 1 kev while reference [9] provides the absorption cross sections. The energy distribution after inelastic scattering is that recommended by K. Parker [21]. The differential elastic scattering cross sections used are given in reference [23].

U-238. The fission and and absorption cross sections used for U-238 are those given in reference [59]. The inelastic scattering cross sections used were those available in the literature and those of

Howerton [60] from 1.5 to 9 mev. Differential scattering cross sections were obtained from reference [23].

Polyethylene. The cross sections used were those of BNL 300. The free atom model was assumed and inelastic scattering in carbon was ignored. The values used compare favorably with values currently reported in pulse neutron literature.

LIST OF REFERENCES

1. R. E. Peterson and G. A. Newby, "An Unreflected U-235 Critical Assembly," Nuclear Sci. and Engr., 9, 357-361, (1961).
2. T. F. Wimett, R. H. White, W. R. Stratton, and D. P. Wood, "Godiva II - Unmoderated Pulse-Irradiation Reactor," Nuclear Sci. and Engr., 8, 691-708, (1960).
3. R. L. Long, Effects of Reflectors on the Burst Characteristics of an Enriched Uranium - 10 W/o Molybdenum Alloy Fast Burst Reactor, Missile Science Division Army Missile Test and Evaluation Directorate, Internal Memorandum No. 26, (1965).
4. R. V. Meghreblean and D. K. Holmes, Reactor Analysis, McGraw-Hill Book Company, Inc., (1960).
5. A. M. Weinberg and E. P. Wigner, The Physical Theory of Neutron Chain Reactors, The University of Chicago Press, (1958).
6. M. A. Schultz, Control of Nuclear Reactors and Power Plants, 2nd Edition, McGraw-Hill Book Company, Inc., (1961).
7. C. E. Cohn, "Reflected Reactor Kinetics," Nuclear Sci. and Engr., 13, 12-17, (1962).
8. G. R. Keepin, T. F. Wimett, R. K. Zeigler, "Delayed Neutrons from Fissionable Isotopes of Uranium, Plutonium and Thorium," The Phys. Rev., 107, 1044-1049, (1957).
9. D. J. Hughes, R. B. Schwartz, Neutron Cross Sections, BNL 325, 331-336, (1958).
10. James Grundl and Arthur Usner, "Spectral Comparisons with High Energy Activation Detectors," Nuclear Sci. and Engr., 8, 598-607, (1960).

11. Cleo C. Byers, "Cross Sections of Various Materials in the Godiva and Jezbel Critical Assemblies," Nuclear Sci. and Engr., 8, 608-614, (1960).

12. G. R. Keepin and C. W. Cox, "General Solution of the Reactor Kinetics Equations," Nuclear Sci. and Engr., 8, 670-690, (1960).

13. G. E. Hansen, D. P. Wood, and W. V. Gar, "Critical Masses of Enriched-Uranium Cylinders with Multiple Reflectors of Medium Z Elements," Nuclear Sci. and Engr., 8, 588-594, (1960).

14. W. R. Stratton, T. H. Calvin and R. B. Lazarus, "Analysis of Prompt Excursions in Simple Systems and Idealized Fast Reactors," Proceedings of the 2nd International Conference on Peaceful Uses of Atomic Energy, 12, 196-205, (1958).

15. T. F. Wimett and J. D. Orndoff, "Application of Godiva II Neutron Pulses," Proceedings of the 2nd International Conference on Peaceful Uses of Atomic Energy, 10, 449-460, (1958).

16. G. R. Keepin and T. F. Wimett, "Reactor Kinetics Functions: A New Evaluation," Nucleonics, Oct., (1958).

17. John T. Mihalczo, "Superprompt-Critical Behavior of an Unmoderated, Unreflected Uranium-Molybdenum Alloy Reactor," Nuclear Sci. and Engr., 16, 291-298, (1963).

18. S. Glasstone, M. C. Edlund, The Elements of Nuclear Reactor Theory, Van Nostrand, (1962).

19. G. S. Brunson, et. al., A Survey of Prompt-Neutron Lifetimes in Fast Critical Systems, Argonne National Laboratory, ANL 6681, August, 1963.

20. D. C. Irving and John T. Mihalczo, "Monte Carlo Calculations for Enriched Uranium Metal Assemblies," Transactions of the American Nuclear Society, Nov., 287-288, (1964).

21. K. Parker, Neutron Cross Sections of U^{235} and U^{238} in the Energy Range 1 Kev - 15 Mev, AWRE Report 0/82/63.

22. G. E. Hansen, "Physics of Fast and Intermediate Reactors," Proc. Seminar, 1, p. 453, International Atomic Energy Agency, Vienna (1962).

23. M. D. Goldberg, et. al., Angular Distributions in Neutron Induced Reactions, BNL-400, (1962).

24. A. B. Smith, "Elastic Scattering of Fast Neutrons from U^{235}, "Nuclear Sci. and Engr., 18, 126-129, (1964).

25. R. A. Karam, "Measurement of Rossi-Alpha in Reflected Reactors," Transactions of the American Nuclear Society, Nov., 283-284, (1964).

26. G. Robert Keepin, Physics of Nuclear Kinetics, Addison Wesley Publishing Company, Inc., (1965).

27. L. E. Weaver, Reactor Kinetics and Control, AEC 2 Symposium Series, March 25-27, (1963).

28. Etherington, Nuclear Engineering Handbook, McGraw-Hill Book Company, Inc., (1958).

29. P. D. O'Brien, The Sandia Pulsed Reactor Facility, SC-4737(M), Oct., (1962), TID-4500.

30. P. D. O'Brien, Hazards Evaluation of the Sandia Pulsed Reactor Facility, Report to the United States Atomic Energy Commission, SC-4357A(RR), Feb., (1961).

31. R. G. Morrison, "Application of Miniature Intrinsic Thermocouples for Reactor Transient Diagnostics," Transactions of the American Nuclear Society, 128-129, June, (1965).

32. Robert L. Long, "Effects of Reflectors on the Burst Characteristics of the WSMR Fast Burst Reactor," Transactions of the American Nuclear Society, 451, November, (1965).

33. Kaman Nuclear, Fast Burst Reactor Facility Technical Manual, KN-685-64-1(TM), (1965).

34. R. L. Long, Modification of FBR Fuel Assembly, FBRF Safeguards Report, White Sands Missile Test and Evaluation Directorate, Jan., (1965).

35. Sandia Corporation, Sandia Pulsed Reactor Operations Manual, SC-M-64-1210, (1965).

36. R. L. Coats, Rod Calibration of the SPR-I Reactor, Sandia Corporation Interdivision Memorandum, (1966).

37. R. L. Long, Private Communication, (1965).

38. T. F. Wimett, Private Communication, (1966).

39. G. E. Hansen, Private Communication, (1966).

40. G. M. Frye, et. al., Energy Spectrum of Neutrons from Thermal Fission of U^{235} and from an Untamped Multiplying Assembly of U^{235}, LA 1670, (1964).

41. J. T. Mihalczo, "Prompt-Neutron Decay Constant in a Two-Component Enriched Uranium Metal Critical Assembly," Transactions of the American Nuclear Society, June, (1960).

42. J. T. Mihalczo, "Prompt Neutron Lifetime in Enriched Uranium Metal Cylinder," Transactions of the American Nuclear Society, 48-49, (1964).

43. Oak Ridge National Laboratory, A General Purpose Monte Carlo Neutron Transport Code, ORNL-3622.

44. U. Benzi, et. al., "A Monte Carlo Analysis of Some Enriched U^{235} Fast Critical Assemblies," Journal of Nuclear Energy, Vol. 20, (1966).

45. J. Orndoff, "Prompt Neutron Periods of Metal Critical Assemblies," Nuclear Sci. and Engr., 2, 450, (1957).

46. H. L. Garabedean and C. B. Leffert, "A Time Dependent Analysis of Spatial Flux Distributions," Nuclear Sci. and Engr., 6, 26, (1959).

47. A. Foderado and H. L. Garabedean, "Two Group Reactor Kinetics," Nuclear Sci. and Engr., 14, 22-29, (1962).

48. Tsutomu Hoshino, et. al., "New Approximate Solution of Space-and Energy-Dependent Reactor Kinetics," Nuclear Sci. and Engr., 23, 170-182, (1965).

49. Chester D. Kylstra and Robert E. Uhreg, "Spatial Dependent Transfer Function for Nuclear Systems," Nuclear Sci. and Engr., 22, 191-205, (1965).

50. D. R. Harris, "Neutron Fluctuations in a Reactor of Finite Size," Nuclear Sci. and Engr., 21, 369-381, (1965).

51. J. T. Mihalczo, "Prompt Neutron Lifetime in Critical Enriched-Uranium Metal Cylinders and Annuli," Nuclear Sci. and Engr., 20, 60, (1964).

52. G. E. Hansen and Clifford Maier, "Perturbation Theory of Reactivity Coefficients for Fast Neutron Cubical Systems," Nuclear Sci. and Engr., 8, 532, (1960).

53. J. R. Beyster, et. al., "Measurements of Neutron Spectra in Water, Polyethylene and Zirconium Hydride," Nuclear Sci. and Engr., 9, 168, (1961).

54. D. T. Goldman and F. D. Federighi, "Calculation of Neutron Flux Spectra in a Polyethylene Moderated Medium," Nuclear Science and Engr., 16, 165, (1965).

55. E. Moller and N. G. Sjostrand, "Measurement of the Slowing-down and Thermalization Time of Neutrons in Water," ARKIV FOR FYSIK BAND 27 NR 31 (1964).

56. G. F. Von Dardel, "The Interaction of Neutrons with Matter Studied with a Pulsed Neutron Source, "Transactions of the Royal Institute of Technology, Stockholm, Sweden, Vol. 2, No. 10, (1964).

57. B. G. Carlson and G. I. Bell, "Solution of the Transport Equation by the S_n Method," Proceedings of the 2nd International Conference on the Peaceful Uses of Atomic Energy, Geneva, 16, 535, (1958).

58. L. Cranbert, G. Frye, N. Nereson, and L. Rosen, "Fission Neutron Spectrum of U^{235}," Physics Review, 103, 662, (1956).

59. W. N. McElroy, et. al., Experimental and Evaluated Cross Section Library of Selected Reactions, Technical Report No. AFWL-TR-65-34, Vol. 1, (1965).

60. Howerton, R. J., Semi-emperical Neutron Cross Sections, Part III, 1, (1958).

GLOSSARY

BARE REACTOR	-	For the purposes of this paper a bare reactor refers to an unreflected fuel region.
BURST ROD	-	A burst rod is a movable fissionable component which is rapidly inserted into the fuel region in order to make the system highly supercritical.
CENT	-	A cent is a unit of reactivity equal to one hundredth of a dollar.
CORE	-	The unreflected fuel region is referred to as the core. The words core, reactor and fuel assembly are used interchangably in the discussion of a Godiva type reactor.
CRITICAL	-	A reactor is said to be critical when the multiplication factor of the reactor is equal to unity.
DELAYED CRITICAL	-	The expression delayed critical is used in this paper interchangeably with critical. It also refers to a range of operation where the reactivity of the system is limited to near critical conditions.
DELAYED NEUTRONS	-	A neutron which results from the decay of certain fission products. These neutrons do not appear immediately after the fission event since the normal decay scheme of the parent emitter is followed. Hense, these neutrons are referred to as delayed neutrons.
DOLLAR	-	One dollar is defined as that amount of reactivity which makes the system prompt critical
FAST NEUTRONS	-	High energy neutrons and, therefore, neutrons with high velocities are referred to as fast neutrons.

FAST REACTOR	-	A reactor system which offers little or no moderation to the fission neutrons is called a fast reactor.
GLORY HOLE	-	The term glory hole refers to an opening through which access to the inner region of the core is obtained without dismantling the assembly.
INHOUR RELATION	-	The inhour relation is a conditional equation relating reactivity to stable reactor period for a solution of the reactor kinetics equations. The name "inhour" results from early reactor terminology in which an inhour unit was that amount of reactivity required to give a stable reactor period of one hour.
KIVA	-	The building or room in which the reactor is housed. .
MODERATOR	-	A moderator is a material of relatively low mass number. If a neutron undergoes elastic scattering with such a material the resulting neutron energy is significantly lower than before the collision.
MULTIPLICATION FACTOR	-	The ratio of neutron production rate to neutron loss rate.
NEUTRON EFFECTIVENESS	-	The relative efficiency of a neutron in producing fission as compared to a typical reactor neutron.
PLATEAU	-	The region of the burst where the neutron level is governed by the decay of delayed neutron precursors produced during the pulse.
PROMPT CRITICAL	-	The term prompt critical refers to that state of the reactor in which the system is critical on the basis of prompt neutrons alone.
PROMPT NEUTRON	-	A neutron which arises directly from the fission event.

REFLECTED NEUTRON - For the purposes of this paper, a neutron which has been scattered in the direction of the fuel assembly from a reflector is called a reflected neutron.

WORTH OF A COMPONENT - The worth of a given component is the amount of reactivity added to the reactor by the presence of the component.